Structure-function relationship between plastid morphology and carbon partitioning during secondary cell wall synthesis in *Arabidopsis thaliana*

by

Medha Sood

Submitted in partial fulfilment of the requirements for the degree

Magister Scientiae

In the Faculty of Natural and Agricultural Sciences
Department of Biochemistry, Genetics and Microbiology
University of Pretoria

April 2022

Supervisor: Prof Eshchar Mizrachi
Co-supervisors: Dr Desre Pinard,
Prof Vida Van Staden and
Dr Victoria J. Maloney

DECLARATION

I, **Medha Sood**, declare that the dissertation, which I hereby submit for the degree **M.Sc. Biotechnology** at the University of Pretoria, is my own work and has not been submitted by me for a degree at this or any other tertiary institution.

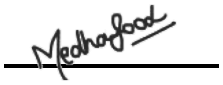

April 2022

Medha Sood

Date

DISSERTATION SUMMARY

Structure-function relationship between plastid morphology and carbon partitioning during secondary cell wall synthesis in *Arabidopsis thaliana*

Medha Sood

Supervised by **Prof Eshchar Mizrachi**

Co-supervised by **Dr Desre Pinard, Prof Vida van Staden** and **Dr Victoria J. Maloney**

Submitted in partial fulfilment of the requirements of the degree *Magister Scientiae*

Department of Biochemistry, Genetics and Microbiology

University of Pretoria

Approximately 82% of fixed carbon present in living biomass is found in terrestrial plants of which an estimated 70% exists in the secondary cell wall (SCW) of vascular plants. The SCW, comprised of cellulose, hemicellulose and lignin, serves as the main source of lignocellulosic biomass, a renewable feedstock for timber, paper, pulp, biomaterials and biofuel production. Lignin comprises about 15 to 36% of the dry weight of wood making it one of the most abundantly found natural polymers on earth. Lignin is made up of three major monolignols, namely p-coumaryl, coniferyl and sinapyl alcohols. Its composition, structure and quantity all impact recalcitrance to industrial processing and saccharification, making it an important research target for industrial applications.

Although research into the molecular regulation of lignin synthesis has greatly advanced in the last 20 years, the role and regulation of organelles in carbon allocation between polysaccharides and lignin during xylogenesis has received far less attention. This is despite the fact that plastids are the exclusive sites of the pentose phosphate pathway (PPP) and the shikimate pathway. The PPP is responsible for the production of erythrose 4-phosphate (E4P) catalysed by the plastid-localised enzymes transketolase (TK) and/or transaldolase (TAL). E4P, combined with

phosphoenolpyruvate (PEP) from glycolysis, feed into the shikimate pathway which produces chorismate, the precursor of the aromatic amino acids (AAA) such as phenylalanine (Phe) and many aromatic secondary metabolites. Phe is used by the phenylpropanoid pathway for monolignol and ultimately lignin formation. Plastids also play a crucial role in regulating the plant's carbon budget by acting as sites for starch biosynthesis for energy storage and as reserves for growth, development and response to stress. Recent study of organellar biology in *Eucalyptus* xylem tissue has shown that not only are plastid targeted (i.e. nuclear-encoded) genes preferentially co-regulated with distinct phases of xylogenesis; plastidial gene expression itself is also uniquely regulated during xylogenesis and may play a distinct role in facilitating carbon partitioning for cell wall biosynthesis. This data supports the notion of a new plastid type, specific to secondary xylem formation, namely the xyloplast.

This MSc study aimed to gain deeper insights into the ultrastructural changes that may accompany chloroplast differentiation into xyloplasts during SCW formation. A VND7(Vascular-related NAC domain 7)-inducible system in *Arabidopsis* was used, for which transcriptomic and some metabolomic data is publicly available. In the VND7 system, most cells in Arabidopsis plants differentiate into xylem vessel elements upon induction, resulting in SCW deposition. Using this system, SCW formation was induced to characterise changes in plastid ultrastructure at different time points after induction using transmission electron microscopy. This study provided novel insight into some of the major transitional steps involved in the conversion of chloroplasts to xyloplasts. The findings revealed that SCW induction resulted in major ultrastructural changes in chloroplasts, with an intermediate morphology typical of plastid interconversion. Integration of morphology and gene expression analysis showed that plastid differentiation is accompanied by rapid Phe synthesis and plastid degradation plays a key role in making Phe available for the monolignol biosynthetic pathway. These findings shed insight on vascular plant development and evolution, and pave the way for advanced biotechnological applications in engineering biomass crops.

Preface

The plant SCW provides mechanical strength and rigidity for the upright growth of vascular plants. In addition to this, it also reinforces tracheary elements and channels for long-distance transport of water in xylem. The predominant constituents of the SCW are lignin, cellulose, and hemicellulose which form the bulk of the plant's woody biomass – an abundant, sustainable resource for the bio-based economy. However, one of the major reasons for the untapped potential of woody biomass is the recalcitrance of highly lignified tissue to industrial processing, with the removal of lignin playing a major role. In addition to fixing carbon through photosynthesis, plastids found in vascular plants are also involved in the mass production of aromatic amino acids needed for monolignol biosynthesis in woody tissues – which accounts for ~57% of total global carbon in living biomass. In South Africa, following the acceptance of the Long Term Mitigation Scenarios (LTMS), a solution to carbon constraints is needed and in order to maximize the yield of woody biomass, it is important to gain a holistic understanding of wood formation as a process.

Approximately 30% of woody cell wall biomass is comprised of lignin which makes it an important component of the SCW and a major carbon sink. Lignin is a phenolic heteropolymer formed through the polymerization of monolignols, which are synthesized through the phenylpropanoid biosynthesis pathway. In dicots, the carbon skeleton precursor for phenylpropanoid synthesis is provided by the aromatic amino acid – Phe – which is synthesized by the plastid-localized shikimate pathway, along with tyrosine (Tyr) and tryptophan (Trp). Other compounds formed from the end products of the shikimate pathway include flavonoids, alkaloids, indole glucosinolates and hydroxycinnamic acids. Phosphoenolpyruvate (PEP) - generated during glycolysis - and erythrose 4-phosphate (E4P) - synthesized by the pentose phosphate pathway - act as precursors for the shikimate pathway. The shikimate pathway therefore plays a critical role in carbon partitioning, as it irreversibly shunts carbon from sugars which can be used as precursors for cellulose, hemicellulose or pectin to phenolic biopolymers, such as lignin. This emphasizes the key role that is played by plastids and their metabolism during lignin formation, a topic that has historically been ignored in studies of plant secondary growth.

Plastids are a unique group of organelles that arose from a single endosymbiotic event in eukaryotes. In vascular plants especially, plastids can interconvert between different types of varying morphologies and functions. Although the most commonly studied plastid is the chloroplast, many non-photosynthetic plastid types which are highly integrated with specialised cellular metabolism have evolved in this lineage. These plastids have distinct functions and play key roles in plant developmental processes. One such recently proposed plastid is the xyloplast, which plays a key role in providing Phe for lignin synthesis in woody tissues during xylogenesis. This finding is supported by the unique transcriptional regulation of nuclear-encoded as well as plastidial-encoded proteins and metabolism coordinated with wood formation in *Eucalyptus*.

In addition to their specialised metabolic functions, distinct plastid types are largely defined by their unique morphological characteristics. **The aim of this study** was to obtain a broader understanding of the plastid ultrastructural dynamics that accompany the carbon shunt to phenylalanine and monolignol synthesis in developing xylem, to broaden current knowledge of organellar biology during secondary growth. One of the major drawbacks to studying xylem is the complexity of the SCW in trees. To overcome this, we used a post-translational induction system of VND7 (master regulator of xylem vessel differentiation) in *Arabidopsis* to study SCW formation at different time points. Transmission electron microscopy analysis of trans-differentiating *Arabidopsis* leaves revealed an amoeboid plastid, which is commonly seen during plastid interconversion, followed by plastids with unique morphology. Using publicly available transcriptomic and metabolic data of the VND7 system, this study also highlighted the link between changes in plastid morphology and carbon partitioning towards the synthesis of SCW phenolic constituents, emphasizing plastid structure-function relationship. This study provides considerable insight into plastid ontogeny and ultrastructure in xylem as well as further evidence for the existence of a distinct plastid derivative — the ‘xyloplast’ in developing xylem.

These findings provide insight into vascular plant development and evolution which, in the future, can be applied to advanced biotechnological applications in engineering biomass crops. These results highlight the importance of understanding plastid function in secondary growth in order to further model xylogenesis and identify targets to optimize carbon allocation and partitioning.

The dissertation is structured as follows:

Chapter 1 is a literature review which comprehensively covers organellar biology which includes the origin of plastids through endosymbiosis, their subsequent evolution and specialization to perform tissue-specific functions as well as new, recently described plastid types. I discuss the changes in ultrastructure that accompany the interconversion of plastid types and how the changes in morphology relate to their ultimate function. I then discuss in detail the roles of important plastidial pathways such as the Calvin Cycle, the Shikimate pathway and the PPP in the partitioning of carbon between sugars, starch and aromatic amino acids in source and sink tissue. I discuss how organellar biology is uniquely regulated during xylogenesis by describing a newly proposed morphologically distinct, xylem-specific plastid – the xyloplast. I also highlight the importance of the VND7 post-translational induction system in *Arabidopsis* which serves as an important tool to study xylem differentiation. I conclude the chapter by reviewing the recent advances in our understanding of lignin and its recalcitrance to industrial processing in order to improve lignin engineering.

Chapter 2 is a research chapter which describes the ultrastructural differentiation of chloroplasts into xyloplasts. Using the VND7 inducible system and transmission electron microscopy I show a detailed temporal analysis of the morphological changes that occur during the plastid interconversion over a 48 hour period. The identification of a common transitional intermediate amoeboid plastid partially supports that the xyloplast is a distinct plastid type. I also wanted to gain insight into the role of plastids in partitioning carbon (C) into the shikimate pathway for Phe and subsequent monolignol synthesis. I analysed published transcriptomic and metabolic data from the VND7-inducible system to discuss changes gene expression in the context of the morphological changes seen in plastids during secondary cell wall (SCW) deposition. I found that there is a structure-function relationship between the shunting of carbon towards phenolic synthesis and the transition from chloroplast to xyloplast and ultimate plastid degradation.

In **Chapter 3,** I conclude the dissertation by addressing the remaining gaps in knowledge, highlight future perspectives and outline work not discussed in detail in this thesis. Specifically, I created CRISPR/Cas9 mutant lines targeting starch metabolism genes in plastids which can be used downstream to gain knowledge on the role starch plays as a carbon source for the xyloplast.

Acknowledgements

"Before the reward there must be labour. You plant before you harvest. You sow in tears before you reap joy." – Ralph Ransom

- **Prof Eshchar Mizrachi** – None of this would have been possible without you. It would be safe to say I was nowhere close to being a scientist when I started this degree and even though I'm not 100% there yet (I still need to perfect my use of dashes as parenthesis), I have learnt an incredible amount from you. Thank you for being an extraordinary mentor, always thinking out loud and encouraging us to do the same. It is impossible to not be excited about science in your presence and I have learnt to find a feeling of accomplishment in every "adequate" you've thrown at me. I hope you continue to inspire and shape young minds for many years to come.
- **Dr Desré Pinard** – Des, I thought it was because of my interesting work that you'd nod so enthusiastically in every presentation but turns out it's in your nature to be so kind and supportive of everyone around you. Thank you for the ridiculously detailed feedback, developing an app so I wouldn't have to cry myself to sleep while coding and always having such contagious energy. You are an incredible co-supervisor.
- **Prof Vida van Staden and Dr Victoria Maloney –** You are both incredible mentors, scientists and most importantly an inspiration to all women in science. Thank you for being amazing co-supervisors and teaching me so much on this journey.
- **Mom and Dad** – There is so much I am grateful for, I don't even know where to begin. Mom, thank you for always reminding me that I am capable of achieving anything I set my mind to, you made sure I persevered even when I felt like I couldn't. I am who I am today, all because of you. Dad, thank you for inspiring me to pursue a career in science, you have always challenged me to be the best in everything I do. Thank you both for being my pillars of strength.

- **Vansh** – Not-so-little broski, thank you for always making me feel like I am the smartest person you know, you clearly don't know a lot of people. Thank you for always believing in me and choosing me as your role model, it makes all my endeavours twice as rewarding. As you start your university career, I have no doubt you'll achieve great success (maybe don't do research). I am proud to be your older sister.
- **Stefan** – Or should I say bro-supervisor? Thank you for being an incredible mentor to me, whether it is in the lab or in life. I will forever cherish our coffees on campus, beers at Capital Craft, all-you-can-eat sushi evenings and the Jakaranda drives. Thank you for all the advice, having the driest sense of humour (which I have somehow learnt to love) and for making my masters a memorable experience.
- **Aparna** – Miles apart in distance, but never in heart. Thank you for the endless phone calls of motivation, sharing the lows of my failures and celebrating my every victory, no matter how small. They're right when they say friends are the family we choose and boy, did I choose well.
- **Elle** – There isn't a day that goes by where I don't thank the stars for making our paths cross. Thank you for teaching me to unapologetically be myself, being patient with me during my "stressed" episodes and for always having confidence in my abilities. Your free-spirit is an inspiration.
- To my friends – **Arun, Jay, Felix and Laksh**, thank you for the endless support, the coffee dates, the drinks and the laughs – you guys have been the greatest gift.
- My lab mates – **Luke, Ipeleng and Lazarus** – I will never forget the laughs, the lab pranks, the gossip and the daily venting. Lab Z was a vibe.
- Finally, **Nani Ma**, you are my greatest blessing and joy, thank you for your love, your support and for instilling in me that education is indeed the most empowering tool needed to build a triumphant future.

Table of Contents

DECLARATION i

DISSERTATION SUMMARY ii

Preface iv

Acknowledgements vii

List of abbreviations xii

Chapter 1 15

The role of plastids in carbon partitioning towards secondary cell wall synthesis 15

1.1. Introduction 16

1.2. Plastid evolution and biology 17

1.2.1. The origin of plastids – the endosymbiotic theory 17

1.2.2. Structure-function relationship in plastids 18

1.3. Carbon partitioning in plants 22

1.3.1. The Calvin Cycle as a starting point of carbon metabolism 23

1.3.2. The role of starch in carbon allocation 25

1.3.3. Transitory and storage starch 25

1.3.4. Starch breakdown 26

1.3.5. The pentose phosphate pathway as a source of reducing power and pentose sugars 27

1.3.6. The Shikimate pathway links carbohydrate metabolism and AAA biosynthesis 28

1.4. Plastid metabolism during xylogenesis 29

1.5. Transcriptional regulation of carbon flux to SCW and the VND7 induction system 30

1.6. Lignin in woody biomass 33

1.6.1. Lignin's role in biomass recalcitrance 34

1.7. Conclusion: A developing secondary xylem-specific plastid, the xyloplast 36

1.8. References 32

Chapter 2 47

The ultrastructure and role of plastids in carbon partitioning during xylogenesis in VND7-inducible *Arabidopsis* 47

2.1. Summary 48

2.2. Introduction 49

2.3. Materials and Methods 52

2.3.1. Plant growth, DEX treatment and VND induction 52

2.3.2. Light microscopy 52
2.3.3. Transmission electron microscopy 53
2.3.4. VND7 transcriptional and metabolic analysis 53
2.4. Results 54
2.4.1. VND7 induction results in secondary cell wall deposition and changes in plastid ultrastructure 54
2.4.2. Finer scale TEM analysis revealed a morphologically unique plastid, the xyloplast 59
2.4.3. Plastid structure is related to function in carbon partitioning during SCW formation 62
2.5. Discussion 67
2.6. Acknowledgments 75
2.7. References 76
2.8. Supporting Information 83
Supplemental Figure S1 83
Supplemental Figure S2 84
Supplemental Figure S3 85
Supplemental Figure S4 86
Supplemental Figure S5 87
Supplemental Figure S6 88
Supplemental Figure S7 89
Supplemental Figure S8 90
Supplemental Figure S9 91
Supplemental Figure S10 91
Supplemental Figure S11 92
Supplemental Figure S12 92
Supplemental Figure S13 93
Supplemental Figure S14 94
Supplemental Figure S15 95
Supplemental Figure S16 96
Supplemental Figure S17 97
Supplemental Figure S18 97
Supplemental Figure S19 97
Supplemental Figure S20 98

Supplemental Figure S21 98
Supplemental Figure S22 99
Supplemental Figure S23 99
Supplemental Figure S24 99
Supplemental Figure S25 100
Supplemental Figure S26 100
Chapter 3 101
3.1. Concluding remarks 102
3.2. References 105
3.3. Supplementary note 108
3.3.1. Background 108
3.3.2. CRISPR/Cas9 target site selection and sgRNAs design 108
3.3.3. Cloning and plant transformation 109
3.3.4. Conclusion 110

List of abbreviations

35S CaMV	35S Cauliflower mosaic virus
3PG	3-phosphoglycerate
4CL	4-Coumarate-CoA Ligase
AAA	Aromatic amino acid
ADP	Adenosine diphosphate
ADP-Glc	ADP-glucose
AGP	ADPG pyrophosphorylase
AGPase	ADP-Glc pyrophosphorylase
ATP	Adenosine triphosphate
BAM3	Beta-amylase 3
C3H	4-coumarate 3-hydroxylase
C4H	Cinnamate-4-Hydroxylase
CAD	Cinnamyl alcohol dehydrogenase (CAD)
CCoAOMT	Caffeoyl-CoA O-methyltransferase
CCR	Cinnamoyl-CoA reductase
CesA	Cellulose synthase A
CIM	Chromoplast internal membrane
cINV	Cytosolic invertase
CO2	Carbon dioxide
COMT	Caffeic acid 3-O-methyltransferase
CRISPR	Clustered Regularly Interspaced Palindromic Repeats
DEX	Dexamethasone
DHAP	Dihydroxyacetone phosphate
E4P	Erythrose 4-phosphate
F1,6BP	Fructose 1,6-bisphosphate
F5H	Ferulate-5-hydroxylase
F6P	Fructose 6-phosphate
FBP aldolase	Fructose bisphosphate aldolase
FBPase	Fructose bisphosphatase
Fru	Fructose
G1P	Glucose 1-phosphate
G3P	Glyceraldehyde 3-phosphate
G3PDH	Glyceraldehyde 3-phosphate dehydrogenase
G6PDH	Glucose 6-phosphate dehydrogenase
GBSSI	Granule-bound starch synthase
Glc	Glucose
G-lignin subunit	Guaiacyl
GPT	Glucose 6-phosphate/phosphate translocator
GR	Glucocorticoid receptor
gRNA	Guide RNA
GWD	Glucan, water dikinase
HCT	hydroxycinnamoyltransferase
HPI	Hours post induction
H-lignin subunit	Hydroxyphenyl

HXK	Hexokinase
Ile	Isoleucine
IRX	Irregular xylem
Leu	Leucine
Lys	Lysine
Met	Methionine
NADPH	Nicotinamide adenine dinucleotide phosphate
PAL	Phenylalanine ammonia-lyase
PCD	Programmed cell death
PEP	Phosphoenolpyruvate
PG	Plastoglobules
PGI	Phosphoglucose isomerase
PGM	Phosphoglucomutase
PPi	Inorganic pyrophosphate
PPP	Pentose phosphate pathway
pPGI	Plastidial phosphoglucose isomerase
pPGM	Plastidial phosphoglucomutase
Phe	Phenylalanine
PWD	Phosphoglucan, water dikinase
RL5P	Ribulose 5-phosphate
Rubisco	Ribulose-1,5-bisphosphate carboxylase oxygenase
RuBP	Ribulose1,5-bisphosphate
S7P	Sedoheptulose 7-phosphate
SBE	Starch branching enzymes
SCW	Secondary cell wall
SDE	Starch debranching enzymes
SPS	Sucrose phosphate synthase
SS	Starch synthase
Sucrose-6P	Sucrose 6-phosphate
S-lignin subunit	Syringyl
SuSy	Sucrose synthase
TAL	Transladolase
TALEN	Transcription activator-like effector nuclease
TE	Tracheary element
TEM	Transmission electron microscopy
TF	Transcription factor
Thr	Threonine
TK	Transketolase
TPT	Triose phosphate translocator
Trp	Tryptophan
Tyr	Tyrosine
UDP-G	UDP-glucose
UGP	UDPG pyrophosphorylase
Val	Valine
VND	Vascular-related NAC domain
WT	Wildtype

XL5P	Xylulose 5-phosphate
ZFN	Zinc finger nucleases

Chapter 1
Literature Review:

The role of plastids in carbon partitioning towards secondary cell wall synthesis

1.1. Introduction

Plastids are a diverse group of sub-cellular organelles that occur in plants as well as a large number of diverse eukaryotic lineages (Inaba and Ito-Inaba, 2010; Keeling, 2013) and originated through the process of endosymbiosis (McFadden, 2001) when a free-living, single-celled organism (cyanobacterium-like prokaryote) was engulfed by the eukaryotic ancestor of plants (López-Juez, 2006; Keeling, 2010). This partnership was important during the evolution of land plants, especially vascular plants (de Vries et al., 2016), as it led to the incorporation of novel metabolic pathways into the cell and further plastid specialisation (Inaba and Schnell, 2008). Most research has focussed on dissecting photosynthetic plastid biology i.e. CO_2 fixation in chloroplasts however, heterotrophic plastids such as amyloplasts and chromoplasts also play pivotal roles in carbon metabolism and synthesis of essential storage compounds (Neuhaus and Emes, 2000). Additionally, many plant metabolic pathways essential for carbon partitioning during wood formation are compartmentalized to plastids such as the pentose phosphate pathway (PPP) and the shikimate pathway. During xylogenesis, the plastid-localized shikimate pathway links carbohydrate metabolism to the synthesis of aromatic amino acids which include tyrosine, phenylalanine (Phe) and tryptophan (Dewick, 2009). Phe is the primary precursor for lignin formation and other major plant products such as flavonoids, benzoic acid derivatives, stilbenes, and coumarins (Dixon and Paiva, 1995; Holton and Cornish, 1995; Whetten and Sederoff, 1995; Maeda and Dudareva, 2012). Despite the great significance of plastidial metabolism to xylogenesis, its role in SCW formation has been largely ignored.

Woody biomass is the most abundant sustainable carbon resource on earth (Liu et al., 2020) with many uses in industrial applications and as a sustainable, renewable energy source (Novaes et al., 2010b; Myburg et al., 2019; Ali et al., 2020). Lignin is a phenolic heteropolymer of 4-hydroxyphenylpropanoids derived from Phe and comprises approximately 30% of woody cell wall biomass which makes it an important component of the SCW and a major carbon sink (Takenaka et al., 2018). Although lignin is an essential component of woody biomass, conferring mechanical strength (Zhong and Ye, 2014) and pathogen resistance by forming a physical barrier against pathogen infection (Vance et al., 1980; Bhuiyan et al., 2009; Zhong and Ye, 2014), these same properties hinder saccharification (Yoo et al., 2020). Lignin forms a physical barrier for the binding of cellulases and is also an insoluble substrate for hydrolytic enzyme activity (Lynd et

al., 1999; Himmel et al., 2007; Chandra et al., 2016; Yoo et al., 2020). Lignin's contribution to recalcitrance significantly increases costs of biomass processing, thus modification of lignin to reduce recalcitrance, without affecting yield, is extremely important (Mosier et al., 2005; Pu et al., 2011; Pu et al., 2013; Nguyen et al., 2015; Li et al., 2016b; Mottiar et al., 2016). In the past years, many studies have dissected the lignin biosynthetic pathway in *Arabidopsis* and *Populus* in order to identify targets for genetic engineering of lignin content, composition and structure to reduce recalcitrance (Bjurhager et al., 2010; Vanholme et al., 2012; Liu et al., 2018; Chanoca et al., 2019; Mahon and Mansfield, 2019). However, how carbon is partitioned towards lignin biosynthesis is not fully understood. Understanding carbon partitioning is an important step in providing valuable insight into targeted metabolic/genetic engineering/breeding strategies for improvement of biomass recalcitrance.

This literature review explores our current knowledge of plastid metabolism and its integration with xylem development. It focuses on dissecting the changes accompanying the interconversion of plastids between different plastid types, the relationship between plastid morphology and function as well as the transcriptomic regulation of plastids found in wood forming tissues during secondary growth. The use of an important tool for understanding the molecular mechanism of xylem vessel differentiation – the VND7 post-translational induction system – is also reviewed. This literature study is also aimed at providing a thorough understanding of the important regulatory link that the shikimate and pentose phosphate pathways form between primary and secondary metabolism in trees, the regulation of carbon partitioning to lignocellulosic biomass as well as lignin's contribution to SCW recalcitrance.

1.2. Plastid evolution and biology

1.2.1. The origin of plastids – the endosymbiotic theory

Similar to the endosymbiotic origins of mitochondria, plastids arose when a free-living, single-celled organism (cyanobacterium-like prokaryote) was engulfed by eukaryotic phagotroph through so-called 'primary' endosymbiosis which resulted in the formation of the three lineages: green algae/plants, red algae and glaucophytes **(Fig 1)** (McFadden, 2001; Lopez-Juez and Pyke, 2004; Keeling, 2010).

Plastids resulting from primary endosymbiosis are characterized by the presence of two surrounding membranes derived from the prokaryotic ancestor (Inaba and Ito-Inaba, 2010). Through the process of secondary and tertiary endosymbioses, these primary plastids spread to other eukaryotic lineages (Archibald, 2009; Keeling, 2013). Secondary endosymbiosis takes place when a eukaryotic cell is engulfed by another eukaryotic cell that has previously been formed as a result of primary endosymbiosis (McFadden, 2001). These plastids are seen in chlorarachniophytes, euglenoid algae and cryptophytes (McFadden, 2001; Keeling, 2013).

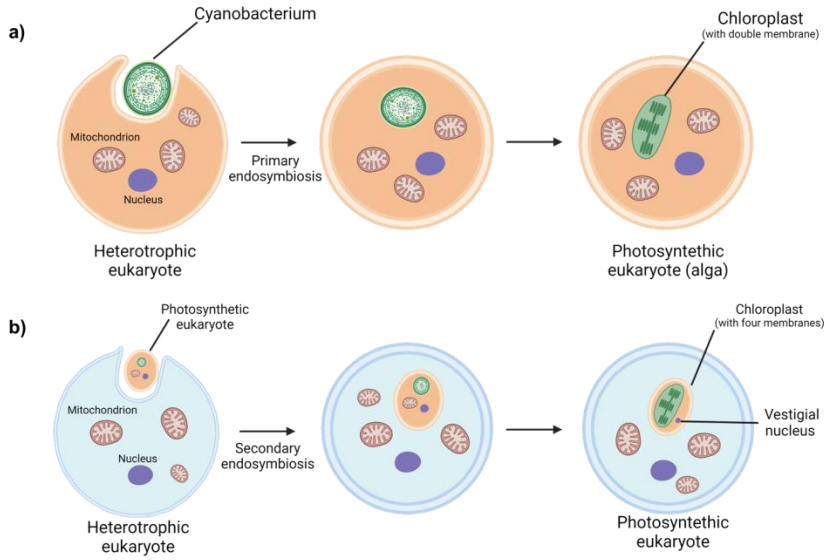

Figure 1 The origin of plastids through a) primary and b) secondary endosymbiosis. Created with Biorender.com

The evolution of these organelles was accompanied by the reduction of the prokaryotic symbiont genome with the majority of genes being transferred to the host nuclear genome (Adams et al., 2002; Inaba et al., 2011), as well as the development of a protein-targeting system (Keeling, 2010). Due to this, plastid biogenesis is dependent on the expression of proteins encoded by the host nucleus and the posttranslational transport of these proteins into plastids (Inaba and Schnell, 2008), making coordination between these genomes important for plant fitness, adaptation and evolution.

1.2.2. Structure-function relationship in plastids

As multicellular plants evolved to form specialized tissues and cells, distinct plastid types also became specialized for metabolic and signalling functions within plant cells (Inaba and Schnell,

2008; de Vries et al., 2016). This resulted in plastids that have distinct morphologies and functions in various tissues and cell types and also respond to diverse array of environmental stimuli (Wise 2007; Choi et al. 2021).

The interconversion of plastids between various types is very important as new plastids can only arise from existing plastids (Inaba and Ito-Inaba, 2010; Zechmann, 2019; Choi et al., 2021). Proplastids (diameter 1 to 1.5 µm) are undifferentiated plastids that occur in plant meristematic and reproductive tissues (Marinos, 1967; Inaba and Ito-Inaba, 2010; Jarvis and López-Juez, 2013; Liebers et al., 2017). Compared to other plastid types, proplastids display minimal structural morphology, are colourless and small in size (Whatley, 1977; Jarvis and López-Juez, 2013; Liebers et al., 2017; Choi et al., 2021). Proplastids can convert into chloroplasts, etioplasts or leucoplasts while chromoplasts and gerontoplasts are usually formed from chloroplasts (Vothknecht and Westhoff, 2001; Rottet et al., 2015). Chloroplasts are the lens-shaped archetypical plastids present in photosynthetic cells (Sarafis, 1998). They contain an internal thylakoid membrane system which forms disc-shaped stacks called grana where photosynthetic protein complexes are anchored for photosynthesis (Granick, 1961; Rottet et al., 2015; Roston et al., 2018). At the edges of thylakoids, osmiophilic droplets called plastoglobules (PG) are found (Larcher et al., 1988; Austin et al., 2006). Their main role is the storage of α-tocopherol, plastoquinone, and triacylglycerols as well as the synthesis of lipid molecules (Bailey and Whyborn, 1963; Greenwood et al., 1963; Steinmüller and Tevini, 1985; Tevini and Steinmüller, 1985; Vidi et al., 2006b; Ytterberg et al., 2006). PG are also found in chromoplasts where they mainly function in the storage of carotenoids (Emter et al., 1990; Deruère et al., 1994).

Chromoplasts are carotenoid-accumulating plastids and confer colour to fruits (Büker et al., 1998; Bouvier and Camara, 2007) and flowers (Tetlow et al., 2003; Egea et al., 2010). In addition to the PG, large structures called fibrils containing carotenoids are also found (Deruère et al., 1994). During fruit ripening, chloroplasts convert into chromoplasts (Egea et al., 2010). Photosynthetic ability is lost due to granal and thylakoid disassembly, which is accompanied by the formation of new carotenoid-bearing membrane systems, called chromoplast internal membranes (CIMs), derived from vesicles of the inner plastid membrane (Spurr and Harris, 1968; Wrischer and Devide, 2002; Simkin et al., 2007). A special carotenoid-containing CIM, known as the chromoplast reticulum is abundant in flower chromoplasts (Ljubešić, 1979) and has

been described in some *Capsicum* varieties (Carde et al., 1988). The reticulum is formed from the invagination of the inner plastidial membrane and lacks chlorophyll (Ljubešić, 1977, 1979). An increase in the reticulum is associated with transport activity of the plastid envelope (Ljubešić, 1979). The synthetic differentiation of chloroplasts to chromoplasts can be triggered metabolically through phytoene induction (Llorente et al., 2020b). These chloroplast-derived chromoplasts showed absence of an organized thylakoid membrane system and grana, contained tightly appressed lipid membrane stacks a well as PG (Llorente et al., 2020b). **Table 1** provides an overview of the various plastid types that are known, such as proplastids, chromoplasts, leucoplasts and chloroplasts. A lesser studied plastid type, not included in the table, includes the desiccoplast, found in desiccation-tolerant plants that can interconvert between proplastids and chloroplasts (Solymosi and Keresztes, 2012)

Table 1: Various known plastid types and their characteristic features

Plastid type	Tissue	Morphological characteristics	Function	Reference
Proplastid	Meristematic tissues, germ cells	Small, low internal differentiation	Specialized plastid precursors, trans-generational transfer of plastids	(Pyke, 2007; Liebers et al., 2017)
Chromoplast	Fruits, flowers and root tissues	Shows great heterogeneity, characterized by storage structures present i.e. globular, membranous, or crystalline	Provide distinctive colours to tissues, carotenoid production	(Thomson and Whatley, 1980; Egea et al., 2010)
Etioplast	Cotyledons of dark-grown seedlings	Contain prolamellar bodies which are paracrystalline lattices of membrane tubules containing chlorophyll	Dark-matured chloroplast progenitors	(Sperling et al., 1998; Cortleven et al., 2016)

Chloroplast	All photo-synthetically active tissues such as leaves, stems	At least three membrane systems present including the thylakoid membrane system	Photosynthesis, metabolite biosynthesis	(Staehelin, 1986; Jarvis and López-Juez, 2013)
Gerontoplast	Senescing foliage	Presence of a large number of PG and a reduced thylakoid system	Senescing chloroplast which can be reverted to a chloroplast until terminal senescence phase is reached and cell death is observed	(Wise and Hoober, 2007; Solymosi and Keresztes, 2012)
Elaioplast	Embryonic leaves of oilseeds, citrus fruits and specialized cells, e.g.,tapetal cells of anthers	Small, rounded organelles filled by oil droplets, also contain PG-associated proteins e.g. fibrillins	Storage and metabolism of lipids	(Ting et al., 1998; Wu et al., 1999)
Proteinoplast	Seeds	Crystalline bodies of protein present which could be enzyme activity sites	Protein storage	(Wise and Hoober, 2007)
Amyloplast	Roots and storage tissues, collumella cells	Starch grains presents	Starch synthesis and storage. Specialized amyloplasts called Statoliths also play a key role in gravitropism	(Naeem et al., 1997; Pyke, 2007)
Phenyloplast	Mesocarp	Presence of lens-shaped loculi between thylakoids	Phenol glucoside accumulation and storage	(Brillouet et al., 2014)
Tannosome	Thracheophyta chlorophyllous organs	Pearling of thylakoid membranes, budding off of vesicles and shuttles	Tannin polymerization	(Brillouet et al., 2013)

In the last few years, two new non-photosynthetic and structurally unique plastid types, derived from chloroplasts, have been reported. The tannosome is responsible for the synthesis of condensed tannins, which are then transported to the vacuole in tannosome shuttles (Brillouet et al., 2013). The differentiation from chloroplasts to the tannosome begins with an increase in size and circularization of the plastid, followed by the unstacking of the thylakoid membrane and swelling of the grana (Brillouet et al., 2013). These changes are also seen in plants exposed to UV stress which also triggers the synthesis of phenolics (He et al., 1994; Jansen et al., 1998; Selga and Selga, 1998; Berli et al., 2011). Following this, there is further disorganization of the thylakoid membranes and osmiophilic material, identified as phenolics, seen in the thylakoid lumen (van Steveninck and Van Steveninck, 1980; Keresztes and Sárvári, 2001; Brillouet et al., 2013). The chloroplast double membrane becomes diffuse and tannosomes are formed from the pearling of the thylakoid membranes, which become encapsulated in spherical structures called shuttles. These shuttles bud off from the plastid and are transported to the vacuole (Brillouet et al., 2013). Another organelle, the phenyloplast, is found in vanilla fruit (Brillouet et al., 2014). During redifferentiation from chloroplasts, ribosomes fill the stroma and loculi are formed between thylakoid membranes which store the β-D-glucosides (Brillouet et al., 2014). The interconversion of plastids from one type to another requires extensive ultrastructural reorganization which corresponds to its function (Vothknecht and Westhoff, 2001). Although plastids are the exclusive sites of aromatic amino acids (AAA) synthesis needed for monolignol production, limited evidence of plastid morphology and structure-function relationship in xylem has been generated (Pinard and Mizrachi, 2018).

1.3. Carbon partitioning in plants

Many plant metabolic pathways that are essential to secondary growth and wood formation and are compartmentalized to plastids including the Calvin cycle, the pentose phosphate pathway (PPP) and the shikimate pathway. In wood forming tissues, the plastidial shikimate pathway plays a key role in the synthesis of AAA from sugars including phenylalanine (Phe), which is the main precursor for monolignol synthesis (Novaes et al., 2010b). In this way, plastids create a unique link between secondary metabolism (shikimate pathway for AAA and monolignol production) and primary carbon metabolism (pentose phosphate pathway).

1.3.1. The Calvin Cycle as a starting point of carbon metabolism

The first important metabolic pathway involved in carbon partitioning is the Calvin cycle (Figure 2a) (Sarafis, 1998; Sugiura et al., 1998; Li and Chiu, 2010; Adams, 2019). During photosynthesis, CO_2 from the atmosphere is fixed via the Calvin cycle, in the chloroplasts, to yield triose phosphates in order to facilitate the growth and development of plants (Stein and Granot, 2019).

The Calvin cycle can be divided into three distinct phases: fixation, reduction, and regeneration. In the *carboxylation* phase, CO_2 is fixed into 3-phosphoglycerate (3PG) by ribulose-1,5-bisphosphate carboxylase oxygenase (Rubisco). In the *reduction* phase, through the use of ATP and NADPH, glyceraldehyde-3-phosphate dehydrogenase reduces 3PG into glyceraldehyde-3-phosphate (G3P) (Sillero et al., 2006). In the final *regenerative* phase, some G3P molecules are recycled to produce ribulose1,5-bisphosphate (RuBP) for carbon fixation by the enzymes fructose bisphosphatase (FBPase), fructose bisphosphate aldolase (FBP aldolase), triosephosphate isomerase, ribulose 5-phosphate 3-epimerase, ribulose 5-phosphate isomerase and transketolase (TK) (Geiger and Servaites, 1994; Tamoi et al., 2005; Sillero et al., 2006). The triose-phosphates generated act as important intermediates and can be allocated into to either the starch or sucrose biosynthetic pathway depending on sink strength (Figure 2b) (Woodrow and Berry, 1988; Geiger and Servaites, 1994; Marcelis, 1996; Tamoi et al., 2005).

For sucrose biosynthesis, the triose-phosphates are exported into the cytosol where one molecule of fructose 1,6-biphosphate (F1,6BP) is formed from two molecules of triose-phosphate, followed by a de-phosphorylation reaction which forms fructose-6-phosphate (F6P) **(**Figure 2a**)**. F6P is isomerized via phosphoglucose isomerase (PGI) to form glucose 6-phosphate (G6P) which is used to form UDP-glucose (UDP-G). Sucrose phosphate synthase (SPS) then catalyses the formation of sucrose 6-phosphate (sucrose-6P) form F6P and UDP-G (Stein and Granot, 2019). Sucrose-6P is dephosphorylated by sucrose phosphate phosphatase to form sucrose, which is the primary sugar transported from source tissues to sink tissues through the phloem in order to provide carbon for metabolic pathways (Dennis and Miernyk, 1982; Stein and Granot, 2018, 2019).

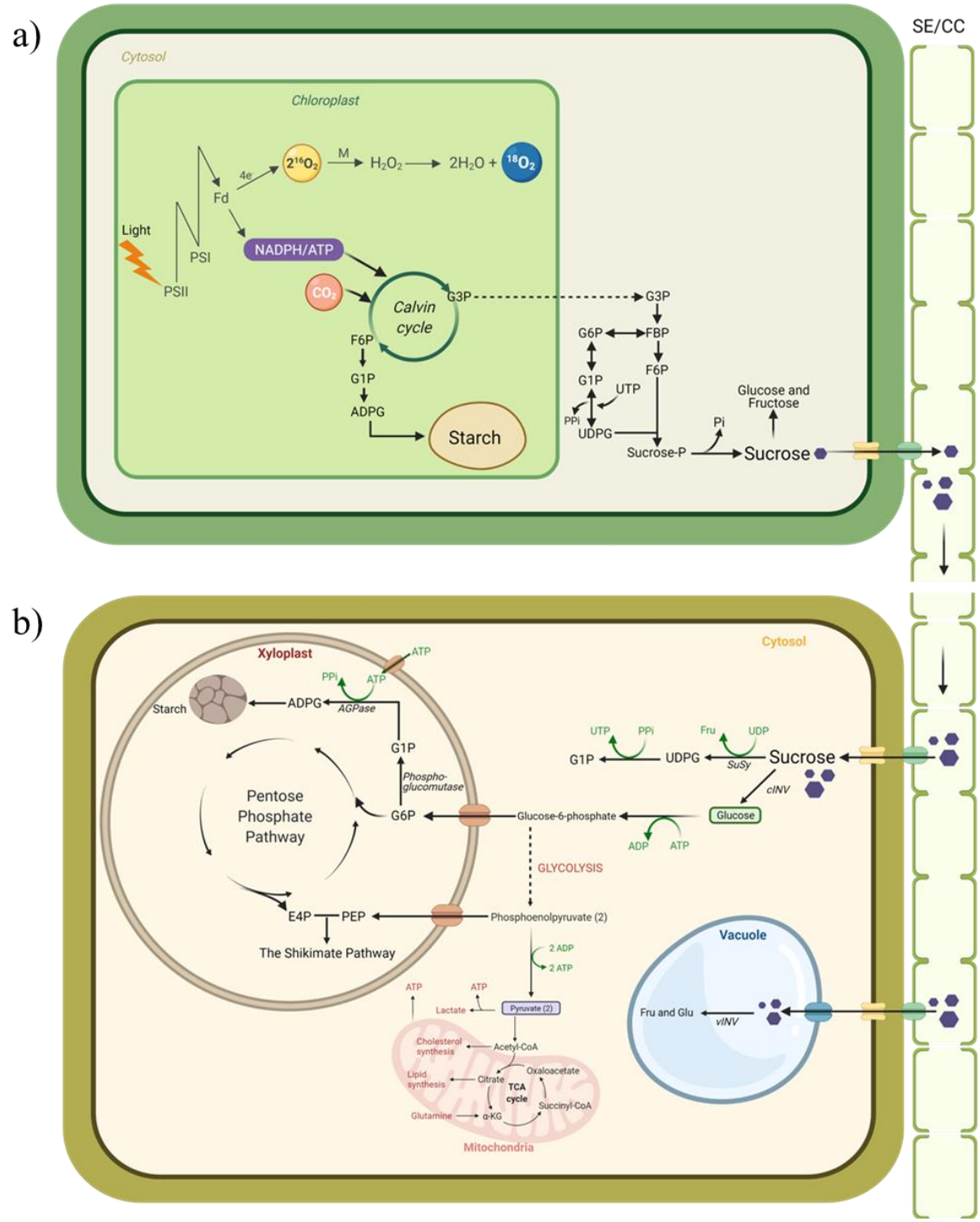

Figure 2 Carbon partitioning in plants. (a) Simplified model of the Calvin cycle in source tissue. Triose-phosphates synthesized in the chloroplast can be exported to the cytosol for sucrose synthesis or be used for transitory starch synthesis. (b) Simplified schematic presentation of sugar metabolism in sink tissue cells Glu can be phosphorylated by a hexokinase (HXK) to yield glucose-6-phosphate (G6P). G6P can be used for glycolysis and then respiration in the mitochondria, or be translocated into the plastid to be fed into plastidic metabolic pathways including starch synthesis, the pentose phosphate pathway and the shikimate pathway. Created with Biorender.com

1.3.2. The role of starch in carbon allocation

Starch is synthesized in plastids and is a semi-crystalline carbon storage polymer that is made up of amylose and amylopectin, both consisting of α-(1,4)-linked glucose (Glc) chains (Badenhuizen, 1963; Smith et al., 1997; Whistler and Daniel, 2000; MacNeill et al., 2017). The two main types of starch include: transitory starch and storage starch (Lu and Sharkey, 2006; Gámez-Arjona et al., 2011; Lloyd and Kossmann, 2015). Starch can act as a carbon reserve in leaves for growth and respiration at night or act as a storage component in seeds and tubers (Bahaji et al., 2014; Cho and Kang, 2020). Thus, the synthesis and breakdown of starch in plant tissues plays a major role in the physiology and development of plants by regulating the partitioning of free sugars which subsequently controls plant growth and other developmental processes (Geigenberger, 2003; Smith and Stitt, 2007; Bahaji et al., 2014).

1.3.3. Transitory and storage starch

Transitory starch is synthesized in chloroplasts from triose-phosphates during the day and is degraded at night to support non-photosynthetic metabolism and growth (Fig 2a) (Caspar et al., 1985; Stitt and Quick, 1989; Schulze et al., 1991; Huber and Hanson, 1992; Ludewig et al., 1998; Liu et al., 2012; Aliche et al., 2020). In non-photosynthetic (heterotrophic) sink tissues such as seeds, stems, roots or tubers, storage starch is synthesized in amyloplasts and serves as long term storage which has been well established and reviewed (Martin and Smith, 1995; Neuhaus and Emes, 2000; Emes et al., 2003; Streb et al., 2009; Pfister and Zeeman, 2016). In heterotrophic cells (Fig 2b), sucrose can be broken down by sucrose synthase (SuSy) or invertase. In the presence of UDP, SuSy breaks down sucrose to yield fructose and UDP-Glucose (UDP-G) (Stein and Granot, 2019). In contrast, invertase cleaves sucrose to yield glucose and fructose (Nguyen-Quoc and Foyer, 2001). UDP-G is converted to G1P and PPi by UDPG pyrophosphorylase (UGP) and the former is metabolized to G6P by cytosolic phosphoglucomutase (PGM) which enters the amyloplast for starch synthesis (Mühlbach and Schnarrenberger, 1978; Keeling et al., 1988; Hatzfeld and Stitt, 1990; Hill and Smith, 1991; Wischmann et al., 1999) via the glucose 6-phosphate/phosphate translocator (GPT) (Flügge et al., 1989; Kammerer et al., 1998).

In the amyloplast, G6P is converted to G1P and subsequently ADP-glucose (ADP-Glc) by plastidial PGM (Hill and Smith, 1991; Bahaji et al., 2014) and ADP-Glc pyrophosphorylase

(AGPase), respectively (Ghosh and Preiss, 1966; Emes and Neuhaus, 1997; Neuhaus and Emes, 2000; Bahaji et al., 2014; Preiss and Sivak, 2017). The Glc moiety is incorporated to the non-reducing end of an existing α-glucan chain by starch synthases (SS) (MacNeill et al., 2017). The granule-bound starch synthase (GBSSI) is responsible for amylose synthesis (Denyer et al.; Smith and Martin, 1993; Martin and Smith, 1995; Goren et al., 2018) and multiple isoforms of SS *i.e.* SSI, SSII, and SSIII are involved in amylopectin biosynthesis (Brust et al., 2013; Cuesta-Seijo et al., 2016; Pfister and Zeeman, 2016; Goren et al., 2018). Branch points are introduced by starch branching enzymes (SBEs) while starch debranching enzymes (SDEs) trim excess branched chains (Nakamura et al., 1992; Martin and Smith, 1995; Larsson et al., 1996; Larsson et al., 1998). Alternatively to starch synthesis in plastids, cytosolic invertase can irreversibly hydrolyze Suc to form the hexose monomers (Glc and Fru) in the cytosol, that can be phosphorylated and directed to other metabolic pathways such as the PPP in the plastid or glycolysis followed by respiration in the mitochondria (Fig 2b) (Stein and Granot, 2019).

1.3.4. Starch breakdown

Starch degradation has been extensively studied within living cells in most plant tissues, the nature and regulation of which differs from endosperms, which is essentially dead tissue (Smith et al., 2003; Smith et al., 2005; Smith and Stitt, 2007; Hannah and James, 2008; Zeeman et al., 2010; Stitt and Zeeman, 2012). Remobilization of transitory starch in leaves requires the enzyme glucan, water dikinase (GWD) which alters the phosphate content of amylopectin by transferring the β-phosphate of ATP to the C6-position of glucosyl residues (Ritte et al., 2002; Mikkelsen et al., 2004; Ritte et al., 2006). Mutants lacking the GWD protein display the starch excess 1 (*sex1*) phenotype (Caspar et al., 1991; Zeeman and Rees, 1999; Yu et al., 2001). A second glucan, phosphoglucan, water dikinase (PWD) further facilitates starch degradation by adding a phosphate group to the C3 position of glucosyl residues (Baunsgaard et al., 2005; Kötting et al., 2005) and making amylopectin structure more accessible to breakdown by the further action of debranching enzymes, β-amylases and α-amylases (Stitt and Zeeman, 2012).

After soluble, linear glucans have been formed through the activity of glucans and DBEs, two pathways or further degradation can take place (Smith et al., 2005). First, G1P can be released by the activity of chloroplastic glucan phosphorylase (Lin et al., 1988; Zeeman et al., 1998) followed by the formation of triose-phosphates which are then exported to the cytosol via the

triose phosphate translocator (TPT) (Häusler et al., 1998). Second, maltose can be synthesized by β-amylase activity which acts at the non-reducing ends of α-1,4–linked glucan chains (Fulton et al., 2008). Nine β-amylases are encoded for by the *Arabidopsis* genome of which one has been shown to be localized in the chloroplast, providing evidence for the role of β-amylase in chloroplast-localized transitory starch metabolism (Lao et al., 1999). Knowledge of starch breakdown pathways play a key role in our understanding of their integration with plant primary metabolism (Zeeman et al., 2007).

1.3.5. The pentose phosphate pathway as a source of reducing power and pentose sugars

G6P can also enter the PPP which is also central to primary carbon metabolism. This pathway consists of two stages: the oxidative non-reversible phase and the non-oxidative reversible phase (Horecker, 2002; Sillero et al., 2006). During the oxidative phase, ribulose-5-phosphate is formed through the dehydrogenation and decarboxylation of G6P which is catalyzed by a series of three enzymes namely glucose-6-phosphate dehydrogenase (G6PDH), gluconolactonase and 6-phosphogluconate dehydrogenase (Schnarrenberger et al., 1973; Herbert et al., 1979; Mayes and Bender, 2003; Sillero et al., 2006). In non-photosynthetic cells, the oxidative phase provides NADPH for reductive biosynthetic processes, such as steroid and fatty acid synthesis as well as lignin synthesis (Stafford, 1974; Pryke and ap Rees, 1977; Kruger and von Schaewen, 2003; Mayes and Bender, 2003). The non-oxidative phase provides ribose for nucleotide synthesis and metabolic intermediates for the synthesis of aromatic amino acids and phenylpropanoids (Herrmann, 1995; Kruger and von Schaewen, 2003)

As cells generally require more NADPH for reductive biosynthesis compared to ribose-5-phosphate for nucleotides, the non-oxidative phase of the cycle converts ribose-5-phosphate into G3P and fructose 6-phosphate (F6P) (Murray et al., 2009; Bhagavan and Ha, 2011). The plastid-localized enzymes, transketolase (TK) and transaldolase (TAL) play an important role in regulating the flux of carbon into the shikimate pathway by controlling E4P levels (Kruger and von Schaewen, 2003; Murray et al., 2009). TK catalyzes the formation of sedoheptulose-7-phosphate (S7P) and glyceraldehyde-3-phosphate (G3P) from xylulose 5-phosphate (XL5P) and ribulose 5-phosphate (RL5P) as well as the conversion of XL5P and E4P to G3P and F6P (Racker et al., 1953; Murray et al., 2009; Kochetov and Solovjeva, 2014). TAL catalyzes the

reversible reaction in which F6P and E4P are formed from S7P and G3P (Horecker and Smyrniotis, 1953). E4P, together with PEP (generated by glycolysis) is converted by the shikimate pathway into chorismate to form AAAs (Tzin and Galili, 2010b; Maeda and Dudareva, 2012).

1.3.6. The Shikimate pathway links carbohydrate metabolism and AAA biosynthesis

In wood forming tissues, the plastidial shikimate pathway, exclusively localized within the plastid stroma (Herrmann, 1995; Herrmann and Weaver, 1999; Schmid and Amrhein, 1999), plays a key role in the synthesis of AAAs from sugars i.e. Tyr, Trp and Phe (Herrmann and Weaver, 1999; Novaes et al., 2010b). E4P from the PPP and PEP from glycolysis act as precursors for the shikimate pathway (Herrmann, 1995). In the first step, PEP and E4P undergo aldol condensation to form 2-dehydro-3-deoxy-D-arabino-heptonate-7-phosphate (DAHP) and inorganic phosphate by the activity of DAHP synthase (Tzin and Galili, 2010a; Kumar et al., 2019). The enzyme, 3-dehydroquinate synthase converts DAHP to 3-dehydroquinic acid, the reduction of which leads to the formation of quinic acid (Herrmann, 1995; Tzin and Galili, 2010a). Shikimate is formed via the dehydration and reduction of 3-dehydroquinic acid by the enzymes, 3-dehydroquinate dehydratase and shikimate-3-dehydrognase (Herrmann, 1995; Whetten and Sederoff, 1995; Dewick, 2009). The final product of the main shikimate pathway branch is chorismate which is the substrate for the AAA biosynthetic pathways (Herrmann, 1995; Kumar et al., 2019).

Chorismate mutase catalyzes prephenate biosynthesis after which arogenate is obtained through transamination (Fraser and Chapple, 2011). Following this, the Tyr and Phe pathways diverge and the ring carboxylate and hydroxyl groups are removed via arogenate dehydratase for Phe synthesis (Fraser and Chapple, 2011). Phe is the primary precursor for many major secondary plant metabolites such as flavonoids, benzoic acid derivatives, stilbenes, and coumarins (Dixon and Paiva, 1995; Holton and Cornish, 1995; Whetten and Sederoff, 1995) and most importantly monolignols for lignin formation in vascular plants (Boerjan et al., 2003). In grasses however, Tyr can also be used for lignin synthesis (Barros et al., 2016; Maeda, 2016).

1.4. Plastid metabolism during xylogenesis

Xylem tissue plastids play a key role during SCW biosynthesis as the plastid-localized shikimate pathway acts as an irreversible carbon-partitioning step between sugars and aromatic phenolic precursors for lignin biosynthesis (Rippert et al., 2009a). Although organellar metabolism is integral to xylogenesis, the first real study of gene expression of plastid-targeted genes was only performed in 2019 (Pinard and Mizrachi, 2018; Pinard et al., 2019). Previous transcriptional and translational studies of non-green plastids such as chromoplasts (Kahlau and Bock, 2008) and amyloplasts (Valkov et al., 2009) have shown that in non-green plastids, there is down-regulation of photosynthesis-related genes, a down-regulation of plastidial gene expression genes (ribosomal proteins, rRNAs, tRNAs and RNA polymerase subunits) and an overall down-regulation of plastid genome expression with an exception of *accD* and *clpP* (Kahlau and Bock, 2008; Valkov et al., 2009; Zhang et al., 2012). These genes play crucial roles in lipid metabolism and protein turnover, respectively, needed for the functioning of these plastids (Shanklin et al., 1995; Lee et al., 2004; Kode et al., 2005; Kahlau and Bock, 2008; Valkov et al., 2009).

Analysis of plastid-encoded genes, using total mRNA-seq data, in *E. grandis* mature leaf, phloem, and immature xylem tissues showed that in xylem, 13 plastid-encoded non-photosynthetic genes are up-regulated to levels much higher than in chromoplasts or amyloplasts (Pinard et al., in preparation) (Kahlau and Bock, 2008; Valkov et al., 2009). These genes included *E. grandis* housekeeping and genes such as *ycf1*, *ycf2*, and *accD* (Pinard et al., in preparation). The *ycf2* gene was the most highly differentially expressed and encodes an essential TIC (translocon on the inner chloroplast membrane)-complex-associated protein (Kessler and Schnell, 2006; Kikuchi et al., 2018), which indicates the importance of non-photosynthetic protein import in non-green plastid metabolism and secondary growth (Pinard et al., in preparation).

Small-RNA sequencing data revealed clusters of organellar small RNAs (cosRNAs) (Pinard et al., in preparation), which are small RNA footprints left by nuclear-encoded RNA-binding proteins (RBPs) that stabilize organellar transcripts by binding to them (Ruwe et al., 2016). The identification of a cosRNA footprint overlapping the 3’ end of the *ycf2* transcript indicates the possible active regulation of *ycf2* by an unknown RBP (Pinard et al., in preparation). Together, the analysis of plastid gene expression - using total RNA, mRNA and small RNA sequencing - in

immature xylem (heterotrophic tissue) compared to mature leaf (photosynthetic tissues) revealed a unique differential expression of plastid-encoded transcripts in xylem through possible active regulation by RBPs (Pinard et al., in preparation). Together with different plastid-targeted protein expression from the nuclear genome (Pinard et al., 2019), this suggests that there is distinct regulation of xylem plastid biology in facilitating carbon partitioning towards SCW growth, providing evidence for the existence of a wood-specific plastid, the xyloplast (Pinard and Mizrachi, 2018).

1.5. Transcriptional regulation of carbon flux to SCW and the VND7 induction system

In order to fully understand the development of the SCW in plants it is important to understand the transcriptional regulation of SCW synthesis (Ohtani et al., 2016) and the role organellar biology play therein (Pinard and Mizrachi, 2018). However, accessing xylem vessel elements for molecular and observational studies is a major obstacle (Zimmermann, 2013; Brodersen et al., 2019; Tan et al., 2019). This is due to the complexity with which xylem vessels are embedded in the plant body as well as the high variability resulting from the fact that xylem tissue is made up of several kinds of cells i.e. xylem fibers and parenchyma cells (Tan et al., 2019). To overcome this, *in vitro* induction systems have been widely used to study xylem vessel cell differentiation by induction through either phytohormonal stimuli (Fukuda and Komamine, 1980; Kubo et al., 2005; Oda et al., 2005; Pesquet et al., 2010; Kondo et al., 2014; Kondo et al., 2015; Kondo et al., 2016) or by overexpressing SCW-related transcription factors (Yamaguchi et al., 2008; Yamaguchi et al., 2010; Yamaguchi et al., 2011; Tan et al., 2018).

A good example of such an induction system is the glucocorticoid-mediated posttranslational induction system of VASCULAR-RELATED NAC-DOMAIN 6/7 (VND6/7) (Yamaguchi et al., 2010). *A thaliana irregular xylem* (*irx*) mutant studies have identified VND1–VND7 transcription factors, belonging to the NAC family, as master regulators of xylem vessel cell differentiation that promote the up-regulation of SCW- and programmed cell death (PCD)-related genes (Kubo et al., 2005; Yamaguchi et al., 2008; Ohashi-Ito et al., 2010; Zhong et al., 2010; Yamaguchi et al., 2011; Endo et al., 2015; Nakano et al., 2015). The over-expression of VND6 and VND7 results in the trans-differentiation of various cells into metaxylem-like vessels

in *Arabidopsis* and protoxylem-like vessels in poplar whereas repression leads to the inhibition of xylem vessel differentiation (Kubo et al., 2005). In the VND6/7 induction system, a construct with a 35SCaMV promoter in which the VND6 or VND7 gene is fused to the activation domain of the herpes virus VP16 protein and hormone-binding glucocorticoid receptor (GR) domain was created (Fig 3) (Yamaguchi et al., 2010). The VP16 activation domain can directly interact with general transcription factors (TF) including the TATA-binding protein, TFIIB, and the SAGA histone acetylase complex (Shen et al., 1996).

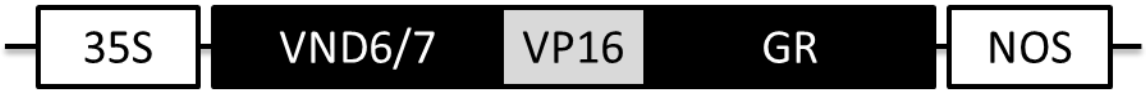

Figure 3 Schematic of the VND6- VP16-GR and VND7-VP16-GR constructs. 35S, CaMV 35S promoter; VP16, activation domain of herpes virus VP16 protein; GR, hormone binding domain of rat GR; NOS, terminator of nopaline synthase

The expression of the construct is induced when transformed *A thaliana* are treated with dexamethasone (DEX), a synthetic glucocorticoid (Yamaguchi et al., 2010). Treatment with DEX results in ectopic secondary wall thickening and the trans-differentiation of non-vascular cells into xylem vessels (Yamaguchi et al., 2010). The SCW of the trans-differentiated cells exhibit a helical pattern which reflects protoxylem-like vessels (Yamaguchi et al., 2011). This is also accompanied by the up-regulation of other genes related to xylem vessel differentiation (Yamaguchi et al., 2010), including genes encoding enzymes involved in cellulose biosynthesis such as CesA4/A7/A8 or IRREGULAR XYLEM3 [IRX3], IRX5, and IRX1 respectively (Pear et al., 1996; Taylor et al., 1999; Yamaguchi et al., 2010) as well lignin biosynthesis (CCoAOMT7 and IRX12)(Raes et al., 2003; Brown et al., 2005) and hemicellulose biosynthesis (IRX8 and IRX10)(Brown et al., 2005). However, in the absence of DEX, GR binds to heat shock proteins to form an inactivated complex in the cytosol (Louvion et al., 1993; Aoyama and Chua, 1997). The receptor is released from this complex when the GR is bound by DEX and is translocated to the nucleus where it functions as a TF (Aoyama and Chua, 1997).

Although many proteomic and transcriptomic studies in trees (Allona et al., 1998; Sterky et al., 2004; Rengel et al., 2009; Sundell et al., 2017) and *in vitro* systems (Demura et al., 2002;

Ohashi-Ito et al., 2010; Zhong et al., 2010; Yamaguchi et al., 2011) have focused on dissecting xylem cell differentiation, primary metabolic changes accompanying SCW differentiation are poorly studied (Ohtani et al., 2016). Transcriptional and metabolomic analyses of VND7 *Arabidopsis* seedlings showed crucial alterations of the shikimate pathway (Trp, Phe, Try, and His), the branched-chain amino acid pathway (Ile, Leu, and Val) and the Asp family pathway (Lys, Met, Ile, and Thr) after induction, during early stages of SCW synthesis (Li et al., 2016b). Transcriptional analysis of VND7 *Arabidopsis* seedlings showed that over 2000 genes showed changes in expression at various time points after induction (Li et al., 2016b). Genes encoding enzymes involved in F6P, PEP and Phe (including the shikimate pathway) synthesis were actively up-regulated during vessel induction (Ohtani et al., 2016). Metabolome analysis showed a transient increase in Phe 12 hours after induction (HAI) accompanied by a transient increase in p-coumaric acid levels, which is a monolignol precursor, 24 HAI (Li et al., 2016b; Ohtani et al., 2016). This was followed by lignin deposition seen 36 HAI in DEX-treated plants (Ohtani et al., 2016).

These results show that the association between xylem vessel differentiation and changes in primary metabolism for monolignol synthesis is evident and that the VND7 post translational induction system is an excellent tool to understanding the molecular mechanisms which underlie xylem differentiation and SCW formation in trees (Yamaguchi et al., 2011). Major advantages of this system include the non-toxicity and absence of negative physiological effects of glucocorticoid treatment on plants, while allowing the precise activation of target genes and its use in tobacco BY-2 cells and poplar trees (Yamaguchi et al., 2011).

A major gap in our knowledge of plastidial biology during secondary growth is the ultrastructural changes in plastids accompanying SCW formation (Pinard and Mizrachi, 2018). This is due to the fact that microscopic analysis in wood is very challenging and extraction of plastids directly from xylem results in variability and is very harsh causing microscopic artifacts. The VND7 induction system has previously been used to perform confocal and transmission electron microscopy (TEM) to study cell wall production machinery in the Golgi apparatus, which is central to hemicellulose (glucuronoxylan) biosynthesis, during SCW formation (Meents et al., 2019). However, as of yet, no study has used the VND induction system to study plastid dynamics or morphology during this transition.

1.6. Lignin in woody biomass

Over the past years, the use of fossil fuels for energy and organic compounds has negatively impacted the climate (Chanoca et al., 2019). This climate crisis urgently requires the transition to a bio-based economy, led by the use of lignocellulosic biomass for the production of fuels, chemicals and bio-materials (Demirbas, 2004; Novaes et al., 2010a; Lauri et al., 2014; Zoghlami and Paës, 2019).

Today, wood provides about 6% of the total primary energy supply worldwide (Sreevani, 2018). Wood consists of secondary xylem which contains essential cells such as tracheary elements (TEs) for water transport, xylary fibers which provide mechanical support as well as xylary parenchyma cells (Myburg and Sederoff, 2001; Plomion et al., 2001; Turner et al., 2007; Smith et al., 2017; Meents et al., 2018). Of these, fiber and TE cells deposit thick SCWs which are predominantly composed of lignin (~30%), cellulose (~45%), and hemicellulose (~25%) (Sjostrom, 1993). These complex biopolymers determine the physical and chemical properties of wood as well as its energy content (Sjostrom, 1993; Mellerowicz and Sundberg, 2008; Campbell et al., 2015).

Lignin is a phenolic heteropolymer of 4-hydroxyphenylpropanoids derived from Phe and differs from cellulose and hemicellulose, which are polysaccharides (Rippert et al., 2009b). Three monolignols, which differ in their aromatic ring substitution patterns can be polymerized into lignin (Whetten and Sederoff, 1995). These monolignols include the mono-methoxylated coniferyl alcohol, the non-methoxylated p-coumaryl alcohol and the dimethoxylated sinapyl alcohol which are transported to the SCW where they undergo oxidation by the activity of laccases and peroxidases to form monolignol radicals namely G- (guaicyl), H- (hydroxyphenyl) and S- (syringyl) units (Freudenberg and Neish, 1968; Tobimatsu and Schuetz, 2019). The monolignol radicals are then polymerized into lignin (Boerjan et al., 2003; Ralph et al., 2004; Barros et al., 2015).

Until recently, it was unknown how monolignols are transported to the apoplastic space across the plasma membrane for lignin polymerization by laccases and peroxidases. A recent study incubated coniferyl alcohol, a monolignol, with liposomes which contained fungal laccases (Perkins et al., 2019). This resulted in the formation of a monolignol gradient, as the polymerization-inducing enzymes used up coniferyl alcohol to polymerize larger phenolics

inside the liposome. From this, they were able to deduce that monolignols use simple diffusion to cross the plasma membrane which is driven by the monolignol gradient (Perkins et al., 2019).

Variation in composition of lignin is seen across taxa and different cell wall layers however, G and S units principally comprise angiosperm lignins while mostly G units with traces of H units are generally seen in gymnosperm lignins (Baucher et al., 1998; Boerjan et al., 2003). This variation in the H/G/S ratios as well as lignin content affects the efficiency of biomass processing and plays a key role in determining biomass recalcitrance (Zeng et al., 2014; McCann and Carpita, 2015; Wang et al., 2018).

1.6.1. Lignin's role in biomass recalcitrance

The cellulose and hemicellulose components of wood are central to pulp, paper, bioethanol production etc. (Vanholme et al., 2013a) while lignin can be used to provide aromatic building blocks for chemicals (Upton and Kasko, 2016; Schutyser et al., 2018; Wang et al., 2019). However, a major obstacle in the use of woody biomass for the production of these value-added products is the resistance of plant cell walls to enzymatic and microbial degradation, which is also known as recalcitrance (Himmel et al., 2007). Hydrophobic networks of lignin form cross-linked complexes with SCW polysaccharides which makes lignin one of the most significant contributors to recalcitrance (Jung and Vogel, 1986; Hatfield et al., 1999; Moxley et al., 2012; Pu et al., 2015; Qin et al., 2015; Wang et al., 2018). Lignin prevents the hydrolysis of biomass through enzymatic reactions in two major ways. It can either act as a physical barrier by forming complexes with carbohydrates and preventing access of enzymes to polysaccharides or inhibit enzymatic activity by binding with them (Zeng et al., 2014; McCann and Carpita, 2015; Li et al., 2016a).

Strategies to improve recalcitrance of lignin includes (i) maximising lignin removal though pre-treatment (Lynd et al., 1999; Li et al., 2010; Ding et al., 2012; Haghighi Mood et al., 2013; Pu et al., 2015) (ii) perturbation of lignin biosynthesis to reduce lignin content (Bonawitz and Chapple, 2010; Simmons et al., 2010; Vanholme et al., 2019) and (iii) engineering/ modifying the structure of lignin (Grabber et al., 2012; Vanholme et al., 2013b; Mottiar et al., 2016). One way to modify plant lignin content is by down-regulating key enzymes involved in lignin biosynthesis such as CCR (Derikvand et al., 2008; Wadenbäck et al., 2008; Van Acker et al., 2014), coumarate 3-hydroxylase (C3H) (Ralph et al., 2006; Ralph et al., 2012), hydroxycinnamoyl

CoA: shikimate hydroxycinnamoyl transferase (HCT) (Wagner et al., 2007), caffeoyl CoA 3-O-methyltransferase (CCoAOMT)(Guo et al., 2001), ferulate 5-hydroxylase (F5H)(Reddy et al., 2005) and caffeic acid 3-O-methyltransferase (COMT)(Guo et al., 2001). In Alfalfa (*Medicago sativa* L.), down regulation of C4H, C3H, and F5H showed changes in lignin composition and content (Reddy et al., 2005). C4H mutants showed reduction in lignin, no changes in composition but displayed increased digestibility (Reddy et al., 2005). In dicots, pulping and digestion was also improved through the down regulation of the CAD gene although no reduction in lignin content was seen (Baucher et al., 1999; Halpin, 2004).

However, reduction of lignin content is often associated with increased susceptibility to pathogens and a growth penalty (Maher et al., 1994; Shadle et al., 2003; Sattler and Funnell-Harris, 2013; Van Acker et al., 2013). An emerging trend is to 'redesign' lignin's chemical structure without drastic alteration of lignin content or function (Mottiar et al., 2016; Ralph et al., 2019). This includes engineering of lignin that is (i) less hydrophobic to increase solubility during delignification processes (Grabber et al., 2012) or (ii) has shorter chains with minimal branching such as in poplar, where the overexpression of F5H increased digestibility through an increase syringyl monomer levels and decreased degree of polymerisation (Huntley et al., 2003; Stewart et al., 2009). Another approach includes the incorporation of phenolics or molecules into lignin in order to reduce recalcitrance (Simmons et al., 2010; Ralph et al., 2019). This has been demonstrated by the incorporation of coniferyl ferulate, which is a methoxylated analog of coniferyl p-coumarate, along with normal monolignols into primary cell walls in maize (Grabber et al., 2008). This allowed the easier solubilization of lignin as the backbone now had newly introduced ester linkages which are more readily cleavable at lower temperature (Grabber et al., 2008; Simmons et al., 2010; Vanholme et al., 2010).

Biomass recalcitrance leads to increased energy requirements and increased cost of bio-refinery operations and is clearly affected by SCW composition and biomass structure (McCann and Carpita, 2015). The valorisation of SCW polymers in the bio-based economy is rooted in understanding the molecular basis of biomass recalcitrance (McCann and Carpita, 2015). This includes identifying existing genotypes with desirable traits, using transgenic approaches, such as CRISPR/Cas9, to modify the expression of SCW-related genes and engineering trees using synthetic biology approaches to redesign labile polymers (McCann and Carpita, 2015; Zhou et

al., 2015; Wang et al., 2018). With the emerging climate crash, economic challenges and need for renewable energy, there is an imminent need to fast-track the use of wood energy in a bio-based economy (Chanoca et al., 2019)

1.7. Conclusion: A developing secondary xylem-specific plastid, the xyloplast

Over the years, anthropogenic activities and the use of fossil fuels have created an imminent need to shift towards a bio-based economy that uses renewable energy (Mansfield et al., 2012; Vanholme et al., 2013a; Schutyser et al., 2018; Wang et al., 2018). Lignin is the most abundant renewable aromatic feedstock with high energy content and zero net CO_2 release when burned, making it an excellent fuel in addition to be used for making carbon fibres, dispersants, phenols, sorbents and surfactants etc. (Qin and Phil, 2009; Smolarski, 2012; Bajpai, 2018). Annually, about 50 million tons of lignin is generated from pulping processes however, only approximately 2% of it is used for industrial applications (Lora and Glasser, 2002; Kai et al., 2015; Cannatelli and Ragauskas, 2016). In order to tailor wood that can be efficiently converted into value-added products and fully utilize lignin, it is critical to dissect the molecular and biochemical mechanisms controlling wood formation (Plomion et al., 2001; Zhang, 2003; Foston and Ragauskas, 2012; Phitsuwan et al., 2013).

Plastids are the exclusive site of the shikimate pathway which produces the key amino acid, Phe, for monolignol and ultimately lignin formation (Boerjan et al., 2003; Maeda and Dudareva, 2012). However, very little is known regarding the flow of carbon through them (Pinard and Mizrachi, 2018). A comprehensive analysis of nuclear and organellar transcriptomes in *Eucalyptus* leaf, immature xylem, and phloem in comparison to other heterotrophic plastids showed that plastid-encoded gene expression in xylem is uniquely regulated to facilitate effective carbon partitioning towards SCW synthesis (Pinard *et al*., in preparation). These data support the notion of a developing secondary xylem-specific plastid, the xyloplast and makes it important to understand their role in carbon partitioning (Pinard and Mizrachi, 2018). The aim of this study is to dissect the ultrastructural changes that accompany the differentiation of chloroplasts into xyloplasts and determine the relationship between plastid morphology and function in the production of Phe for SCW synthesis in the VND7-inducible system in *Arabidopsis*. Time-point

specific analysis of plastid ultrastructure during xylem differentiation will be performed using transmission electron microscopy in VND7-inducible *Arabidopsis* seedlings (Yamaguchi et al., 2011). This study will play a key role in addressing the general gap in our understanding of sink tissue plastids, specifically xyloplasts

1.8. References

Adams, K.L., Qiu, Y.-L., Stoutemyer, M., and Palmer, J.D. (2002). Punctuated evolution of mitochondrial gene content: high and variable rates of mitochondrial gene loss and transfer to the nucleus during angiosperm evolution. PNAS **99,** 9905-9912.

Adams, R.P. (2019). Inheritance of chloroplasts and mitochondria in conifers: a review of paternal, maternal, leakage and facultative inheritance. Phytologia **101,** 134-138.

Ali, S.S., Kornaros, M., Manni, A., Sun, J., El-Shanshoury, A.E.-R.R., Kenawy, E.-R., and Khalil, M.A. (2020). Enhanced anaerobic digestion performance by two artificially constructed microbial consortia capable of woody biomass degradation and chlorophenols detoxification. J. Hazard. Mater. **389,** 122076.

Aliche, E.B., Theeuwen, T.P.J.M., Oortwijn, M., Visser, R.G.F., and van der Linden, C.G. (2020). Carbon partitioning mechanisms in potato under drought stress. Plant Physiol. Biochem. **146,** 211-219.

Allona, I., Quinn, M., Shoop, E., Swope, K., Cyr, S.S., Carlis, J., Riedl, J., Retzel, E., Campbell, M.M., and Sederoff, R. (1998). Analysis of xylem formation in pine by cDNA sequencing. PNAS **95,** 9693-9698.

Aoyama, T., and Chua, N.H. (1997). A glucocorticoid-mediated transcriptional induction system in transgenic plants. PlJ **11,** 605-612.

Archibald, J.M. (2009). The puzzle of plastid evolution. Curr. Biol. **19,** R81-R88.

Austin, J.R., II, Frost, E., Vidi, P.-A., Kessler, F., and Staehelin, L.A. (2006). Plastoglobules are lipoprotein subcompartments of the chloroplast that are permanently coupled to thylakoid membranes and contain biosynthetic enzymes. The Plant Cell **18,** 1693-1703.

Badenhuizen, N. (1963). Formation and distribution of amylose and amylopectin in the starch granule. Nature **197,** 464-467.

Bahaji, A., Li, J., Sánchez-López, Á.M., Baroja-Fernández, E., Muñoz, F.J., Ovecka, M., Almagro, G., Montero, M., Ezquer, I., and Etxeberria, E. (2014). Starch biosynthesis, its regulation and biotechnological approaches to improve crop yields. Biotechnol. Adv. **32,** 87-106.

Bailey, J.L., and Whyborn, A. (1963). The osmiophilic globules of chloroplasts II. Globules of the spinach-beet chloroplast. AcBB **78,** 163-174.

Bajpai, P. (2018). Value-added products from lignin. In Biotechnology for pulp and paper processing. Springer, pp. 561-571.

Barros, J., Serk, H., Granlund, I., and Pesquet, E. (2015). The cell biology of lignification in higher plants. Ann. Bot. **115,** 1053-1074.

Barros, J., Serrani-Yarce, J.C., Chen, F., Baxter, D., Venables, B.J., and Dixon, R.A. (2016). Role of bifunctional ammonia-lyase in grass cell wall biosynthesis. Nature Plants **2,** 1-9.

Baucher, M., Monties, B., Montagu, M.V., and Boerjan, W. (1998). Biosynthesis and genetic engineering of lignin. Crit. Rev. Plant Sci. **17,** 125-197.

Baucher, M., Bernard-Vailhé, M.A., Chabbert, B., Besle, J.-M., Opsomer, C., Van Montagu, M., and Botterman, J. (1999). Down-regulation of cinnamyl alcohol dehydrogenase in transgenic alfalfa (Medicago sativa L.) and the effect on lignin composition and digestibility. Plant Mol. Biol. **39,** 437-447.

Baunsgaard, L., Lütken, H., Mikkelsen, R., Glaring, M.A., Pham, T.T., and Blennow, A. (2005). A novel isoform of glucan, water dikinase phosphorylates pre-phosphorylated α-glucans and is involved in starch degradation in Arabidopsis. PlJ **41,** 595-605.

Berli, F.J., Fanzone, M., Piccoli, P., and Bottini, R. (2011). Solar UV-B and ABA are involved in phenol metabolism of Vitis vinifera L. increasing biosynthesis of berry skin polyphenols. J. Agric. Food Chem. **59,** 4874-4884.

Bhagavan, N.V., and Ha, C.-E. (2011). Chapter 14 - Carbohydrate Metabolism II: Gluconeogenesis, glycogen synthesis and breakdown, and alternative pathways. In Essentials of Medical Biochemistry, N.V. Bhagavan and C.-E. Ha, eds (San Diego: Academic Press), pp. 151-168.

Bhuiyan, N.H., Selvaraj, G., Wei, Y., and King, J. (2009). Role of lignification in plant defense. Plant Signal. Behav. **4,** 158-159.

Bjurhager, I., Olsson, A.-M., Zhang, B., Gerber, L., Kumar, M., Berglund, L.A., Burgert, I., Sundberg, B., and Salmén, L. (2010). Ultrastructure and mechanical properties of Populus wood with reduced lignin content caused by transgenic down-regulation of cinnamate 4-hydroxylase. Biomacromolecules **11,** 2359-2365.

Boerjan, W., Ralph, J., and Baucher, M. (2003). Lignin biosynthesis. Annu. Rev. Plant Biol. **54,** 519-546.

Bonawitz, N.D., and Chapple, C. (2010). The genetics of lignin biosynthesis: connecting genotype to phenotype. Annu. Rev. Genet. **44,** 337-363.

Bouvier, F., and Camara, B. (2007). The role of plastids in ripening fruits. In The Structure and Function of Plastids. Springer, pp. 419-432.

Brillouet, J.-M., Verdeil, J.-L., Odoux, E., Lartaud, M., Grisoni, M., and Conéjéro, G. (2014). Phenol homeostasis is ensured in vanilla fruit by storage under solid form in a new chloroplast-derived organelle, the phenyloplast. JExB **65,** 2427-2435.

Brillouet, J.-M., Romieu, C., Schoefs, B., Solymosi, K., Cheynier, V., Fulcrand, H., Verdeil, J.-L., and Conéjéro, G. (2013). The tannosome is an organelle forming condensed tannins in the chlorophyllous organs of Tracheophyta. Ann. Bot. **112,** 1003-1014.

Brodersen, C.R., Roddy, A.B., Wason, J.W., and McElrone, A.J. (2019). Functional status of xylem through time. Annu. Rev. Plant Biol. **70,** 407-433.

Brown, D.M., Zeef, L.A., Ellis, J., Goodacre, R., and Turner, S.R. (2005). Identification of novel genes in Arabidopsis involved in secondary cell wall formation using expression profiling and reverse genetics. The Plant Cell **17,** 2281-2295.

Brust, H., Orzechowski, S., Fettke, J., and Steup, M. (2013). Starch synthesizing reactions and paths: in vitro and in vivo studies. Journal of applied glycoscience **60,** 3-20.

Büker, M., Schünemann, D., and Borchert, S. (1998). Enzymic properties and capacities of developing tomato (Lycopersicon esculentum L.) fruit plastids. JExB **49,** 681-691.

Campbell, L., Kumar, M., and Turner, S. (2015). Secondary cell walls: biosynthesis and manipulation. JExB **67,** 515-531.

Cannatelli, M.D., and Ragauskas, A.J. (2016). Conversion of lignin into value-added materials and chemicals via laccase-assisted copolymerization. Appl. Microbiol. Biotechnol. **100,** 8685-8691.

Carde, J., Camara, B., and Cheniclet, C. (1988). Absence of ribosomes in Capsicum chromoplasts. Planta **173,** 1-11.

Caspar, T., Huber, S.C., and Somerville, C. (1985). Alterations in growth, photosynthesis, and respiration in a starchless mutant of Arabidopsis thaliana (L.) deficient in chloroplast phosphoglucomutase activity. Plant Physiol. **79,** 11-17.

Caspar, T., Lin, T.-P., Kakefuda, G., Benbow, L., Preiss, J., and Somerville, C. (1991). Mutants of *Arabidopsis* with altered regulation of starch degradation. Plant Physiol. **95,** 1181-1188.

Chandra, R.P., Chu, Q., Hu, J., Zhong, N., Lin, M., Lee, J.-S., and Saddler, J. (2016). The influence of lignin on steam pretreatment and mechanical pulping of poplar to achieve high sugar recovery and ease of enzymatic hydrolysis. Bioresour. Technol. **199,** 135-141.

Chanoca, A., de Vries, L., and Boerjan, W. (2019). Lignin Engineering in Forest Trees. Front. Plant Sci. **10**.

Cho, Y.G., and Kang, K.K. (2020). Functional Analysis of Starch Metabolism in Plants. Plants **9**.

Choi, H., Yi, T., and Ha, S.-H. (2021). Diversity of Plastid Types and Their Interconversions. Front. Plant Sci. **12**.

Cortleven, A., Marg, I., Yamburenko, M.V., Schlicke, H., Hill, K., Grimm, B., Schaller, G.E., and Schmülling, T. (2016). Cytokinin Regulates the Etioplast-Chloroplast Transition through the Two-Component Signaling System and Activation of Chloroplast-Related Genes. Plant Physiol. **172,** 464.

Cuesta-Seijo, J.A., Nielsen, M.M., Ruzanski, C., Krucewicz, K., Beeren, S.R., Rydhal, M.G., Yoshimura, Y., Striebeck, A., Motawia, M.S., and Willats, W.G. (2016). In vitro biochemical characterization of all barley endosperm starch synthases. Front. Plant Sci. **6,** 1265.

de Vries, J., Stanton, A., Archibald, J.M., and Gould, S.B. (2016). Streptophyte Terrestrialization in Light of Plastid Evolution. Trends Plant Sci. **21,** 467-476.

Demirbas, A. (2004). The importance of biomass. EnS **26,** 361-366.

Demura, T., Tashiro, G., Horiguchi, G., Kishimoto, N., Kubo, M., Matsuoka, N., Minami, A., Nagata-Hiwatashi, M., Nakamura, K., and Okamura, Y. (2002). Visualization by comprehensive microarray analysis of gene expression programs during transdifferentiation of mesophyll cells into xylem cells. PNAS **99,** 15794-15799.

Dennis, D., and Miernyk, J. (1982). Compartmentation of nonphotosynthetic carbohydrate metabolism. Annu. Rev. Plant Physiol. **33,** 27-50.

Denyer, K., Barber, L., Burton, C., Hedley, C., and Hylton, C. John-son S, Jones DA, Marshall J, Smith AM, Tatge H, Tomlinson K, Wang TL (1995a) The isolation and characterization of novel low-amylose mutants of Pisum sativum L. Plant, Cell Environ. 18, 1019-1026.

Derikvand, M.M., Sierra, J.B., Ruel, K., Pollet, B., Do, C.-T., Thévenin, J., Buffard, D., Jouanin, L., and Lapierre, C. (2008). Redirection of the phenylpropanoid pathway to feruloyl malate in Arabidopsis mutants deficient for cinnamoyl-CoA reductase 1. Planta **227,** 943-956.

Deruère, J., Römer, S., d'Harlingue, A., Backhaus, R.A., Kuntz, M., and Camara, B. (1994). Fibril assembly and carotenoid overaccumulation in chromoplasts: a model for supramolecular lipoprotein structures. The Plant Cell **6,** 119-133.

Dewick, P.M. (2009). The shikimate pathway: aromatic amino acids and phenylpropanoids. J. Nat. Prod. **137,** 86.

Ding, S.-Y., Liu, Y.-S., Zeng, Y., Himmel, M.E., Baker, J.O., and Bayer, E.A. (2012). How does plant cell wall nanoscale architecture correlate with enzymatic digestibility? Sci **338,** 1055-1060.

Dixon, R.A., and Paiva, N.L. (1995). Stress-induced phenylpropanoid metabolism. The Plant Cell **7,** 1085.

Egea, I., Barsan, C., Bian, W., Purgatto, E., Latché, A., Chervin, C., Bouzayen, M., and Pech, J.-C. (2010). Chromoplast differentiation: current status and perspectives. PCPhy **51,** 1601-1611.

Emes, M., and Neuhaus, H. (1997). Metabolism and transport in non-photosynthetic plastids. JExB **48,** 1995-2005.

Emes, M.J., Bowsher, C.G., Hedley, C., Burrell, M.M., Scrase-Field, E.S.F., and Tetlow, I.J. (2003). Starch synthesis and carbon partitioning in developing endosperm. JExB **54,** 569-575.

Emter, O., Falk, H., and Sitte, P. (1990). Specific carotenoids and proteins as prerequisites for chromoplast tubule formation. Protoplasma **157,** 128-135.

Endo, H., Yamaguchi, M., Tamura, T., Nakano, Y., Nishikubo, N., Yoneda, A., Kato, K., Kubo, M., Kajita, S., and Katayama, Y. (2015). Multiple classes of transcription factors regulate the expression of VASCULAR-RELATED NAC-DOMAIN7, a master switch of xylem vessel differentiation. PCPhy **56,** 242-254.

Flügge, U., Fischer, K., Gross, A., Sebald, W., Lottspeich, F., and Eckerskorn, C. (1989). The triose phosphate-3-phosphoglycerate-phosphate translocator from spinach chloroplasts: nucleotide sequence of a full-length cDNA clone and import of the in vitro synthesized precursor protein into chloroplasts. EMBO **8,** 39-46.

Foston, M., and Ragauskas, A.J. (2012). Biomass Characterization: Recent Progress in Understanding Biomass Recalcitrance. Ind Biotechnol **8,** 191-208.

Fraser, C.M., and Chapple, C. (2011). The phenylpropanoid pathway in Arabidopsis. The *arabidopsis* book **9,** e0152-e0152.

Freudenberg, K., and Neish, A.C. (1968). Constitution and biosynthesis of lignin. Constitution and biosynthesis of lignin.

Fukuda, H., and Komamine, A. (1980). Establishment of an experimental system for the study of tracheary element differentiation from single cells isolated from the mesophyll of *Zinnia elegans*. Plant Physiol. **65,** 57-60.

Fulton, D.C., Stettler, M., Mettler, T., Vaughan, C.K., Li, J., Francisco, P., Gil, M., Reinhold, H., Eicke, S., Messerli, G., Dorken, G., Halliday, K., Smith, A.M., Smith, S.M., and Zeeman, S.C. (2008). β-AMYLASE4, a noncatalytic protein required for starch breakdown acts upstream of three active β-amylases in *Arabidopsis* chloroplasts. The Plant Cell **20,** 1040.

Gámez-Arjona, F.M., Li, J., Raynaud, S., Baroja-Fernández, E., Muñoz, F.J., Ovecka, M., Ragel, P., Bahaji, A., Pozueta-Romero, J., and Mérida, Á. (2011). Enhancing the expression of starch synthase class IV results in increased levels of both transitory and long-term storage starch. Plant Biotechnol. J. **9,** 1049-1060.

Geigenberger, P. (2003). Regulation of sucrose to starch conversion in growing potato tubers. JExB **54,** 457-465.

Geiger, D.R., and Servaites, J.C. (1994). Diurnal regulation of photosynthetic carbon metabolism in C3 Plants. Annu. Rev. Plant Physiol. Plant Mol. Biol. **45,** 235-256.

Ghosh, H.P., and Preiss, J. (1966). Adenosine diphosphate glucose pyrophosphorylase: a regulatory enzyme in the biosynthesis of starch in spinach leaf chloroplasts. J. Biol. Chem. **241,** 4491-4504.

Goren, A., Ashlock, D., and Tetlow, I.J. (2018). Starch formation inside plastids of higher plants. Protoplasma **255,** 1855-1876.

Grabber, J.H., Ress, D., and Ralph, J. (2012). Identifying new lignin bioengineering targets: impact of epicatechin, quercetin glycoside, and gallate derivatives on the lignification and fermentation of maize cell walls. J. Agric. Food Chem. **60,** 5152-5160.

Grabber, J.H., Hatfield, R.D., Lu, F., and Ralph, J. (2008). Coniferyl ferulate incorporation into lignin enhances the alkaline delignification and enzymatic degradation of cell walls. Biomacromolecules **9,** 2510-2516.

Granick, S. (1961). The chloroplasts: inheritance, structure, and function. In The cell (Elsevier), pp. 489-602.

Greenwood, A., Leech, R.M., and Williams, J. (1963). The osmiophilic globules of chloroplasts: I. Osmiophilic globules as a normal component of chloroplasts and their isolation and composition in Vicia faba L. AcBB **78,** 148-162.

Guo, D., Chen, F., Inoue, K., Blount, J.W., and Dixon, R.A. (2001). Downregulation of caffeic acid 3-O-methyltransferase and caffeoyl CoA 3-O-methyltransferase in transgenic alfalfa: impacts on lignin structure and implications for the biosynthesis of G and S lignin. The Plant Cell **13,** 73-88.

Haghighi Mood, S., Hossein Golfeshan, A., Tabatabaei, M., Salehi Jouzani, G., Najafi, G.H., Gholami, M., and Ardjmand, M. (2013). Lignocellulosic biomass to bioethanol, a comprehensive review with a focus on pretreatment. Renewable and Sustainable Energy Reviews **27,** 77-93.

Halpin, C. (2004). Investigating and manipulating lignin biosynthesis in the postgenomic era. Adv. Bot. Res. **41,** 63-106.

Hannah, L.C., and James, M. (2008). The complexities of starch biosynthesis in cereal endosperms. Curr. Opin. Biotechnol. **19,** 160-165.

Hatfield, R., Ralph, J., and Grabber, J. (1999). Cell wall structural foundations: Molecular basis for improving forage digestibilities. Crop Sci. **39,** 27-37.

Hatzfeld, W.-D., and Stitt, M. (1990). A study of the rate of recycling of triose phosphates in heterotrophic Chenopodium rubrum cells, potato tubers, and maize endosperm. Planta **180,** 198-204.

Häusler, R.E., Schlieben, N.H., Schulz, B., and Flügge, U.-I. (1998). Compensation of decreased triose phosphate/phosphate translocator activity by accelerated starch turnover and glucose transport in transgenic tobacco. Planta **204,** 366-376.

He, J., Huang, L.K., and Whitecross, M. (1994). Chloroplast ultrastructure changes in *Pisum sativum* associated with supplementary ultraviolet (UV-B) radiation. Plant, Cell Environ. **17,** 771-775.

Herbert, M., Burkhard, C., and Schnarrenberger, C. (1979). A survey for isoenzymes of glucosephosphate isomerase, phosphoglucomutase, glucose-6-phosphate dehydrogenase and 6-Phosphogluconate dehydrogenase in C 3-, C 4-and crassulacean-acid-metabolism plants, and green algae. Planta **145,** 95-104.

Herrmann, K.M. (1995). The shikimate pathway: early steps in the biosynthesis of aromatic compounds. The Plant Cell **7,** 907.

Herrmann, K.M., and Weaver, L.M. (1999). The shikimate pathway. Annu. Rev. Plant Biol. **50,** 473-503.

Hill, L.M., and Smith, A.M. (1991). Evidence that glucose 6-phosphate is imported as the substrate for starch synthesis by the plastids of developing pea embryos. Planta **185,** 91-96.

Himmel, M.E., Ding, S.-Y., Johnson, D.K., Adney, W.S., Nimlos, M.R., Brady, J.W., and Foust, T.D. (2007). Biomass recalcitrance: engineering plants and enzymes for biofuels production. Sci **315,** 804-807.

Holton, T.A., and Cornish, E.C. (1995). Genetics and biochemistry of anthocyanin biosynthesis. The Plant Cell **7,** 1071.

Horecker, B., and Smyrniotis, P. (1953). The coenzyme function of thiamine pyrophosphate in pentose phosphate metabolism. J. Am. Chem. Soc. **75,** 1009-1010.

Horecker, B.L. (2002). The pentose phosphate pathway. J. Biol. Chem. **277,** 47965-47971.

Huber, S.C., and Hanson, K.R. (1992). Carbon partitioning and growth of a starchless mutant of *Nicotiana sylvestris*. Plant Physiol. **99,** 1449-1454.

Huntley, S.K., Ellis, D., Gilbert, M., Chapple, C., and Mansfield, S.D. (2003). Significant increases in pulping efficiency in C4H-F5H-transformed poplars: improved chemical savings and reduced environmental toxins. J. Agric. Food Chem. **51,** 6178-6183.

Inaba, T., and Schnell, D.J. (2008). Protein trafficking to plastids: one theme, many variations. Biochem. J. **413,** 15-28.

Inaba, T., and Ito-Inaba, Y. (2010). Versatile roles of plastids in plant growth and development. PCPhy **51,** 1847-1853.

Inaba, T., Yazu, F., Ito-Inaba, Y., Kakizaki, T., and Nakayama, K. (2011). Chapter Five - Retrograde signaling pathway from plastid to nucleus. In International Review of Cell and Molecular Biology, K.W. Jeon, ed (Academic Press), pp. 167-204.

Jansen, M.A., Gaba, V., and Greenberg, B.M. (1998). Higher plants and UV-B radiation: balancing damage, repair and acclimation. Trends Plant Sci. **3,** 131-135.

Jarvis, P., and López-Juez, E. (2013). Biogenesis and homeostasis of chloroplasts and other plastids. Nat. Rev. Mol. Cell Biol. **14,** 787-802.

Jung, H., and Vogel, K.P. (1986). Influence of lignin on digestibility of forage cell wall material. J. Anim. Sci. **62,** 1703-1712.

Kahlau, S., and Bock, R. (2008). Plastid transcriptomics and translatomics of tomato fruit development and chloroplast-to-chromoplast differentiation: chromoplast gene expression largely serves the production of a single protein. The Plant Cell **20,** 856-874.

Kai, D., Low, Z.W., Liow, S.S., Abdul Karim, A., Ye, H., Jin, G., Li, K., and Loh, X.J. (2015). Development of lignin supramolecular hydrogels with mechanically responsive and self-healing properties. ACS Sustain. Chem. Eng. **3,** 2160-2169.

Kammerer, B., Fischer, K., Hilpert, B., Schubert, S., Gutensohn, M., Weber, A., and Flügge, U.-I. (1998). Molecular characterization of a carbon transporter in plastids from heterotrophic tissues: the glucose 6-phosphate/phosphate antiporter. The Plant Cell **10,** 105-117.

Keeling, P.J. (2010). The endosymbiotic origin, diversification and fate of plastids. Philosophical Transactions of the Royal Society B: Biological Sciences **365,** 729-748.

Keeling, P.J. (2013). The number, speed, and impact of plastid endosymbioses in eukaryotic evolution. Annu. Rev. Plant Biol. **64,** 583-607.

Keeling, P.L., Wood, J.R., Tyson, R.H., and Bridges, I.G. (1988). Starch biosynthesis in developing wheat grain: evidence against the direct involvement of triose phosphates in the metabolic pathway. Plant Physiol. **87,** 311-319.

Keresztes, Á., and Sárvári, É. (2001). Investigations into the» inverse contrast «of chloroplast thylakoids. Acta Bot. Croat. **60,** 253-265.

Kessler, F., and Schnell, D.J. (2006). The function and diversity of plastid protein import pathways: a multilane GTPase highway into plastids. Traffic **7,** 248-257.

Kikuchi, S., Asakura, Y., Imai, M., Nakahira, Y., Kotani, Y., Hashiguchi, Y., Nakai, Y., Takafuji, K., Bédard, J., and Hirabayashi-Ishioka, Y. (2018). A Ycf2-FtsHi heteromeric AAA-ATPase complex is required for chloroplast protein import. The Plant Cell **30,** 2677-2703.

Kochetov, G.A., and Solovjeva, O.N. (2014). Structure and functioning mechanism of transketolase. Biochim Biophys Acta Proteins Proteom **1844,** 1608-1618.

Kode, V., Mudd, E.A., Iamtham, S., and Day, A. (2005). The tobacco plastid *accD* gene is essential and is required for leaf development. PlJ **44,** 237-244.

Kondo, Y., Fujita, T., Sugiyama, M., and Fukuda, H. (2015). A novel system for xylem cell differentiation in *Arabidopsis thaliana*. Mol Plant **8,** 612-621.

Kondo, Y., Ito, T., Nakagami, H., Hirakawa, Y., Saito, M., Tamaki, T., Shirasu, K., and Fukuda, H. (2014). Plant GSK3 proteins regulate xylem cell differentiation downstream of TDIF-TDR signalling. Nat Commun **5,** 3504.

Kondo, Y., Nurani, A.M., Saito, C., Ichihashi, Y., Saito, M., Yamazaki, K., Mitsuda, N., Ohme-Takagi, M., and Fukuda, H. (2016). Vascular cell induction culture system using *Arabidopsis* leaves (VISUAL) Reveals the Sequential Differentiation of Sieve Element-Like Cells. Plant Cell **28,** 1250-1262.

Kötting, O., Pusch, K., Tiessen, A., Geigenberger, P., Steup, M., and Ritte, G. (2005). Identification of a novel enzyme required for starch metabolism in *Arabidopsis* leaves. The phosphoglucan, water dikinase. Plant Physiol. **137,** 242-252.

Kruger, N.J., and von Schaewen, A. (2003). The oxidative pentose phosphate pathway: structure and organisation. Curr. Opin. Plant Biol. **6,** 236-246.

Kubo, M., Udagawa, M., Nishikubo, N., Horiguchi, G., Yamaguchi, M., Ito, J., Mimura, T., Fukuda, H., and Demura, T. (2005). Transcription switches for protoxylem and metaxylem vessel formation. Genes Dev. **19,** 1855-1860.

Kumar, S., Kumar, R., Pal, A., and Chopra, D.S. (2019). Chapter 16 - Enzymes. In Postharvest Physiology and Biochemistry of Fruits and Vegetables, E.M. Yahia, ed (Woodhead Publishing), pp. 335-358.

Lao, N.T., Schoneveld, O., Mould, R.M., Hibberd, J.M., Gray, J.C., and Kavanagh, T.A. (1999). An *Arabidopsis* gene encoding a chloroplast-targeted β-amylase. PlJ **20,** 519-527.

Larcher, W., Lütz, C., Nagele, M., and Bodner, M. (1988). Photosynthetic functioning and ultrastructure of chloroplasts in stem tissues of Fagus sylvatica. J. Plant Physiol. **132,** 731-737.

Larsson, C.-T., Khoshnoodi, J., Ek, B., Rask, L., and Larsson, H. (1998). Molecular cloning and characterization of starch-branching enzyme II from potato. Plant Mol. Biol. **37,** 505-511.

Larsson, C.-T., Hofvander, P., Khoshnoodi, J., Ek, B., Rask, L., and Larsson, H. (1996). Three isoforms of starch synthase and two isoforms of branching enzyme are present in potato tuber starch. Plant Sci. **117,** 9-16.

Lauri, P., Havlík, P., Kindermann, G., Forsell, N., Böttcher, H., and Obersteiner, M. (2014). Woody biomass energy potential in 2050. Energy Policy **66,** 19-31.

Lee, S.S., Jeong, W.J., Bae, J.M., Bang, J.W., Liu, J.R., and Harn, C.H. (2004). Characterization of the plastid-encoded carboxyltransferase subunit (accD) gene of potato. Mol. Cells (Springer Science & Business Media BV) **17**.

Li, C., Knierim, B., Manisseri, C., Arora, R., Scheller, H.V., Auer, M., Vogel, K.P., Simmons, B.A., and Singh, S. (2010). Comparison of dilute acid and ionic liquid pretreatment of switchgrass: biomass recalcitrance, delignification and enzymatic saccharification. Bioresour. Technol. **101,** 4900-4906.

Li, H.-m., and Chiu, C.-C. (2010). Protein transport into chloroplasts. Annu. Rev. Plant Biol. **61,** 157-180.

Li, M., Pu, Y., and Ragauskas, A.J. (2016a). Current understanding of the correlation of lignin structure with biomass recalcitrance. Front. Chem. **4,** 45.

Li, Z., Omranian, N., Neumetzler, L., Wang, T., Herter, T., Usadel, B., Demura, T., Giavalisco, P., Nikoloski, Z., and Persson, S. (2016b). A transcriptional and metabolic framework for secondary wall formation in Arabidopsis. Plant Physiol. **172,** 1334-1351.

Liebers, M., Grübler, B., Chevalier, F., Lerbs-Mache, S., Merendino, L., Blanvillain, R., and Pfannschmidt, T. (2017). Regulatory shifts in plastid transcription play a key role in morphological conversions of plastids during plant development. Front. Plant Sci. **8**.

Lin, T.-P., Spilatro, S.R., and Preiss, J. (1988). Subcellular localization and characterization of amylases in *Arabidopsis* leaf. Plant Physiol. **86,** 251-259.

Liu, D.D., Chao, W.M., and Turgeon, R. (2012). Transport of sucrose, not hexose, in the phloem. JExB **63,** 4315-4320.

Liu, Q., Luo, L., and Zheng, L. (2018). Lignins: Biosynthesis and biological functions in plants. Int. J. Mol. Sci. **19,** 335.

Liu, Y.-J., Li, B., Feng, Y., and Cui, Q. (2020). Consolidated bio-saccharification: Leading lignocellulose bioconversion into the real world. Biotechnol. Adv. **40,** 107535.

Ljubešić, N. (1977). The formation of chromoplasts in fruits of *Cucúrbita maxima* Duch.'turbaniformis'. Bot. Gaz. **138,** 286-290.

Ljubešić, N. (1979). Chromoplasts in the petals of *Liriodendron tulipifera L. Zeitschrift für* Pflanzenphysiologie **91,** 49-51.

Llorente, B., Torres-Montilla, S., Morelli, L., Florez-Sarasa, I., Matus, J.T., Ezquerro, M., D'Andrea, L., Houhou, F., Majer, E., Picó, B., Cebolla, J., Troncoso, A., Fernie, A.R., Daròs, J.-A., and Rodriguez-Concepcion, M. (2020). Synthetic conversion of leaf chloroplasts into carotenoid-rich plastids reveals mechanistic basis of natural chromoplast development. PNAS **117,** 21796-21803.

Lloyd, J.R., and Kossmann, J. (2015). Transitory and storage starch metabolism: two sides of the same coin? Curr. Opin. Biotechnol. **32,** 143-148.

Lopez-Juez, E., and Pyke, K.A. (2004). Plastids unleashed: their development and their integration in plant development. Int. J. Dev. Biol. **49,** 557-577.

López-Juez, E. (2006). Plastid biogenesis, between light and shadows. JExB **58,** 11-26.

Lora, J.H., and Glasser, W.G. (2002). Recent industrial applications of lignin: a sustainable alternative to nonrenewable materials. J. Polym. Environ. **10,** 39-48.

Louvion, J.-F., Havaux-Copf, B., and Picard, D. (1993). Fusion of GAL4-VP16 to a steroid-binding domain provides a tool for gratuitous induction of galactose-responsive genes in yeast. Gene **131,** 129-134.

Lu, Y., and Sharkey, T.D. (2006). The importance of maltose in transitory starch breakdown. Plant, Cell Environ. **29,** 353-366.

Ludewig, F., Sonnewald, U., Kauder, F., Heineke, D., Geiger, M., Stitt, M., Müller-Röber, B.T., Gillissen, B., Kühn, C., and Frommer, W.B. (1998). The role of transient starch in acclimation to elevated atmospheric CO2. FEBS Lett. **429,** 147-151.

Lynd, L.R., Wyman, C.E., and Gerngross, T.U. (1999). Biocommodity engineering. Biotechnol. Prog. **15,** 777-793.

MacNeill, G.J., Mehrpouyan, S., Minow, M.A.A., Patterson, J.A., Tetlow, I.J., and Emes, M.J. (2017). Starch as a source, starch as a sink: the bifunctional role of starch in carbon allocation. JExB **68,** 4433-4453.

Maeda, H., and Dudareva, N. (2012). The Shikimate pathway and aromatic amino acid biosynthesis in plants. Annu. Rev. Plant Biol. **63,** 73-105.

Maeda, H.A. (2016). Lignin biosynthesis: Tyrosine shortcut in grasses. Nature Plants **2,** 16080.

Maher, E.A., Bate, N.J., Ni, W., Elkind, Y., Dixon, R.A., and Lamb, C.J. (1994). Increased disease susceptibility of transgenic tobacco plants with suppressed levels of preformed phenylpropanoid products. PNAS **91,** 7802-7806.

Mahon, E.L., and Mansfield, S.D. (2019). Tailor-made trees: engineering lignin for ease of processing and tomorrow's bioeconomy. Curr. Opin. Biotechnol. **56,** 147-155.

Mansfield, S.D., Kang, K.-Y., and Chapple, C. (2012). Designed for deconstruction – poplar trees altered in cell wall lignification improve the efficacy of bioethanol production. New Phytol. **194,** 91-101.

Marcelis, L.F.M. (1996). Sink strength as a determinant of dry matter partitioning in the whole plant. JExB **47,** 1281-1291.

Marinos, N.G. (1967). Multifunctional plastids in the meristematic region of potato tuber buds. J. Ultrastruct. Res. **17,** 91-113.

Martin, C., and Smith, A.M. (1995). Starch biosynthesis. The Plant Cell **7,** 971.

Mayes, P.A., and Bender, D.A. (2003). The pentose phosphate pathway and other pathways of hexose metabolism. Harpers illustrated biochemistry. San Francisco (CA): McGraw-Hill Companies, Inc**,** 163-173.

McCann, M.C., and Carpita, N.C. (2015). Biomass recalcitrance: a multi-scale, multi-factor, and conversion-specific property. JExB **66,** 4109-4118.

McFadden, G.I. (2001). Primary and secondary endosymbiosis and the origin of plastids. J. Phycol. **37,** 951-959.

Meents, M.J., Watanabe, Y., and Samuels, A.L. (2018). The cell biology of secondary cell wall biosynthesis. Ann. Bot. **121,** 1107-1125.

Meents, M.J., Motani, S., Mansfield, S.D., and Samuels, A.L. (2019). Organization of xylan production in the golgi during secondary cell wall biosynthesis1 [OPEN]. Plant Physiol. **181,** 527-546.

Mellerowicz, E.J., and Sundberg, B. (2008). Wood cell walls: biosynthesis, developmental dynamics and their implications for wood properties. Curr. Opin. Plant Biol. **11,** 293-300.

Mikkelsen, R., Baunsgaard, L., and Blennow, A. (2004). Functional characterization of alpha-glucan, water dikinase, the starch phosphorylating enzyme. Biochem. J. **377,** 525-532.

Mosier, N., Wyman, C., Dale, B., Elander, R., Lee, Y.Y., Holtzapple, M., and Ladisch, M. (2005). Features of promising technologies for pretreatment of lignocellulosic biomass. Bioresour. Technol. **96,** 673-686.

Mottiar, Y., Vanholme, R., Boerjan, W., Ralph, J., and Mansfield, S.D. (2016). Designer lignins: harnessing the plasticity of lignification. Curr. Opin. Biotechnol. **37,** 190-200.

Moxley, G., Gaspar, A.R., Higgins, D., and Xu, H. (2012). Structural changes of corn stover lignin during acid pretreatment. J. Ind. Microbiol. Biotechnol. **39,** 1289-1299.

Mühlbach, H., and Schnarrenberger, C. (1978). Properties and intracellular distribution of two phosphoglucomutases from spinach leaves. Planta **141,** 65-70.

Murray, K., Rodwell, V., Bender, D., Botham, K.M., Weil, P.A., and Kennelly, P.J. (2009). Harper's illustrated biochemistry. 28. (Citeseer).

Myburg, A.A., and Sederoff, R.R. (2001). Xylem structure and function. e LS.

Myburg, A.A., Hussey, S.G., Wang, J.P., Street, N.R., and Mizrachi, E. (2019). Systems and synthetic biology of forest trees: A bioengineering paradigm for woody biomass feedstocks. Front. Plant Sci. **10**.

Naeem, M., Tetlow, I., and Emes, M. (1997). Starch synthesis in amyloplasts purified from developing potato tubers. PlJ **11,** 1095-1103.

Nakamura, Y., Takeichi, T., Kawaguchi, K., and Yamanouchi, H. (1992). Purification of two forms of starch branching enzyme (Q-enzyme) from developing rice endosperm. Physiol. Plant. **84,** 329-335.

Nakano, Y., Yamaguchi, M., Endo, H., Rejab, N.A., and Ohtani, M. (2015). NAC-MYB-based transcriptional regulation of secondary cell wall biosynthesis in land plants. Front. Plant Sci. **6,** 288.

Neuhaus, H., and Emes, M. (2000). Nonphotosynthetic metabolism in plastids. Annu. Rev. Plant Biol. **51,** 111-140.

Nguyen-Quoc, B., and Foyer, C.H. (2001). A role for 'futile cycles' involving invertase and sucrose synthase in sucrose metabolism of tomato fruit. JExB **52,** 881-889.

Nguyen, T.Y., Cai, C.M., Kumar, R., and Wyman, C.E. (2015). Co-solvent pretreatment reduces costly enzyme requirements for high sugar and ethanol yields from lignocellulosic biomass. ChemSusChem **8,** 1716-1725.

Novaes, E., Kirst, M., Chiang, V., Winter-Sederoff, H., and Sederoff, R. (2010a). Lignin and biomass: a negative correlation for wood formation and lignin content in trees. Plant Physiol. **154,** 555-561.

Novaes, E., Kirst, M., Chiang, V., Winter-Sederoff, H., and Sederoff, R. (2010b). Lignin and Biomass: A Negative Correlation for Wood Formation and Lignin Content in Trees. Plant Physiol. **154,** 555.

Oda, Y., Mimura, T., and Hasezawa, S. (2005). Regulation of secondary cell wall development by cortical microtubules during tracheary element differentiation in Arabidopsis cell suspensions. Plant Physiol. **137,** 1027-1036.

Ohashi-Ito, K., Oda, Y., and Fukuda, H. (2010). Arabidopsis VASCULAR-RELATED NAC-DOMAIN6 directly regulates the genes that govern programmed cell death and secondary wall formation during xylem differentiation. The Plant Cell **22,** 3461-3473.

Ohtani, M., Morisaki, K., Sawada, Y., Sano, R., Uy, A.L.T., Yamamoto, A., Kurata, T., Nakano, Y., Suzuki, S., Matsuda, M., Hasunuma, T., Hirai, M.Y., and Demura, T. (2016). Primary Metabolism during Biosynthesis of Secondary Wall Polymers of Protoxylem Vessel Elements. Plant Physiol. **172,** 1612.

Pear, J.R., Kawagoe, Y., Schreckengost, W.E., Delmer, D.P., and Stalker, D.M. (1996). Higher plants contain homologs of the bacterial celA genes encoding the catalytic subunit of cellulose synthase. PNAS **93,** 12637-12642.

Perkins, M., Smith, R.A., and Samuels, L. (2019). The transport of monomers during lignification in plants: Anything goes but how? Curr. Opin. Biotechnol. **56,** 69-74.

Pesquet, E., Korolev, A.V., Calder, G., and Lloyd, C.W. (2010). The microtubule-associated protein AtMAP70-5 regulates secondary wall patterning in *Arabidopsis* wood cells. Curr. Biol. **20,** 744-749.

Pfister, B., and Zeeman, S.C. (2016). Formation of starch in plant cells. Cell. Mol. Life Sci. **73,** 2781-2807.

Phitsuwan, P., Sakka, K., and Ratanakhanokchai, K. (2013). Improvement of lignocellulosic biomass in planta: A review of feedstocks, biomass recalcitrance, and strategic manipulation of ideal plants designed for ethanol production and processability. Biomass Bioenergy **58,** 390-405.

Pinard, D., and Mizrachi, E. (2018). Unsung and understudied: plastids involved in secondary growth. Curr. Opin. Plant Biol. **42,** 30-36.

Pinard, D., Fierro, A.C., Marchal, K., Myburg, A.A., and Mizrachi, E. (2019). Organellar carbon metabolism is coordinated with distinct developmental phases of secondary xylem. New Phytol. **222,** 1832-1845.

Plomion, C., Leprovost, G., and Stokes, A. (2001). Wood formation in trees. Plant Physiol. **127,** 1513.

Preiss, J., and Sivak, M.N. (2017). Starch synthesis in sinks and sources. In Photoassimilate Distribution in Plants and Crops (Routledge), pp. 63-96.

Pryke, J.A., and ap Rees, T. (1977). The pentose phosphate pathway as a source of NADPH for lignin synthesis. Phytochemistry **16,** 557-560.

Pu, Y., Hu, F., Huang, F., and Ragauskas, A.J. (2015). Lignin structural alterations in thermochemical pretreatments with limited delignification. BioEnergy Research **8,** 992-1003.

Pu, Y., Kosa, M., Kalluri, U.C., Tuskan, G.A., and Ragauskas, A.J. (2011). Challenges of the utilization of wood polymers: how can they be overcome? Appl. Microbiol. Biotechnol. **91,** 1525-1536.

Pu, Y., Hu, F., Huang, F., Davison, B.H., and Ragauskas, A.J. (2013). Assessing the molecular structure basis for biomass recalcitrance during dilute acid and hydrothermal pretreatments. Biotechnol. Biofuels **6,** 15.

Pyke, K. (2007). Plastid biogenesis and differentiation. In Cell and molecular biology of plastids (Springer), pp. 1-28.

Qin, C., and Phil, D. (2009). Lignin as alternative renewable fuel. The Alternative Energy e Magazine **6**.

Qin, L., Li, W.-C., Zhu, J.-Q., Liang, J.-N., Li, B.-Z., and Yuan, Y.-J. (2015). Ethylenediamine pretreatment changes cellulose allomorph and lignin structure of lignocellulose at ambient pressure. Biotechnol. Biofuels **8,** 1-15.

Racker, E., Haba, G.D.L., and Leder, I. (1953). Thiamine pyrophosphate, a coenzyme of transketolase. J. Am. Chem. Soc. **75,** 1010-1011.

Raes, J., Rohde, A., Christensen, J.H., Van de Peer, Y., and Boerjan, W. (2003). Genome-wide characterization of the lignification toolbox in *Arabidopsis*. Plant Physiol. **133,** 1051-1071.

Ralph, J., Lapierre, C., and Boerjan, W. (2019). Lignin structure and its engineering. Curr. Opin. Biotechnol. **56,** 240-249.

Ralph, J., Akiyama, T., Coleman, H.D., and Mansfield, S.D. (2012). Effects on lignin structure of coumarate 3-hydroxylase downregulation in poplar. Bioenergy research **5,** 1009-1019.

Ralph, J., Lundquist, K., Brunow, G., Lu, F., Kim, H., Schatz, P.F., Marita, J.M., Hatfield, R.D., Ralph, S.A., and Christensen, J.H. (2004). Lignins: natural polymers from oxidative coupling of 4-hydroxyphenyl-propanoids. Phytochem. Rev. **3,** 29-60.

Ralph, J., Akiyama, T., Kim, H., Lu, F., Schatz, P.F., Marita, J.M., Ralph, S.A., Reddy, M.S., Chen, F., and Dixon, R.A. (2006). Effects of coumarate 3-hydroxylase down-regulation on lignin structure. J. Biol. Chem. **281,** 8843-8853.

Reddy, M.S., Chen, F., Shadle, G., Jackson, L., Aljoe, H., and Dixon, R.A. (2005). Targeted down-regulation of cytochrome P450 enzymes for forage quality improvement in alfalfa (Medicago sativa L.). PNAS **102,** 16573-16578.

Rengel, D., San Clemente, H., Servant, F., Ladouce, N., Paux, E., Wincker, P., Couloux, A., Sivadon, P., and Grima-Pettenati, J. (2009). A new genomic resource dedicated to wood formation in Eucalyptus. BMC Plant Biol. **9,** 1-14.

Rippert, P., Puyaubert, J., Grisollet, D., Derrier, L., and Matringe, M. (2009a). Tyrosine and phenylalanine are synthesized within the plastids in *Arabidopsis* Plant Physiol. **149,** 1251-1260.

Rippert, P., Puyaubert, J., Grisollet, D., Derrier, L., and Matringe, M. (2009b). Tyrosine and phenylalanine are synthesized within the plastids in *Arabidopsis*. Plant Physiol. **149,** 1251-1260.
Ritte, G., Lloyd, J.R., Eckermann, N., Rottmann, A., Kossmann, J., and Steup, M. (2002). The starch-related R1 protein is an α-glucan, water dikinase. PNAS **99,** 7166-7171.
Ritte, G., Heydenreich, M., Mahlow, S., Haebel, S., Kötting, O., and Steup, M. (2006). Phosphorylation of C6-and C3-positions of glucosyl residues in starch is catalysed by distinct dikinases. FEBS Lett. **580,** 4872-4876.
Roston, R.L., Jouhet, J., Yu, F., and Gao, H. (2018). Editorial: Structure and function of chloroplasts. Front. Plant Sci. **9**.
Rottet, S., Besagni, C., and Kessler, F. (2015). The role of plastoglobules in thylakoid lipid remodeling during plant development. Biochim Biophys Acta Bioenerg **1847,** 889-899.
Ruwe, H., Wang, G., Gusewski, S., and Schmitz-Linneweber, C. (2016). Systematic analysis of plant mitochondrial and chloroplast small RNAs suggests organelle-specific mRNA stabilization mechanisms. NAR **44,** 7406-7417.
Sarafis, V. (1998). Chloroplasts: a structural approach. J. Plant Physiol. **152,** 248-264.
Sattler, S., and Funnell-Harris, D. (2013). Modifying lignin to improve bioenergy feedstocks: strengthening the barrier against pathogens?. Front. Plant Sci. **4**.
Schmid, J., and Amrhein, N. (1999). The shikimate pathway. Plant Amino Acids, Biochemistry and Biotechnology. New York: Marcel Dekker**,** 147-170.
Schnarrenberger, C., Oeser, A., and Tolbert, N. (1973). Two isoenzymes each of glucose-6-phosphate dehydrogenase and 6-phosphogluconate dehydrogenase in spinach leaves. Arch. Biochem. Biophys. **154,** 438-448.
Schulze, W., Stitt, M., Schulze, E.-D., Neuhaus, H.E., and Fichtner, K. (1991). A quantification of the significance of assimilatory starch for growth of *Arabidopsis thaliana* L. Heynh. Plant Physiol. **95,** 890-895.
Schutyser, W., Renders, a.T., Van den Bosch, S., Koelewijn, S.-F., Beckham, G., and Sels, B.F. (2018). Chemicals from lignin: an interplay of lignocellulose fractionation, depolymerisation, and upgrading. ChSRv **47,** 852-908.
Selga, M., and Selga, T. (1998). Interrelated transformation of chloroplast ultrastructure and morphogenesis of plants caused by UV-A radiation. In Photosynthesis: mechanisms and effects (Springer), pp. 2413-2416.
Shadle, G.L., Wesley, S.V., Korth, K.L., Chen, F., Lamb, C., and Dixon, R.A. (2003). Phenylpropanoid compounds and disease resistance in transgenic tobacco with altered expression of L-phenylalanine ammonia-lyase. Phytochemistry **64,** 153-161.
Shanklin, J., DeWitt, N.D., and Flanagan, J.M. (1995). The stroma of higher plant plastids contain ClpP and ClpC, functional homologs of *Escherichia coli* ClpP and ClpA: an archetypal two-component ATP-dependent protease. The Plant Cell **7,** 1713-1722.
Shen, F., Triezenberg, S.J., Hensley, P., Porter, D., and Knutson, J.R. (1996). Transcriptional activation domain of the herpesvirus protein VP16 becomes conformationally constrained upon interaction with basal transcription factors. J. Biol. Chem. **271,** 4827-4837.
Sillero, A., Selivanov, V., and Cascante, M. (2006). Pentose phosphate and Calvin cycles: Similarities and three-dimensional views. Biochemistry and molecular biology education : a bimonthly publication of the International Union of Biochemistry and Molecular Biology **34,** 275-277.
Simkin, A.J., Gaffé, J., Alcaraz, J.-P., Carde, J.-P., Bramley, P.M., Fraser, P.D., and Kuntz, M. (2007). Fibrillin influence on plastid ultrastructure and pigment content in tomato fruit. Phytochemistry **68,** 1545-1556.
Simmons, B.A., Loqué, D., and Ralph, J. (2010). Advances in modifying lignin for enhanced biofuel production. Curr. Opin. Plant Biol. **13,** 312-319.

Sjostrom, E. (1993). Wood chemistry: fundamentals and applications. (Gulf professional publishing).
Smith, A., and Martin, C. (1993). Starch biosynthesis and the potential for its manipulation. In Biosynthesis and manipulation of plant products (Springer), pp. 1-54.
Smith, A.M., and Stitt, M. (2007). Coordination of carbon supply and plant growth. Plant, Cell Environ. **30,** 1126-1149.
Smith, A.M., Denyer, K., and Martin, C. (1997). The synthesis of the starch granule. Annu. Rev. Plant Biol. **48,** 67-87.
Smith, A.M., Zeeman, S.C., and Smith, S.M. (2005). Starch degradation. Annu. Rev. Plant Biol. **56,** 73-98.
Smith, A.M., Zeeman, S.C., Thorneycroft, D., and Smith, S.M. (2003). Starch mobilization in leaves. JExB **54,** 577-583.
Smith, P.J., Wang, H.-T., York, W.S., Peña, M.J., and Urbanowicz, B.R. (2017). Designer biomass for next-generation biorefineries: leveraging recent insights into xylan structure and biosynthesis. Biotechnol. Biofuels **10,** 286.
Smolarski, N. (2012). High-value opportunities for lignin: unlocking its potential. Frost & Sullivan **1,** 1-15.
Solymosi, K., and Keresztes, Á. (2012). Plastid structure, diversification and interconversions II. Land plants. Curr. Chem. Biol. **6,** 187-204.
Sperling, U., Franck, F., van Cleve, B., Frick, G., Apel, K., and Armstrong, G.A. (1998). Etioplast Differentiation in *Arabidopsis*: Both PORA and PORB Restore the Prolamellar Body and Photoactive Protochlorophyllide–F655 to the cop1 Photomorphogenic Mutant. The Plant Cell **10,** 283.
Spurr, A.R., and Harris, W.M. (1968). Ultrastructure of chloroplasts and chromoplasts in *Capsicum annuum* I. Thylakoid membrane changes during fruit ripening. Am. J. Bot. **55,** 1210-1224.
Sreevani, P. (2018). Wood as a renewable source of energy and future fuel. In AIP Conference Proceedings (AIP Publishing LLC), pp. 040007.
Staehelin, L. (1986). Chloroplast structure and supramolecular organization of photosynthetic membranes. In Photosynthesis III (Springer), pp. 1-84.
Stafford, H.A. (1974). The metabolism of aromatic compounds. Annu. Rev. Plant Physiol. **25,** 459-486.
Stein, O., and Granot, D. (2018). Plant Fructokinases: Evolutionary, Developmental, and Metabolic Aspects in Sink Tissues. Frontiers in Plant Science **9**.
Stein, O., and Granot, D. (2019). An Overview of Sucrose Synthases in Plants. Front. Plant Sci. **10**.
Steinmüller, D., and Tevini, M. (1985). Composition and function of plastoglobuli. Planta **163,** 201-207.
Sterky, F., Bhalerao, R.R., Unneberg, P., Segerman, B., Nilsson, P., Brunner, A.M., Charbonnel-Campaa, L., Lindvall, J.J., Tandre, K., and Strauss, S.H. (2004). A Populus EST resource for plant functional genomics. PNAS **101,** 13951-13956.
Stewart, J.J., Akiyama, T., Chapple, C., Ralph, J., and Mansfield, S.D. (2009). The effects on lignin structure of overexpression of ferulate 5-hydroxylase in hybrid poplar1. Plant Physiol. **150,** 621-635.
Stitt, M., and Quick, W.P. (1989). Photosynthetic carbon partitioning: its regulation and possibilities for manipulation. Physiol. Plant. **77,** 633-641.
Stitt, M., and Zeeman, S.C. (2012). Starch turnover: pathways, regulation and role in growth. Curr. Opin. Plant Biol. **15,** 282-292.
Streb, S., Egli, B., Eicke, S., and Zeeman, S.C. (2009). The debate on the pathway of starch synthesis: a closer look at low-starch mutants lacking plastidial phosphoglucomutase supports the chloroplast-localized pathway. Plant Physiol. **151,** 1769-1772.
Sugiura, M., Hirose, T., and Sugita, M. (1998). Evolution and mechanism of translation in chloroplasts. Annu. Rev. Genet. **32,** 437-459.
Sundell, D., Street, N.R., Kumar, M., Mellerowicz, E.J., Kucukoglu, M., Johnsson, C., Kumar, V., Mannapperuma, C., Delhomme, N., and Nilsson, O. (2017). AspWood: high-spatial-resolution

transcriptome profiles reveal uncharacterized modularity of wood formation in Populus tremula. The Plant Cell **29,** 1585-1604.

Takenaka, Y., Watanabe, Y., Schuetz, M., Unda, F., Hill, J.L., Phookaew, P., Yoneda, A., Mansfield, S.D., Samuels, L., and Ohtani, M. (2018). Patterned deposition of xylan and lignin is independent from that of the secondary wall cellulose of *Arabidopsis* xylem vessels. The Plant Cell **30,** 2663-2676.

Tamoi, M., Nagaoka, M., Yabuta, Y., and Shigeoka, S. (2005). Carbon metabolism in the Calvin cycle. Plant Biotechnol. **22,** 355-360.

Tan, T.T., Demura, T., and Ohtani, M. (2019). Creating vessel elements in vitro: Towards a comprehensive understanding of the molecular basis of xylem vessel element differentiation. Plant Biotechnol. J. **36,** 1-6.

Tan, T.T., Endo, H., Sano, R., Kurata, T., Yamaguchi, M., Ohtani, M., and Demura, T. (2018). Transcription factors VND1-VND3 contribute to cotyledon xylem vessel formation. Plant Physiol. **176,** 773-789.

Taylor, N.G., Scheible, W.-R., Cutler, S., Somerville, C.R., and Turner, S.R. (1999). The irregular xylem3 locus of *Arabidopsis* encodes a cellulose synthase required for secondary cell wall synthesis. The Plant Cell **11,** 769-779.

Tetlow, I., Bowsher, C., and Emes, M. (2003). Biochemical properties and enzymic capacities of chromoplasts isolated from wild buttercup (*Ranunculus acris L*.). Plant Sci. **165,** 383-394.

Tevini, M., and Steinmüller, D. (1985). Composition and function of plastoglobuli. Planta **163,** 91-96.

Thomson, W.W., and Whatley, J.M. (1980). Development of nongreen plastids. Annu. Rev. Plant Physiol. **31,** 375-394.

Ting, J.T., Wu, S.S., Ratnayake, C., and Huang, A.H. (1998). Constituents of the tapetosomes and elaioplasts in *Brassica campestris* tapetum and their degradation and retention during microsporogenesis. PlJ **16,** 541-551.

Tobimatsu, Y., and Schuetz, M. (2019). Lignin polymerization: how do plants manage the chemistry so well? Curr. Opin. Biotechnol. **56,** 75-81.

Turner, S., Gallois, P., and Brown, D. (2007). Tracheary element differentiation. Annu. Rev. Plant Biol. **58,** 407-433.

Tzin, V., and Galili, G. (2010a). The biosynthetic pathways for shikimate and aromatic amino acids in *Arabidopsis thaliana*. The Arabidopsis book/American Society of Plant Biologists **8**.

Tzin, V., and Galili, G. (2010b). The biosynthetic pathways for shikimate and aromatic amino acids in *Arabidopsis thaliana*. The arabidopsis book **8,** e0132-e0132.

Upton, B.M., and Kasko, A.M. (2016). Strategies for the conversion of lignin to high-value polymeric materials: review and perspective. Chem. Rev. **116,** 2275-2306.

Valkov, V.T., Scotti, N., Kahlau, S., MacLean, D., Grillo, S., Gray, J.C., Bock, R., and Cardi, T. (2009). Genome-wide analysis of plastid gene expression in potato leaf chloroplasts and tuber amyloplasts: transcriptional and posttranscriptional control. Plant Physiol. **150,** 2030-2044.

Van Acker, R., Vanholme, R., Storme, V., Mortimer, J., Dupree, P., and Boerjan, W. (2013). Perturbation of lignin biosynthesis in *Arabidopsis thaliana* affects secondary cell wall composition and saccharification yield. Biotechnol Bioenergy **6,** 45.

Van Acker, R., Leplé, J.-C., Aerts, D., Storme, V., Goeminne, G., Ivens, B., Légée, F., Lapierre, C., Piens, K., and Van Montagu, M.C. (2014). Improved saccharification and ethanol yield from field-grown transgenic poplar deficient in cinnamoyl-CoA reductase. PNAS **111,** 845-850.

van Steveninck, M.E., and Van Steveninck, R. (1980). Plastids with densely staining thylakoid contents in *Nymphoides indica*. Protoplasma **103,** 343-360.

Vance, C., Kirk, T., and Sherwood, R. (1980). Lignification as a mechanism of disease resistance. Annu. Rev. Phytopathol. **18,** 259-288.

Vanholme, B., Desmet, T., Ronsse, F., Rabaey, K., Van Breusegem, F., De Mey, M., Soetaert, W., and Boerjan, W. (2013a). Towards a carbon-negative sustainable bio-based economy. Front. Plant Sci. **4,** 174.

Vanholme, B., Cesarino, I., Goeminne, G., Kim, H., Marroni, F., Van Acker, R., Vanholme, R., Morreel, K., Ivens, B., and Pinosio, S. (2013b). Breeding with rare defective alleles (BRDA): a natural *P opulus nigra* HCT mutant with modified lignin as a case study. New Phytol. **198,** 765-776.

Vanholme, R., De Meester, B., Ralph, J., and Boerjan, W. (2019). Lignin biosynthesis and its integration into metabolism. Curr. Opin. Biotechnol. **56,** 230-239.

Vanholme, R., Demedts, B., Morreel, K., Ralph, J., and Boerjan, W. (2010). Lignin biosynthesis and structure. Plant Physiol. **153,** 895-905.

Vanholme, R., Storme, V., Vanholme, B., Sundin, L., Christensen, J.H., Goeminne, G., Halpin, C., Rohde, A., Morreel, K., and Boerjan, W. (2012). A systems biology view of responses to lignin biosynthesis perturbations in Arabidopsis. Plant Cell **24,** 3506-3529.

Vidi, P.-A., Kanwischer, M., Baginsky, S., Austin, J.R., Csucs, G., Dörmann, P., Kessler, F., and Bréhélin, C. (2006). Tocopherol Cyclase (VTE1) localization and vitamin E accumulation in chloroplast plastoglobule lipoprotein particles. J. Biol. Chem. **281,** 11225-11234.

Vothknecht, U.C., and Westhoff, P. (2001). Biogenesis and origin of thylakoid membranes. Biochim. Biophys. Acta **1541,** 91-101.

Wadenbäck, J., von Arnold, S., Egertsdotter, U., Walter, M.H., Grima-Pettenati, J., Goffner, D., Gellerstedt, G., Gullion, T., and Clapham, D. (2008). Lignin biosynthesis in transgenic Norway spruce plants harboring an antisense construct for cinnamoyl CoA reductase (CCR). Transgenic Res. **17,** 379-392.

Wagner, A., Ralph, J., Akiyama, T., Flint, H., Phillips, L., Torr, K., Nanayakkara, B., and Te Kiri, L. (2007). Modifying lignin in conifers: the role of HCT during tracheary element formation in *Pinus radiata*. Proc. Natl. Acad. Sci. USA **104,** 11856-11861.

Wang, H., Pu, Y., Ragauskas, A., and Yang, B. (2019). From lignin to valuable products–strategies, challenges, and prospects. Bioresour. Technol. **271,** 449-461.

Wang, J.P., Matthews, M.L., Williams, C.M., Shi, R., Yang, C., Tunlaya-Anukit, S., Chen, H.-C., Li, Q., Liu, J., and Lin, C.-Y. (2018). Improving wood properties for wood utilization through multi-omics integration in lignin biosynthesis. Nat. Commun. **9,** 1-16.

Whatley, J.M. (1977). Variations in the basic pathway of chloroplast development. New Phytol. **78,** 407-420.

Whetten, R., and Sederoff, R. (1995). Lignin biosynthesis. The Plant Cell **7,** 1001.

Whistler, R.L., and Daniel, J.R. (2000). Starch. Kirk-othmer encyclopedia of chemical technology.

Wischmann, B., Nielsen, T.H., and Møller, B.L. (1999). In vitro biosynthesis of phosphorylated starch in intact potato amyloplasts. Plant Physiol. **119,** 455-462.

Wise, R.R., and Hoober, J.K. (2007). The structure and function of plastids. (Springer Science & Business Media).

Woodrow, I.E., and Berry, J.A. (1988). Enzymatic regulation of photosynthetic CO2, fixation in C3 plants. Annu. Rev. Plant Physiol. Plant Mol. Biol. **39,** 533-594.

Wrischer, M., and Devide, Z. (2002). Chromoplasts--the last stages in plastid development. Int. J. Dev. Biol. **35,** 251-258.

Wu, S.S., Moreau, R.A., Whitaker, B.D., and Huang, A.H. (1999). Steryl esters in the elaioplasts of the tapetum in developing *Brassica* anthers and their recovery on the pollen surface. Lipids **34,** 517-523.

Yamaguchi, M., Kubo, M., Fukuda, H., and Demura, T. (2008). VASCULAR-RELATED NAC-DOMAIN7 is involved in the differentiation of all types of xylem vessels in *Arabidopsis* roots and shoots. PlJ **55,** 652-664.

Yamaguchi, M., Mitsuda, N., Ohtani, M., Ohme-Takagi, M., Kato, K., and Demura, T. (2011). VASCULAR-RELATED NAC-DOMAIN 7 directly regulates the expression of a broad range of genes for xylem vessel formation. PlJ **66,** 579-590.

Yamaguchi, M., Goué, N., Igarashi, H., Ohtani, M., Nakano, Y., Mortimer, J.C., Nishikubo, N., Kubo, M., Katayama, Y., and Kakegawa, K. (2010). VASCULAR-RELATED NAC-DOMAIN6 and VASCULAR-RELATED NAC-DOMAIN7 effectively induce transdifferentiation into xylem vessel elements under control of an induction system. Plant Physiol. **153,** 906-914.

Yoo, C.G., Meng, X., Pu, Y., and Ragauskas, A.J. (2020). The critical role of lignin in lignocellulosic biomass conversion and recent pretreatment strategies: A comprehensive review. Bioresour. Technol. **301,** 122784.

Ytterberg, A.J., Peltier, J.-B., and van Wijk, K.J. (2006). Protein profiling of plastoglobules in chloroplasts and chromoplasts. A Surprising Site for Differential Accumulation of Metabolic Enzymes. Plant Physiol. **140,** 984-997.

Yu, T.-S., Kofler, H., Häusler, R.E., Hille, D., Flügge, U.-I., Zeeman, S.C., Smith, A.M., Kossmann, J., Lloyd, J., and Ritte, G. (2001). The Arabidopsis sex1 mutant is defective in the R1 protein, a general regulator of starch degradation in plants, and not in the chloroplast hexose transporter. The Plant Cell **13,** 1907-1918.

Zechmann, B. (2019). Ultrastructure of plastids serves as reliable abiotic and biotic stress marker. PLoS One **14**.

Zeeman, S.C., and Rees, T.A. (1999). Changes in carbohydrate metabolism and assimilate export in starch-excess mutants of Arabidopsis. Plant, Cell Environ. **22,** 1445-1453.

Zeeman, S.C., Kossmann, J., and Smith, A.M. (2010). Starch: its metabolism, evolution, and biotechnological modification in plants. Annu. Rev. Plant Biol. **61,** 209-234.

Zeeman, S.C., Northrop, F., Smith, A.M., and Rees, T.a. (1998). A starch-accumulating mutant of Arabidopsis thaliana deficient in a chloroplastic starch-hydrolysing enzyme. PlJ **15,** 357-365.

Zeeman, S.C., Delatte, T., Messerli, G., Umhang, M., Stettler, M., Mettler, T., Streb, S., Reinhold, H., and Kötting, O. (2007). Starch breakdown: recent discoveries suggest distinct pathways and novel mechanisms. Funct. Plant Biol. **34,** 465-473.

Zeng, Y., Zhao, S., Yang, S., and Ding, S.-Y. (2014). Lignin plays a negative role in the biochemical process for producing lignocellulosic biofuels. Curr. Opin. Biotechnol. **27,** 38-45.

Zhang, J., Ruf, S., Hasse, C., Childs, L., Scharff, L.B., and Bock, R. (2012). Identification of cis-elements conferring high levels of gene expression in non-green plastids. PlJ **72,** 115-128.

Zhang, S. (2003). Wood quality attributes and their impacts on wood utilization. In XII World Forestry Congress, Quebec City, Canada.

Zhong, R., and Ye, Z.-H. (2014). Secondary Cell Walls: Biosynthesis, Patterned Deposition and Transcriptional Regulation. PCPhy **56,** 195-214.

Zhong, R., Lee, C., and Ye, Z.-H. (2010). Global analysis of direct targets of secondary wall NAC master switches in Arabidopsis. Mol Plant **3,** 1087-1103.

Zhou, X., Jacobs, T.B., Xue, L.J., Harding, S.A., and Tsai, C.J. (2015). Exploiting SNP s for biallelic CRISPR mutations in the outcrossing woody perennial Populus reveals 4-coumarate: CoA ligase specificity and redundancy. New Phytol. **208,** 298-301.

Zimmermann, M.H. (2013). Xylem structure and the ascent of sap. (Springer Science & Business Media).

Zoghlami, A., and Paës, G. (2019). Lignocellulosic biomass: understanding recalcitrance and predicting hydrolysis. Front. Chem. **7**.

Chapter 2

The ultrastructure and role of plastids in carbon partitioning during xylogenesis in VND7-inducible *Arabidopsis*

Medha Sood, Desré S. Pinard, Vida Van Staden, Victoria Maloney and Eshchar Mizrachi*

Department of Biochemistry, Genetics and Microbiology, Forestry and Agricultural Biotechnology Institute (FABI), University of Pretoria, Private Bag X20, Pretoria, 0028

*Corresponding author email: eshchar.mizrachi@fabi.up.ac.za.

This chapter has been prepared and formatted as a draft research manuscript for submission to Plant Cell. E.M. is the lead investigator and conceived of the study, provided scientific input, helped to draft and edited the chapter manuscript. M.S. performed all lab experiments, microscopy, and data analysis, generated the figures and drafted the chapter. D.P. provided insight into the interpretation of the results, designed the NExylo application used to perform data analysis and edited the manuscript. VM and VVS assisted with interpretation of microscopy data and provided critical revisions to the manuscript.

2.1. Summary

Lignin is a fundamental component of the secondary cell wall and comprises 30% of woody cell wall biomass. Plastids play a key role in the secondary growth of vascular plants as they are the exclusive sites of the pentose phosphate and the shikimate pathways, which are involved in the synthesis of aromatic amino acids needed for lignin biosynthesis. However, very little is known about plastid biology, ontogeny and ultrastructure in developing secondary xylem tissues.

Using a glucocorticoid-mediated posttranslational induction system of VND7 in *Arabidopsis*, where various cell types trans-differentiate into xylem vessel elements, we performed transmission electron microscopy (TEM) to study the changes in plastid morphology at different time points following induction of secondary cell wall (SCW) deposition in *Arabidopsis* leaves. We also analyzed published transcriptomic and metabolic data for the induced VND7 *Arabidopsis* seedlings to contextualize these morphological changes to construct a coherent integrated view of plastid biology during SCW formation.

Ultrastructural analysis of plastids revealed changes in plastid shape, size and membrane structure during the transition from chloroplast to a xyloplast. We now have new insight into xyloplast differentiation which is accompanied by the formation of a poorly studied, intermediate plastid type, namely an amoeboid plastid. The amoeboid stage transitions into a distinct plastid derivative that we identified as the xyloplast, which lacks an internal membrane system, contains dark electron dense material and has a diffuse outer membrane. Analysis of transcriptional and metabolic data showed that carbon partitioning to aromatic amino acids (AAAs) coincides with notable plastid morphological changes. By integrating detailed plastid ultrastructural changes and transcriptional and metabolic data during SCW formation in the VND7 system, we infer novel plastid structure-functional relationship in xyloplasts which adds to our understanding of the spatial and temporal regulation of SCW biosynthesis.

2.2. Introduction

An endosymbiotic event, where a photosynthetic prokaryote was engulfed by an ancestral eukaryotic cell, first led to the development of plastids (McFadden, 2001; Marin et al., 2005; Choi et al., 2021). Following this, endosymbiotic gene transfer (EGT) allowed the transfer of key metabolic pathways from the cyanobacterial progenitor to the eukaryotic host (Martin et al., 2002; Timmis et al., 2004). Alongside plant terrestrialization and evolution of vascular, seed and flowering plants, plastids evolved to perform specialized functions in different cells and tissues e.g. perform specialized functions in different cells and tissues as functionally (and indeed morphologically) distinct plastid types (Archibald, 2009; Keeling, 2010; de Vries et al., 2016; Choi et al., 2021). These specialized plastids evolved to vary in number, shape, size and genome copy number based on their metabolic function (Liere and Börner, 2013; Hanson and Sattarzadeh, 2014; Beltrán et al., 2018; Choi et al., 2021).

Plastids show great plasticity and diversity in structure which significantly contributes to their specific function (Thomson and Whatley, 1980; Rudowska et al., 2012; Solymosi et al., 2018). Plastid morphological traits are also often used to define specialized plastids types (Thomson and Whatley, 1980; Solymosi et al., 2018). The most studied plastid type is the chloroplast found in photosynthetic tissues, the structure and function of which has been well studied (Rudowska et al., 2012). These lens shaped organelles consist of an outer and inner membrane which regulate protein transport and the thylakoid membrane which harbours light-harvesting complexes (Dilley and Rothstein, 1967; Sarafis, 1998; Chuartzman et al., 2008). The thylakoid membranes are tightly stacked to form the grana, which increases stability and surface area for light capture (Burgess, 1985; Mustárdy et al., 2008). In some chloroplasts, the inner membrane extends to form the peripheral reticulum which contains many vesicles that also increase surface area for cross-membrane transport and may even act as shuttles for transport between the thylakoids and inter-membrane space (Gracen et al., 1972; Huang and van Steveninck, 1990; Wise, 2007; Szczepanik and Sowiński, 2014).

Chloroplasts have the ability to convert into different plastids types usually through light switching, hormonal treatments or *in vitro* induction systems (Buschmann et al., 1978; López-Juez, 2007; Larkin and Ruckle, 2008; Larkin, 2014; Liu et al., 2017). For example, phytoene production (the first step in carotenoid synthesis) synthetically induces chloroplast-to-

chromoplast differentiation in leaves (Llorente et al., 2020a). The differentiation is accompanied by the replacement of photosynthetic thylakoids and grana with tightly arranged, lipid-containing membrane stacks that are electron dense and the proliferation of plastoglobules (PG) (Llorente et al., 2020a). The discovery of phenyloplasts in vanilla fruit (Brillouet et al., 2014) as well as the tannosome (Brillouet et al., 2013) shows that plastid structure can be uniquely adapted for secondary metabolite production (Solymosi et al., 2018). Small vesicles containing condensed tannins, called tannosomes, form from the pearling of thylakoid membranes. These tannosomes bud off into the cytoplasm in tannosome shuttles, where they enter the vacuole and are deposited (Brillouet et al., 2013). Similarly, during the ripening of vanilla fruit, chloroplasts differentiate into phenol-glycosides accumulating phenyloplasts when their thylakoid membranes form large loculi filled with osmiophilic material (Brillouet et al., 2014).

In developing secondary xylem tissue of vascular plants, plastids play a central role in providing the precursors needed for phenolic biopolymer synthesis during plant secondary growth through the plastid-localized shikimate pathway (Rippert et al., 2009b; Pinard and Mizrachi, 2018; Pinard et al., 2019). Nuclear-encoded genes whose proteins are involved in organellar carbon metabolism are transcriptionally co-regulated with SCW biopolymer biosynthesis and deposition (Pinard et al., 2019). A recent study of mRNA-seq data of plastid-encoded genes in *Eucalyptus grandis* mature leaf, phloem and immature xylem, showed that non-photosynthetic genes are uniquely up-regulated in xylem and phloem, even when compared to other heterotrophic tissues (Pinard *et al.* in preparation). This suggests that there is distinct regulation of plastid-encoded genes in xylem to facilitate carbon partitioning towards secondary cell wall biosynthesis, and provides evidence arguing for the existence of a xylem-specific plastid, the xyloplast (Pinard and Mizrachi, 2018).

Ultrastructural analysis of plastids in developing secondary xylem is crucial to gain insight into how xyloplasts might be morphologically distinct from other non-green plastids, and how their structure may reflect their function during xylogenesis (Pinard and Mizrachi, 2018). However, the diverse cell types found in wood i.e. xylem fibers, vessels and parenchyma cells and the complexity with which xylem vessels are embedded in the plant body make it difficult to extract plastids from secondary xylem cells (Zimmermann, 2013; Brodersen et al., 2019; Tan et al., 2019). Expression of VND7 promotes the up-regulation of SCW- and programmed cell death

(PCD)-related genes and results in the trans-differentiation of various cells into metaxylem-like vessels in *Arabidopsis* (Yamaguchi et al., 2008; Zhong et al., 2010; Yamaguchi et al., 2011; Li et al., 2016). The VND7 posttranslational induction system (Yamaguchi et al., 2008; Yamaguchi et al., 2010; Yamaguchi et al., 2011; Tan et al., 2018) allows greater control of sampling critical stages of xylem development. This is due to all cells being induced at the same time as opposed to normal xylem sampling, which contains cells at multiple stages of development which can confound the results. This system has also empowered high resolution studies of SCW synthesis (Farquharson, 2018; Watanabe, 2018; Watanabe et al., 2018; Meents et al., 2019) including transcriptomic (Li et al., 2016; Tong et al., 2021), proteomic (Derbyshire et al., 2015; Noguchi et al., 2018) and metabolomics studies (Li et al., 2016; Ohtani et al., 2016; Ohtani and Demura, 2019). The VND7 system has also been previously used to study the organization of xylan production in the golgi during SCW differentiation (Meents et al., 2019) and would also in theory allow organellar ultrastructural studies to dissect the transition from chloroplasts to xyloplasts.

In this study we utilised the VND7 induction system in *Arabidopsis* to (i) confirm that the VND7 induction system can be a suitable model system to study plastid biology during SCW formation, (ii) investigate organellar morphology under varying time intervals post-induction, and (iii) re-analyze existing transcriptomic and metabolomic data (Li et al., 2016) in light of any ultrastructural changes, to construct a model of plastid structure-function dynamics during xylogenesis. We hypothesized that given the existing molecular support for a unique plastid type (and preliminary microscopy from native *Eucalyptus grandis* trees) – we would observe morphological changes roughly corresponding to the metabolic changes occurring during SCW deposition. For the first time, we were able to use the VND7 system to study plastid morphology and development in induced xylem and provide novel insights into the structural changes that accompany xyloplast differentiation for mass phenylalanine (Phe) production. We describe the xyloplast, a morphologically distinct plastid type found in xylem vessels between 19 and 20 hours after VND7 induction. Analysis of existing expression data in context of the morphological changes seen support the hypothesis that after polysaccharide synthesis, Phe synthesis occurs rapidly and is likely made available to the monolignol biosynthetic pathway through the degradation of plastids, likely as a result of PCD signaling. Knowledge of organellar role in carbon partitioning provides novel insight into understanding the spatial and temporal

regulation of cell wall biosynthesis and provides opportunities for the biotechnological manipulation of plastids to engineer woody biomass in trees in the future.

2.3. Materials and Methods

2.3.1. Plant growth, DEX treatment and VND induction

Arabidopsis thaliana VASCULAR-RELATED NAC-DOMAIN7-inducible line VND7-VP16-GR plants were used (Yamaguchi et al., 2010) which were kindly provided by Misato Ohtani (The University of Tokyo). For bulking, all seeds were kept at 4°C for at least 3 days prior to sowing and then germinated on jiffies. The plants were grown under long day conditions (~16 hours light; 8 hours dark) at 20-22°C. Plants were watered every second day and were fertilised weekly with 2.5g/l of Multifeed Classic 19:8:16 N:P:K. The seeds were harvested after 6 weeks and used for induction experiments.

For the induction experiments, wild type and VND7-VP16-GR seeds were surface sterilized by treatment with 70% ethanol for 5 min, followed by treatment with 0.1% Triton (Sigma) in a 10% bleach solution and subsequently washed 5 times in sterile distilled water. Sterile seeds were then plated on germination media (1× Murashige-Skoog (MS), 1% Sucrose, 0.05% MES, 0.8% agar at pH 5.7). The plates were placed vertically in a growth chamber at 21° C in 24 hours of light and allowed to grow for 7 days. To activate VND7-VP16-GR, whole *Arabidopsis* seedlings were removed from the plates under sterile conditions and soaked in water containing 10 µM (dissolved in DMSO and water) (DEX; Sigma). In order to track the VND7 induction of protoxylem tracheary elements, samples were stored in the dark and removed from the DEX solution and collected at 8, 12, 18, 24, 36 and 48 hours after induction (HAI) for microscopy analysis. These chosen time points and dark conditions allowed direct comparisons to be made with published transcriptome and metabolome data.

2.3.2. Light microscopy

Seven-day old induced *Arabidopsis* leaves were fixed in a solution of 2.5% glutaraldehyde/2.5% formaldehyde in 0.075M sodium phosphate buffer, for a minimum of two hours at room temperature. The leaves were then washed with 0.15M sodium phosphate buffer three times for 15 minutes and dehydrated through a graded ethanol series (30%, 50%, 70%, 90% and 3x100%)

for 15 minutes each. Resin infiltration was performed by adding increasing concentrations of LR White resin in 100% ethanol at room temperature for 1 hour each. 100% LR White was added to the specimens and left at 4°C, overnight. Two more 100% resin exchanges were done followed by the embedding of leaves in gelatine embedding capsules, which were left for 36 to 48 hours in a 60°C oven. Semi-thin (1µm) sections were made with a Reichert Ultracut E microtome and stained with 1% toluidine blue in 1% sodium borate buffer, for 2 min. The semi-thin sections were then imaged with a Zeiss Axio Imager.M2.

2.3.3. Transmission electron microscopy

VND7-induced, VND7-uninduced and WT leaves were prepared for transmission electron microscopy. Samples were fixed and postfixed in the same mixture used for light microscopy. The leaves were positioned vertically and embedded in LR white gelatin capsules. A Reichert Ultracut E microtome was used to obtain ultrathin (100 nm) horizontal leaf sections which were then collected on copper grids, which were then stained in 1% aqueous uranyl acetate for 3 min and Reynold's lead citrate (Reynolds, 1963) for 3 min. The samples were imaged using the FEGTEM: Jeol 2100 transmission electron microscope. Two independent induction experiments were performed and microscopy was performed on leaf cross-sections obtained from individual seedlings (three biological replicates) for each induction experiment at every time point. The two induction experiments will hereon be referred to as trial one and trial two.

2.3.4. VND7 transcriptional and metabolic analysis

Published transcriptomic and metabolomics data (Li et al., 2016) was analysed using a custom designed R application called NExylo (Pinard et.al, in preparation). The NExylo application allows the custom visualisation of gene expression.

2.4. Results

2.4.1. VND7 induction results in secondary cell wall deposition and changes in plastid ultrastructure

To confirm that VND7 induction was successful and led to SCW deposition, we initially performed TEM of leaf cross-sections induced under conditions previously reported (Li et al., 2016). Treatment of 7-day old *A. thaliana* seedlings with DEX for 24 hours successfully resulted in the deposition of SCW in the leaf mesophyll cells between the primary cell wall and the plasma membrane. No SCW deposition was seen in WT seedlings (Figure 1A and B). The first signs of SCW deposition were seen at 24 hours after induction (HAI) (Figure 1C and D) as well as at 36 HAI (Figure 1E and F). By 48 HAI, further cell wall thickening was routinely observed (Figure 1G and H). This confirmed that the expression of VND7 successfully leads to formation of protoxylem.

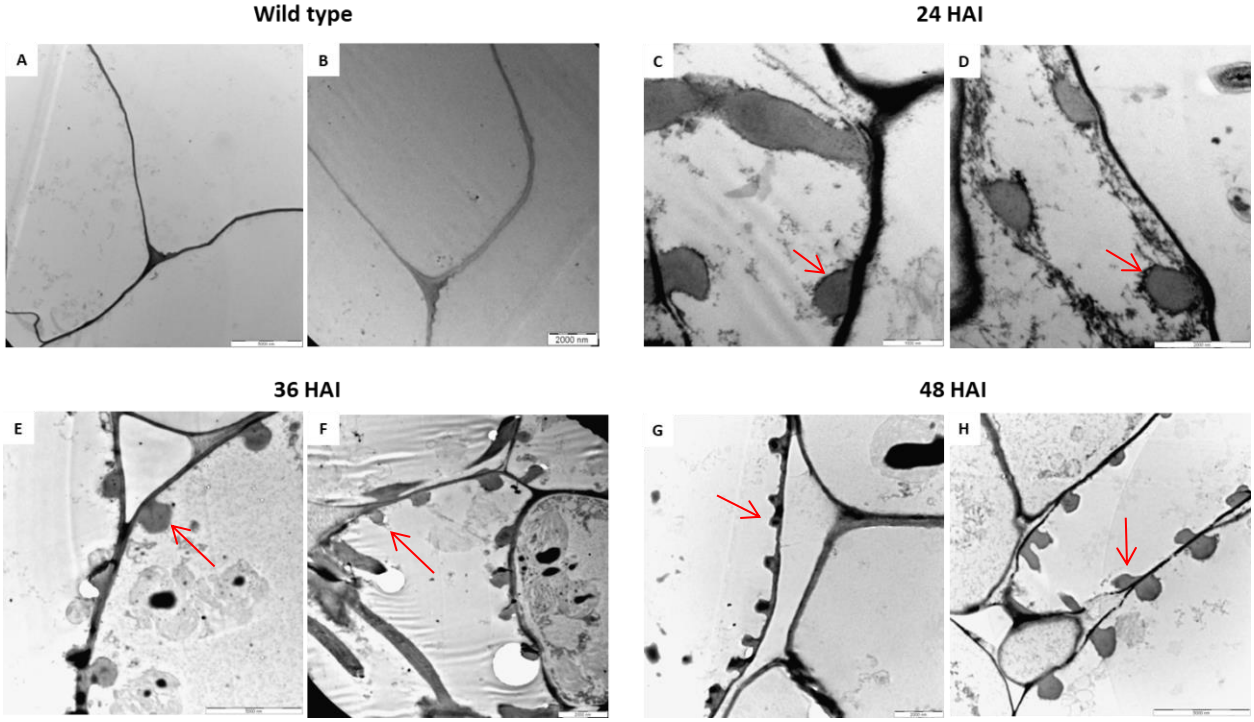

Figure 1 Secondary cell wall deposition in VND7 *Arabidopsis thaliana* leaves. Transmission electron microscope images of VND7 *A. thaliana* leaf cross sections showing normal primary cell walls in WT leaves (A&B) and deposition of SCW at 24 HAI (C&D), 36 HAI (E&F) and 48 HAI (G&H). Red arrows indicate SCW thickening. Images of SCW deposition and changes in morphology have been taken from 2 independent technical replicates. Scale bars - A – 5000nm, B; D; F; G – 2000nm, C – 1000nm, E; H – 5000nm

In order to study organellar morphology during xylem vessel differentiation, we subsequently imaged plastids in induced seedlings at 8, 12, 24, 36 and 48 HAI compared to controls. Light microscopy images performed at 8, 12, 18, 24 and 36 HAI revealed leaf sections containing chloroplasts stained blue using toluidine blue however, due to low magnification; it was difficult to study morphological changes (See Supporting Information Figure S1-7). TEM was then performed to study the fine-scale morphological changes. Normal chloroplasts were seen in both WT *A. thaliana* leaves (Figure 2A-C) and in leaves from 7-day old un-induced VND7 *A. thaliana* seedlings (Figure 2D-F).

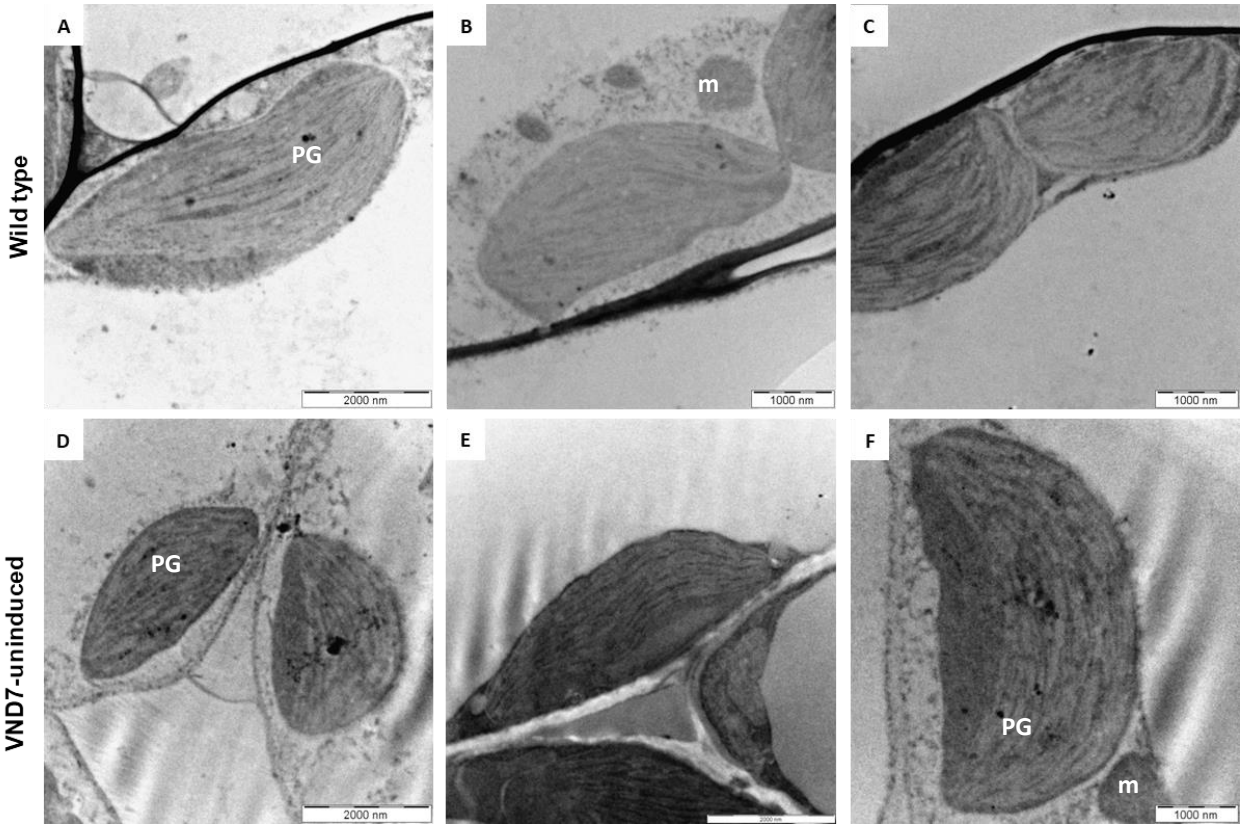

Figure 2 Normal chloroplast structure seen in WT and un-induced *A. thaliana* leaves. Transmission electron microscope images of intact plastids in wild type (A-C) and un-induced VND7 *A. thaliana* leaf cross sections (D-E). PG – plastoglobules; m – mitochondria Scale bars – A; D; E– 2000nm, B; C; F – 1000nm

The chloroplasts showed a typical globular/lens shape and were approximately 5µm long and 2.5µm in width. A well-developed thylakoid membrane system was also seen in the stroma with granal stacks. No starch granules were seen in either WT or un-induced seedlings. This could be due to the fact that the seedlings were stored under dark conditions during induction. Low numbers of PG were present and intact inner and outer membranes of the chloroplast envelope

were seen. Mitochondria were also frequently present and found adjacent to the chloroplasts, e.g. Figure 2D and F.

In DEX-induced VND7 seedlings a number of morphological changes were apparent. The initial changes in ultrastructure at 8 HAI (Figure 3A-C) included the swelling of chloroplasts, and conversion of the conventional disc shape to a horseshoe shape. Compared to WT (Figure 2A-C), dilations of the thylakoid membrane and granal stacks were seen. Changes in the thylakoid membrane system may have also resulted in the proliferation of what we deduce to be vesicles at 8 HAI (Figure 3A).

At 12 HAI, there was an increase in vesicle number and size compared to 8 HAI and the thylakoid membranes appeared more tightly arranged. No starch granules were present. The most notable change was seen in plastid morphology which was significantly different from the conventional disc-shaped chloroplast and had transitioned into a unique amoeboid shape. Invaginations of the plastid membranes resulted in parts of the surrounding cytoplasm (marked with an asterisk) being engulfed into the plastid (Figure 3D-F). No organelles were seen being engulfed along with the cytoplasm however mitochondria were frequently found in close proximity of the plastids (Figure 3D). Some plastids appeared to engulf two portions of cytoplasm, simultaneously (Figure 3E). There was also an increase in the accumulation of PG at 12 HAI (Figure 3D-F) compared to 8 HAI (Figure 3A-C).

At 18 HAI (Figure 4A-C), the vesicles were still visible and no starch granules were seen. The amoeboid plastid shape was no longer observed, as the engulfed portion of the cytoplasm appeared isolated from the surrounding cytoplasm. This was possibly the result of fusion of the opposing plastidial membranes, as has been previously described using 3D reconstruction (Parra-Vega et al., 2015). The engulfed cytoplasm will be referred to as the interplastidial space (IP). The IP appeared to have the same electron density as the surrounding cytoplasm (Figure 4A-C). Even at 18 HAI, the thylakoid membranes were disorganized but still visible.

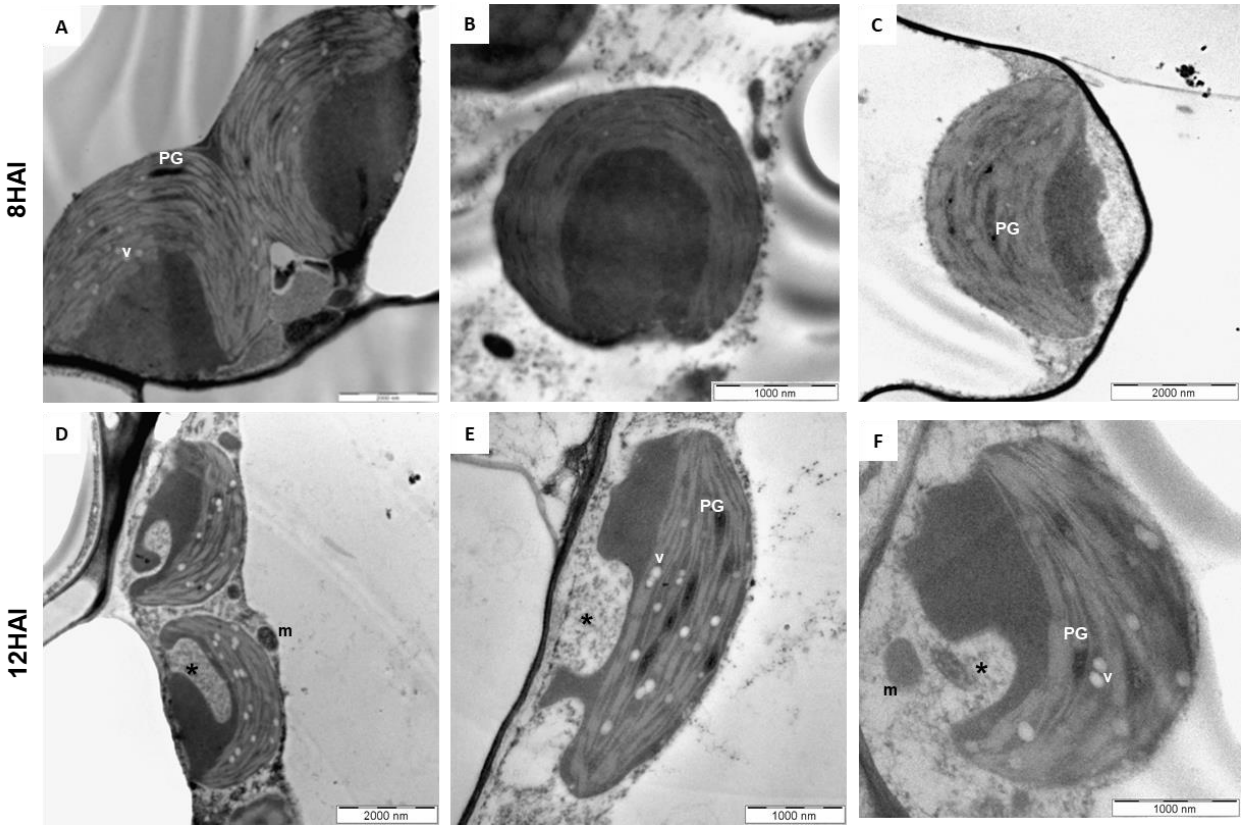

Figure 3 Transition of disc-shaped chloroplasts into unique amoeboid shapes in induced VND7 *A. thaliana* leaves at 8 and 12 HAI. Transmission electron microscope images of VND7 *A. thaliana* leaf cross sections showing changes in plastid ultrastructure at 8 HAI (A-C) and 12 HAI (D-F). m- mitochondria; v- vesicles; PG- plastoglobules; engulfed cytoplasm indicated by asterisk. Scale bars – A; C; D – 2000 nm, B; E; F – 1000 nm

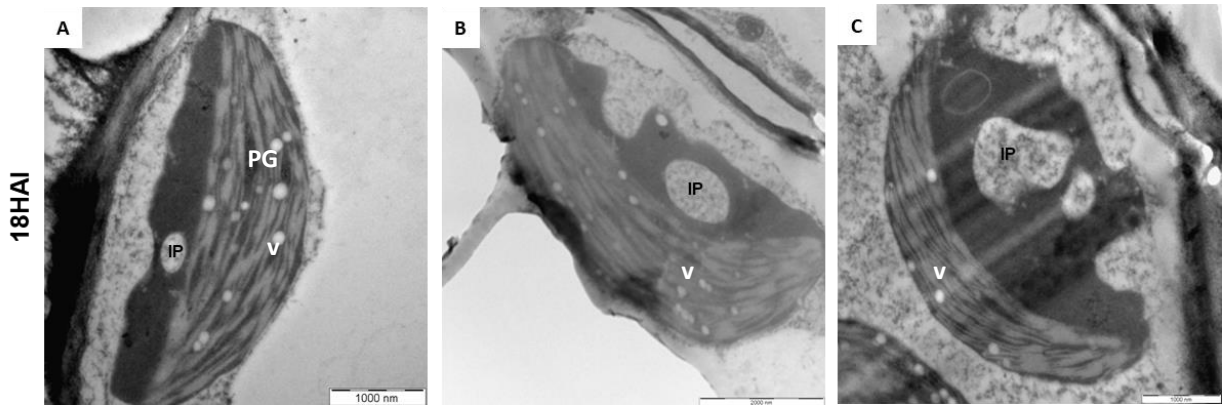

Figure 4 Cytoplasmic engulfment and transition into a unique plastid type in induced VND7 *A. thaliana* leaves at 18 HAI. Transmission electron microscope images of VND7 *A. thaliana* leaf cross sections showing changes in plastid ultrastructure at 18 HAI. PG – plastoglobules; v – vesicles; IP – interplastidial space. Scale bars – A; C – 1000nm, B – 2000nm

From 24 HAI to 48 HAI, when the first signs of SCW deposition were seen (Figure 1) there was further significant degradation of plastids accompanied by swelling and distortion of the inner thylakoid membranes (Figure 5). No starch granules or PG were visible inside the plastid at these time points and the degraded plastids were also surrounded by electron dense spots (indicated by

black arrows). By 48 HAI, the inner plastidial membrane system had completely dissolved, the plastids were surrounded by what appeared to be released plastidial contents and cell death was observed (Figure 5). See Supporting Information Figure S8-11 for supplementary TEM images from the first induction experiment showing changes in plastid ultrastructure from 8 HAI-24 HAI.

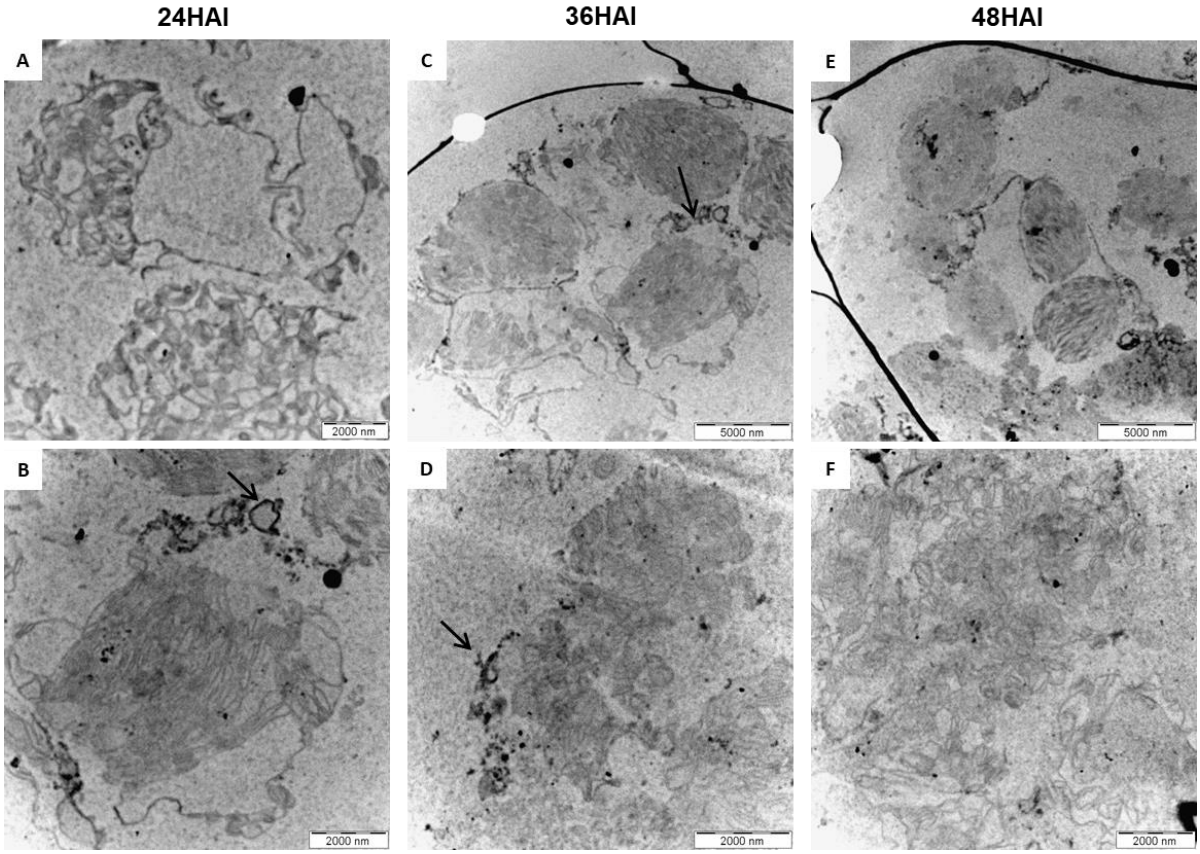

Figure 5 Plastids swell and subsequently degrade at 24, 36 and 48HAI. Transmission electron microscope images of VND7 *A. thaliana* leaf cross sections showing changes in plastid ultrastructure at 24HAI (A&B); 36 HAI (C&D) and 48 HAI (E&F). Arrows indicate released plastidial contents. Scale bars – A; B; D; F – 2000nm, C; E – 5000nm

From these TEM images, we were able to study plastid morphology in this system for the first time. In summary, the initial microscopic study of changes resulting from VND7 induction from 8 to 48 HAI allowed detection of the presence of amoeboid plastids and chloroplast conversion taking place. Major ultrastructural changes were observed between 18 HAI to 24 HAI, this is likely the result of the up-regulation of programmed cell death genes. This highlighted the need for a finer scale analysis of plastid ultrastructure between these time points. As a result, we set up new induction experiments to specifically sample finer time points covering this gap.

2.4.2. Finer scale TEM analysis revealed a morphologically unique plastid, the xyloplast

Time point-based analysis of changes in plastid ultrastructure during VND7 induction revealed the common plastid transitioning intermediate, the amoeboid plastid. However, more insight was required into major plastidial change occurring between 18-24 HAI. Given the gap in our knowledge of plastid morphology between 18 HAI and 24 HAI, we performed a finer scale analysis of VND7 induction by looking at changes in organellar ultrastructure at 19, 19.5, 20, 20.5, 21, 22, 22,5 and 23 HAI. The time points from the previous induction experiment (8; 12; 18; 24; 36 and 48 HAI) were also successfully repeated and showed plastid morphology similar to the results from the first induction experiment (See Supporting Information Figures S12-14; S23-25).

At 19 HAI, unique plastid morphology was seen following previous cytoplasmic engulfment (Figure 6A-C, Supporting Information Figure S15). There was a transition from the lens-shape chloroplast into a round plastid type around approximately 2-2.5 μm in diameter. The plastid lacked an inner membrane system and starch granules but was still surrounded by a double membrane indicative of the endosymbiotic event which gave rise to plastids. An electron dense centre (white asterisk) which could possibly be indicative of phenolic accumulation was seen. We describe this unique plastid type observed at 19 HAI as the xyloplast.

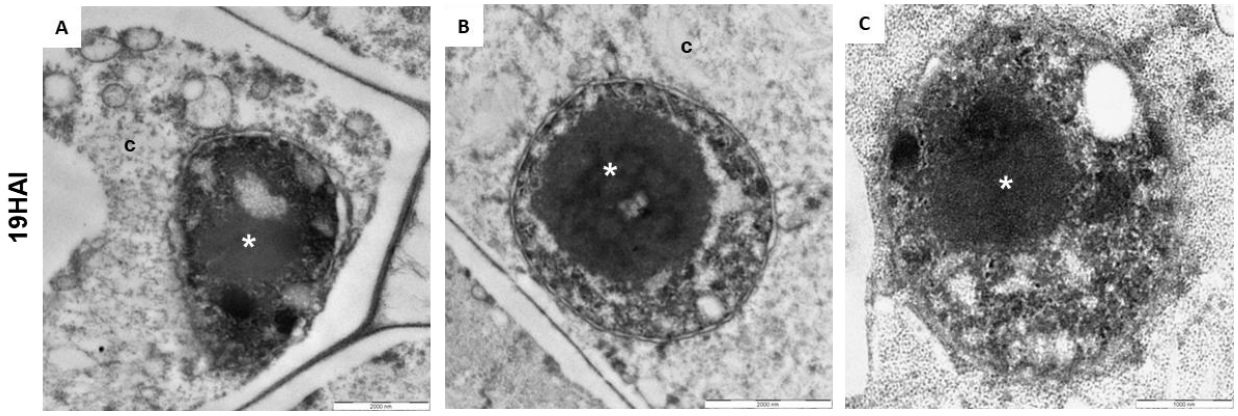

Figure 6 A unique plastid type, the xyloplast, is seen at 19HAI. Transmission electron microscope images of VND7 *A. thaliana* leaf cross sections showing changes in xyloplast ultrastructure at 19 HAI. c-cytoplasm; asterisk shows electron dense centre. Scale bars – A; B – 2000nm and C – 1000nm

At 19.5HAI (Figure 7A-C, Supporting Information Figure S16), the xyloplast could still be seen; however the centre of the xyloplast appeared less electron dense and amorphous electron dense

material was seen accumulating around the circumference. The outer membrane of the plastid appeared to be diffuse and could indicate secretion of plastidial phenolic contents into the surrounding cytoplasm (indicated by arrow in Figure 7C). Interestingly, this morphology was similar to those observed in plastids previously extracted from *Eucalyptus grandis* xylem scrapings (Pinard et al., in revision, supporting information Figure S26). Similar to the plastids we observed, the plastids extracted from *E. grandis* also showed a diffuse outer membrane. However, plastids extracted from *E. grandis* contained starch granules, which were not seen in our study at any time points or in the wild type. This could be due to the fact that in nature xyloplasts may differentiate from amyloplast precursors (Pinard & Mizrachi, 2018), whereas in our induction experiments chloroplasts (which were already lacking starch granules) are the precursors to the xyloplasts observed.

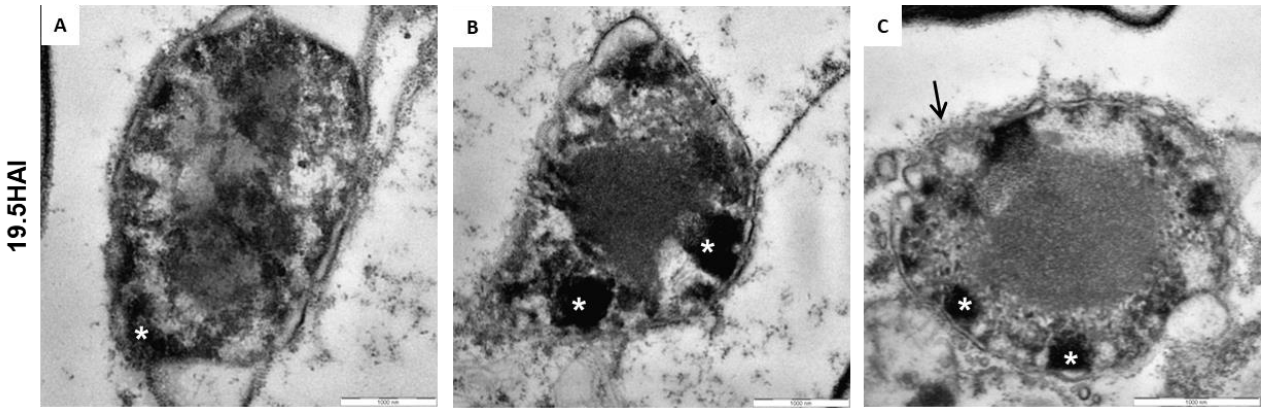

Figure 7 The xyloplast shows a diffuse outer membrane at 19.5HAI. Transmission electron microscope images of VND7 *A. thaliana* leaf cross sections showing changes in plastid ultrastructure at 19.5 HAI (A-C). Asterisk indicates electron dense material; arrow indicates diffuse outer membrane. Scale bars – 1000nm

By 20 HAI, the plastids had become swollen and started to degrade (Figure 8A). Electron dense material was no longer visible and starch granules were still absent. Similar plastid morphology was seen from 20.5 to 23 HAI where the plastids appeared disorganized surrounded by electron dense material (Figure 8B-F; Supporting Information Figure S17-22). Although chloroplasts were sometimes seen in cells after induction (Figure 8B), most plastids formed part of a synchronous process which included xyloplast formation and subsequent plastid degradation.

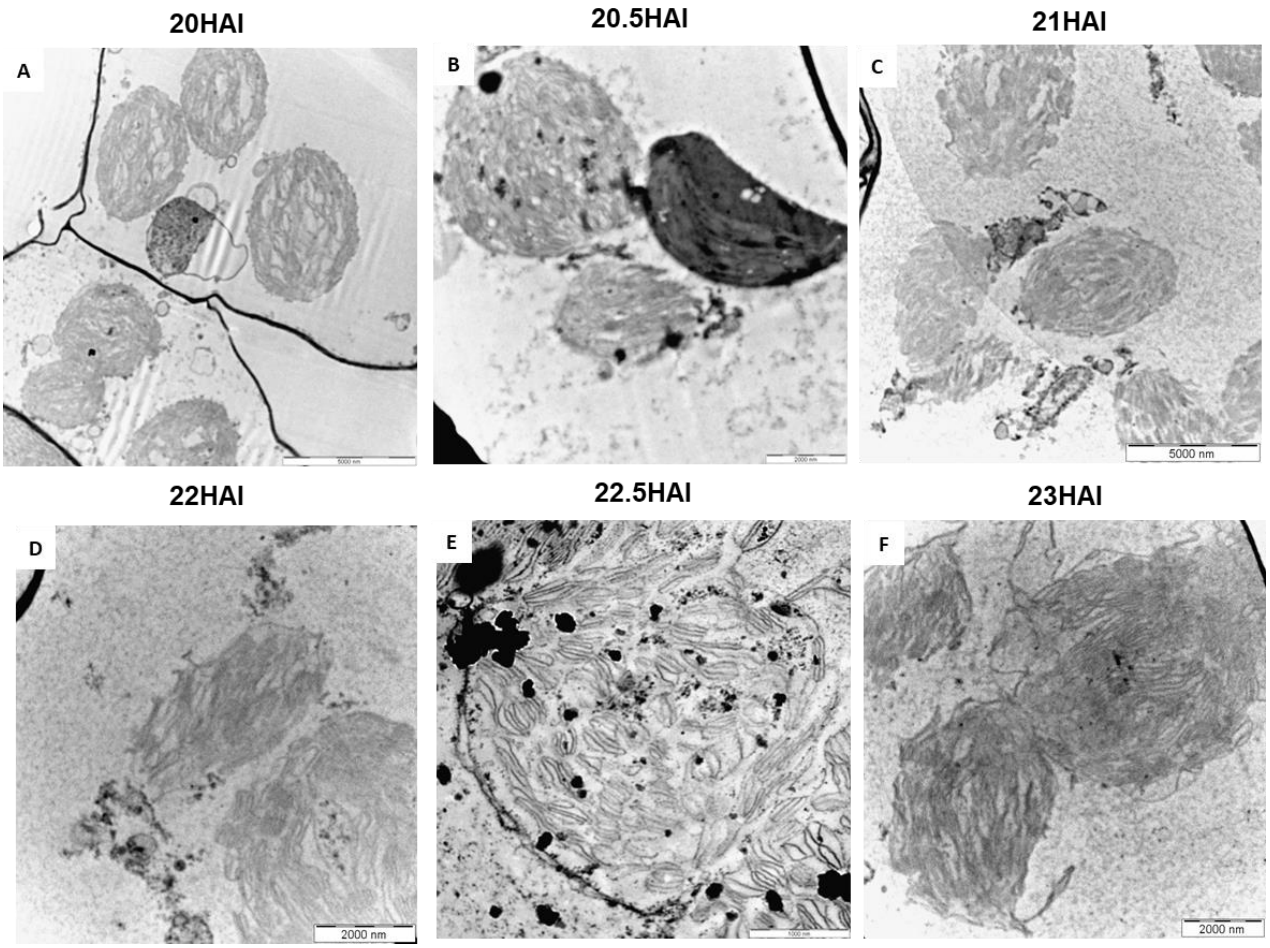

Figure 8 Xyloplasts swell and begin to degrade after 20HAI. Transmission electron microscope images of VND7 *A. thaliana* leaf cross sections showing changes in xyloplast ultrastructure at (A) 20HAI; (B) 20.5HAI; (C) 21HAI; (D) 22HAI; (E) 22.5HAI and (F) 23 HAI. Scale bars –A; C – 5000nm, B; D; F – 2000nm, E – 1000nm

In summary, from the fine scale ultrastructural TEM analysis, we identified four key points in the conversion from chloroplast to xyloplast. These represent (i) native chloroplasts seen prior to induction, (ii) cytoplasmic engulfment occurring from 8-18 HAI to form an amoeboid plastid as a precursor to (iii) the xyloplast with a unique diffuse outer membrane and electron dense contents indicative of phenolics followed by (iv) plastid degradation at 20 HAI followed by cell death (Figure 9).

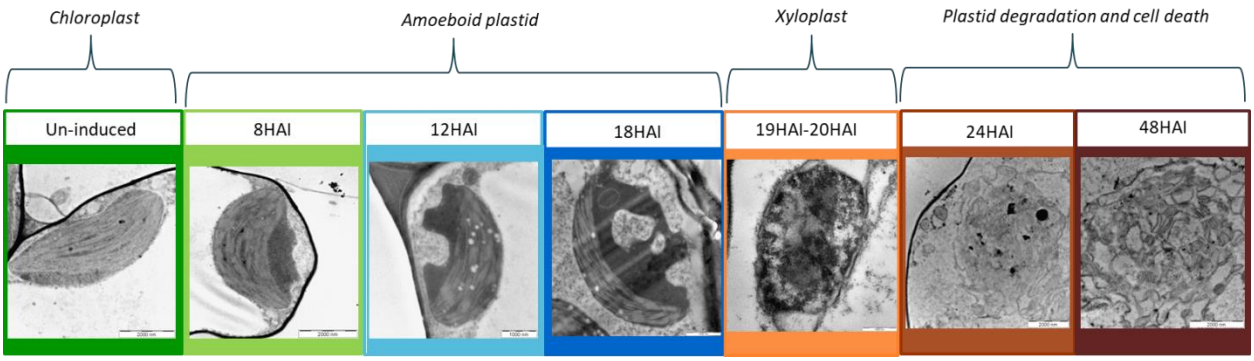

Figure 9 Key steps in the chloroplast to xyloplast conversion in VND7-inducible *A. thaliana* leaves. Native chloroplasts (dark green) engulf surrounding cytoplasm to form an amoeboid plastid (light green to dark blue) followed by the formation of the xyloplast (orange) and cell death (brown).

2.4.3. Plastid structure is related to function in carbon partitioning during SCW formation

In this study, we obtained novel TEM images of plastid structural changes occurring during xylem differentiation, as detailed in the preceding section. This was done using the VND7 system under the same cellular and induction conditions described in previous studies (Li et al., 2016). This allowed us to now investigate the relationship between plastid ultrastructure during xylem differentiation and its function, using published gene expression data, available for certain induced and un-induced time points in the VND7 system (Li et al., 2016). We specifically interrogated groups of genes that would be indicative of biological processes that should accompany the cellular and metabolic transition accompanying SCW formation.

As the chloroplasts transitioned into amoeboid plastids, we analysed the changes in expression of photosynthetic genes. Compared to the control, transcripts of genes involved in photosynthesis were significantly down regulated immediately upon induction of the SCW-related genes (Figure 10A). Morphologically this corresponds to our observations that the chloroplasts lost their internal thylakoid membrane structure and grana, which are sites of light-harvesting complexes and photosynthesis, and started transitioning into the amoeboid plastid from 8 HAI (Figure 3A-C, Figure 9).

Upon induction, there was a rapid increase in the expression of SCW-related genes (Figure 10B). In *Arabidopsis,* several known secondary wall NAC master switches (SWNs) can be found that act as master regulators of SCW biosynthesis including VND1–VND7, SND1, NST1 and NST2 (Zhong et al., 2019). As expected, induction first led to the activation of VND7 expression, which was followed by the sequential activation of general SCW TF-encoding genes such as SND2, MYB85, MYB20, MYB42, MYB83, MYB58 and KNOTTED *ARABIDOPSIS*

*THALIANA*7 (KNAT7) (Figure 10B). Compared to the other general SCW TFs, the expression of MYB63, which is a known lignin-specific regulator (Zhou et al., 2009), was only activated 24 HAI, potentially indicating that at least some genes involved in lignin synthesis are transcribed after the xyloplast has burst (Figure 10B).

After transitioning from primary cell wall synthesis, SCW synthesis and deposition occurs in a series of events starting with the production of polysaccharides i.e. xylan and cellulose (Meents et al., 2018). Xylan (Figure 10C) and cellulose (Figure 10D) synthesis genes were mostly up regulated from 6-12 HAI, and remained expressed throughout. Polysaccharide synthesis is followed by SCW maturation, in which lignification precedes and co-occurs with programmed cell death (Smith et al., 2013; Meents et al., 2018). Upon induction, lignin synthesis and deposition transcripts were up-regulated from 9 HAI, however the complete monolignol biosynthesis pathway (including genes coding for enzymes in early steps of this pathway such as 4CL and C4H) could only be observed from 24 HAI and onwards (Figure 10E). Along with MYB63 expression (Figure 10B), this indicates that monolignol biosynthesis most likely begins to a large extent around or after 24 HAI.

The shikimate pathway plays an important role in lignin synthesis as it is responsible for the shunting of carbon into Phe biosynthesis, which is a precursor for monolignols (Figure 10F). We observed that the shikimate pathway genes are expressed as early as 6 HAI, although Phe synthesis possibly only occurs between 12-24 HAI, as the arogenate dehydratase (ADT) genes, which catalyse the final conversion of arogenate to Phe, are expressed highly between 12-24 HAI (Figure 10F). An important precursor for the shikimate pathway is erythrose-4-phosphate (E4P), which is synthesized by the pentose phosphate pathway (PPP). However, the central PPP genes - TK and TAL - which play a role in the interconversion of sugars to produce E4P did not appear to be transcriptionally co-regulated with SCW synthesis like the other abovementioned pathways, nor was their expression coupled to metabolic functions (Figure 10G). This is mainly because the PPP genes did not show differential regulation in their expression between induced and un-induced samples. However, it is still possible that other regulatory mechanisms such as protein post-translational modification or metabolic regulation could play a role in the PPP regulation for E4P synthesis and carbon partitioning.

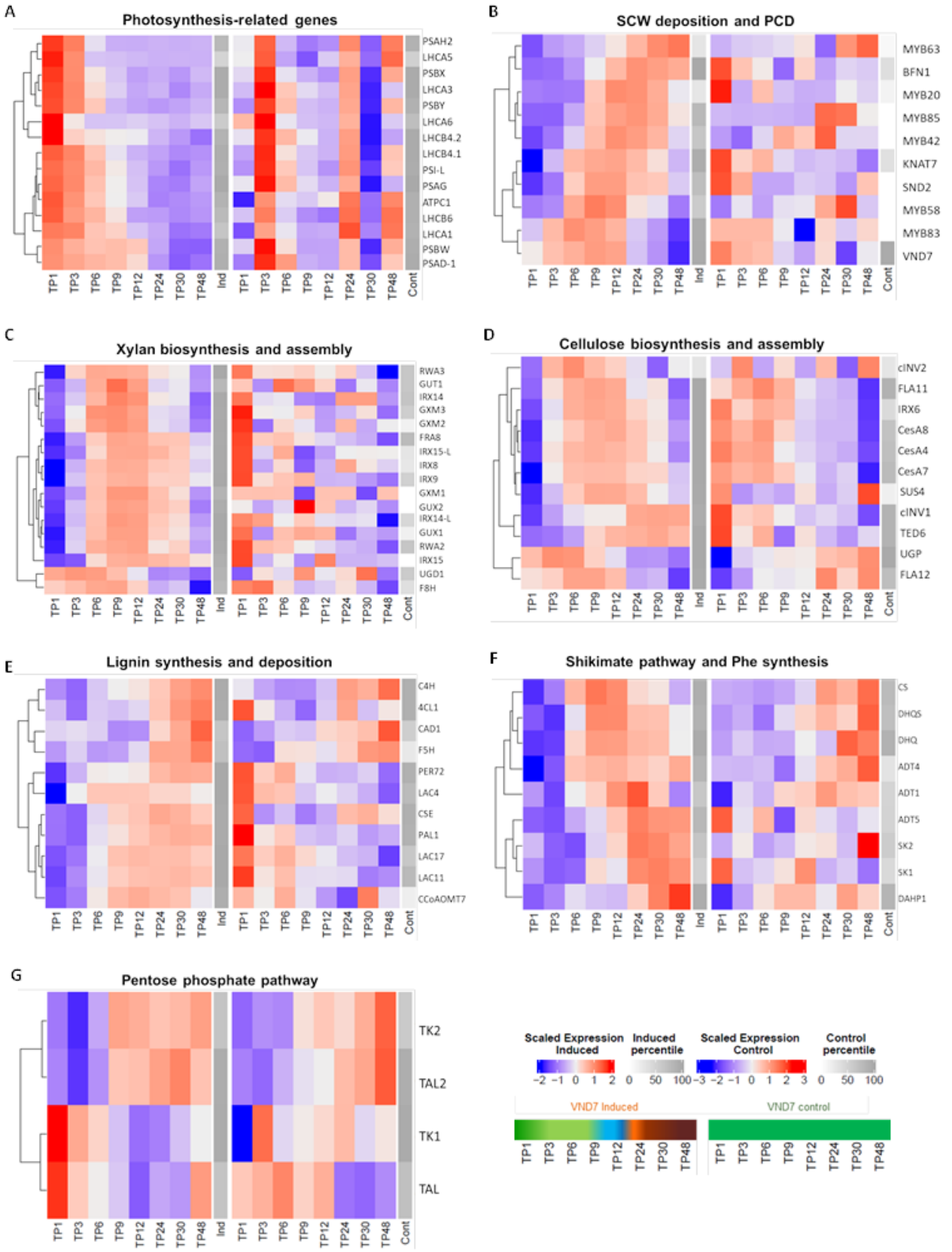

Figure 10 Changes in transcript abundance of genes associated with SCW formation in VND7 seedlings Transcript profiles of selected (A) photosynthesis-related genes, (B) genes involved in patterned deposition of secondary walls, (C) xylan, (D) cellulose and (E) lignin biosynthesis and (F) shikimate and (G) pentose phosphate pathway-related genes at 1, 3, 6, 9, 12, 24, 30 and 48 HAI. Left panel: VND7-induced transcript profiles; right panel: control. Grey scale - percentile rank of expression of the gene in

specific tissue compared to other expressed genes. The coloured bars indicate the different phases shown in Figure 9 vs. the green control bar indicative of chloroplasts. Figures generated using previously published data (Li et al., 2016).

By analysing previously published metabolic data in light of TEM evidence generated in this study, we were able to infer a structure-function relationship between the xyloplast and Phe production for SCW synthesis. During vessel differentiation, increased levels of nucleotide sugars are required as building blocks for cellulose and hemicellulose synthesis. There is high expression of sucrose synthase 4 (SUS4) between 9-12 HAI (Figure 10D), which is mainly responsible for the synthesis of UDP-glucose (UDP-Glc). UDP-Glc is the direct substrate for cellulose synthesis and the precursor to UDP-xylose when converted to UDP-Glucuronic acid (UDP-GlcA). Interestingly, cytosolic invertase 2 (cINV2) - which converts sucrose to glucose – is highly expressed at 6 HAI (Figure 10D). This could increase the cytosolic glucose pool which can then be converted to glucose-1-phosphate and subsequently to UDP-Glc by UDP-glucose pyrophosphorylase (UGP), which is also highly expressed at 3 and 6 HAI (Figure 10D). From this, we can infer that UDP-glucose in this system might be derived both from sucrose via SUS4 as well as directly from glucose via UGP. Both UDP-Glc and UDP-GlcA peak before 9HAI after which they start decreasing, specifically between 12-24 HAI (Figure 11), which is consistent with when polysaccharide synthesis would be beginning and taking place, the decrease in UGP expression (Figure 10D) and the increase in lignin synthesis (Figure 10E).

In Li et al., 2016, the increase in Phe at 24 HAI was said to indicate the increase in/ onset of lignin biosynthesis. Through our analysis, we also observed that Phe levels only seem to increase after 12 HAI and show a peak at 24 HAI (Figure 11) which is consistent with some early (C4H and 4CL) and late (CAD) monolignol synthesis genes only being expressed between 12-24 HAI (Figure 10E). Phe levels drop after 24 HAI– presumably – when the flux of Phe through the monolignol pathway may be at its highest and Phe is no longer being synthesized.

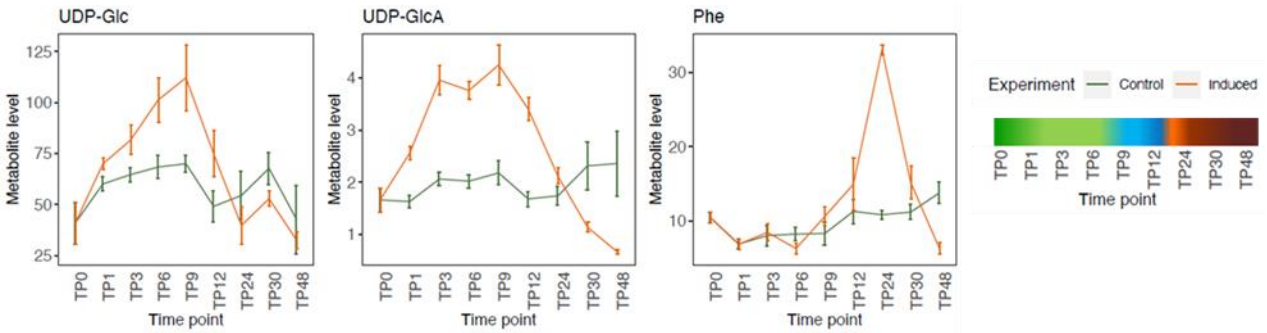

Figure 11 Changes in levels of metabolites needed for SCW synthesis in in VND7-induced seedlings. Alterations in levels of UDP-Glucose (UDP-Glc), UDP-Glucuronic Acid (UDP-GlcA) and Phenylalanine (Phe) needed for cellulose, xylan and lignin synthesis, respectively. Figured generated using previously published data (Li et al., 2016).

The transcriptional and metabolic expression data combined with the morphological changes occurring during the chloroplast-xyloplast conversion provide new insights into organellar biology during xylem differentiation. The drastic morphological changes occurring between 12-24 HAI support that Phe synthesis increases from 12 HAI and peaks at 24 HAI. Plastid disintegration immediately follows the rapid production of Phe at 24 HAI where peak Phe levels are present in the cell (Figure 11).

VND7, being a vessel SCW master regulator, also activates programmed cell death soon after its expression (Laubscher et al., 2018). Using BFN1 as an indicator of this, we looked at its expression. BFN1 which is expressed at 12 HAI and peaks around 24 HAI is involved in programmed cell death (PCD) and coincides with the degradation of plastids and cell death by 48 HAI. This degradation may therefore play a role in making Phe available to be metabolised by the monolignol synthesis pathway as the xyloplasts burst at 24 HAI. Phe levels continue to decrease after 36 HAI (Figure 11) which coincides with the up-regulation and abundance of transcripts for all obligate steps of the monolignol biosynthesis pathway between 24-36 HAI (Figure 10E) and SCW deposition taking place. It is known that the monolignol biosynthetic pathway takes place rapidly as no accumulation of monolignols is seen inside cells and monolignols are rapidly polymerized in secondary cell walls (Smith et al., 2013; Perkins et al., 2022).

We infer from this synthesis and joint lines of evidence that the chloroplast-xyloplast conversion begins around 8 HAI, which coincides with the partitioning of carbon towards Phe synthesis at 9 HAI. The *bona fide* xyloplast exists for a short amount of time (between 19-20 HAI) where it

could play a role in the rapid synthesis of Phe which occurs between 12-24 HAI after which it is fed directly into the monolignol synthetic pathway for ultimate lignification preceding and followed by PCD accompanied by plastid degradation from 36-48 HAI.

2.5. Discussion

The unique differential regulation of organellar-encoded genes in *E. grandis* immature xylem vs leaf forms precedent for a new non-photosynthetic plastid type, the xyloplast (Pinard and Mizrachi, 2018; Pinard et al., 2019). As distinct plastid types are often described based on specialised functions and distinct morphologies (Thomson and Whatley, 1980; Wise, 2007; Solymosi et al., 2018), we studied the ultrastructural dynamics that accompany the conversion of chloroplasts to xyloplasts in *Arabidopsis* VND7-induced seedlings. We also analysed published transcriptional and metabolic changes occurring during the chloroplast to xyloplast interconversion in this system to integrate xyloplast interconversion and structure to its function in the partitioning of carbon during wood formation.

The isolation of intact plastids from wood is a major obstacle as (i) it is difficult to access intact, live cellular material from developing xylem due to secondary cell walls, (ii) the mechanical grinding of tissues often damages the plastidial outer membrane, which (iii) in addition to the potential presence of starch granules within the plastid stroma, leads to plastid lysis (Jain et al., 2008; Tan et al., 2019). This makes it necessary to use an alternative method to study intact plastids in develpoping xylem cells. Comparison of the expression of secondary xylem regulatory and biosynthetic genes between the VND7 induction system in *Arabidopsis* (Li et al., 2016), the *Populus* xylem developmental series (Sundell et al., 2017) as well as *Eucalyptus* immature xylem, showed that 24 HAI in the VND7 system is comparable with xylem in trees (Pinard *et al.* in revision). Transmission electron microscopy of plastids extracted from *E. grandis* secondary xylem scrapings (See Supporting information Figure S3) also revealed morphologically distinct plastids that were structurally comparable to plastids seen at 19 HAI in DEX-induced VND7 *Arabidopsis* leaves (Figure 5 and 6). The similarity between plastid-targeted gene expression and morphology in *E. grandis* immature xylem and *Arabidopsis* VND7 induced plants, during SCW formation, thus makes this a suitable induction system for studying

xyloplast development and inferring structure-function relationships (Li et al., 2016; Pinard et al., in revision).

From our observations, we note distinct phases in the differentiation of xyloplasts from chloroplasts in the VND7 induction system. At VND7 induction, the plastid membrane forms invaginations to facilitate the uptake of cytoplasmic material, to form an amoeboid plastid (Figure 3, 4, see Supporting information Figure S8, S9, S12, S13). This is followed by a rapid change in the membrane structure and subsequent plastid disintegration. Plastid differentiation can be triggered by environmental and/or developmental stimuli (Jarvis and López-Juez, 2013; Liebers et al., 2017) which is essential as it allows cellular specialization based on biological processes taking place in different plant tissues (Llorente et al., 2020a). Based on evidence presented here, we deduce that xyloplast differentiation is regulated by signals directly from or downstream of VND7. This is accompanied by programmed cell death, and is further supported by the decline in UDP-Glc levels (needed for cell wall polysaccharide synthesis) as the expression of the PCD marker, BFN1, increases. Further, the morphological changes are directly related to Phe biosynthesis for monolignol synthesis, as the membranes rupture and peak Phe levels occur with the beginning of SCW deposition at 24 HAI, just prior to monolignol biosynthesis.

Interconversion between different plastid types usually involves remodelling of the internal membrane system (Spurr and Harris, 1968; Suzuki, 1974; Cheung et al., 1993; Simkin et al., 2007), changes in size and number of plastoglobules (Harris and Spurr, 1969) and changes in plastid shape (Waters et al., 2004), size (Egea et al., 2010). Remodelling of the plastidial membrane system is often accompanied by the proliferation of vesicles as seen between 8-18 HAI in our study (Figures 3 and 4). Vesicles originating from plastid membranes have previously been described in various plastid types such as proplastids, chloroplasts, chromoplasts, etioplasts, dessicoplasts and leucoplasts (reviewed in Lindquist et al., 2016). In proplastids, invaginations and vesicles originating from the envelope are often implicated in playing a role in thylakoid biogenesis (Lindquist et al., 2016). Vesicles have also been seen originating from the inner plastid membrane during the chloroplast-to-chromoplast transition (Spurr and Harris, 1968; Egea et al., 2010; Lindquist et al., 2016) as well as in etio-chloroplasts, the intermediates formed during etioplasts-to-chloroplast conversion (Kohn and Klein, 1976;

Orsenigo et al., 1976; Lindquist et al., 2016) which could mean they are commonly seen forming during plastid interconversion. In addition to developmental changes, plastids exposed to stress conditions e.g. metal deficiency (Platt-Aloia et al., 1983; Solymosi and Bertrand, 2010) also often show scattered vesicles formed by swollen thylakoids which are different from the abovementioned peripheral vesicles (Abdelkader et al., 2007). This can sometimes make the classification of vesicles confusing (Lindquist et al., 2016). Vesicles are also occasionally claimed to be artefacts of treatments and fixation conditions. However, a study by Lindquist et al., showed that vesicles are present in various sampling conditions and fixation protocols which suggests that they play a key role in the maintenance and development of the inner membranes of plastids rather than being just artefacts (Lindquist et al., 2016). Based on these TEM images alone, it is still difficult to deduce whether the vesicles seen occurred in response to stress (as the cell is simultanously undergoing PCD during VND7 induction), or whether these vesicles potentially perform a particular role such as in the transport of metabolites or membrane remodelling/maintenance like in the abovementioned studies. Future studies testing multiple fixation conditions, analyzing specific markers, lipid composition and/or labeling sub-cellular components can shed further light on this.

Another observation at early times after induction was the accumulation of spherical osmiophilic globules or plastoglobules (PG) in between the thylakoid membranes (Figures 3 and 4). PG are found in all plastid types such as chloroplasts, chromoplasts, and leucoplasts and are lipid droplets, (Bailey and Whyborn, 1963; Greenwood et al., 1963; Lichtenthaler, 1968; Kessler and Vidi, 2007; Eugeni Piller et al., 2012) that are coated with proteins which include plastoglobulin proteins, enzymes involved in lipid metabolic pathways and unclassified proteins (Vidi et al., 2006a; Ytterberg et al., 2006). An increase in size and number of PG during the chloroplast–chromoplast transition has been described before (Harris and Spurr, 1969). However, this could be due to the role that plastoglobulins play in carotenoid sequestration and unique to chromoplast biogenesis (Bréhélin and Kessler, 2008). Interestingly, biotic and abiotic stress conditions such as nitrogen deprivation, chilling etc. (Nordby and Yelenosky, 1985; Gaude et al., 2007) also often increase the size and number of PG. This is due to the disassembly of thylakoid membranes which leads to the accumulation of fatty acid phytyl esters (FAPEs) (Gaude et al., 2007; Bréhélin and Kessler, 2008; Eugeni Piller et al., 2012).The up-regulation of plastid lipid metabolism during senescence and in response to oxidative stress also leads PG to connect and form grape-

like clusters (Austin et al., 2006) similar to our observations (Figure 3D-F). Similarly to vesicles, the increase in PG during chloroplast to xyloplast conversion could be due to PCD-induced stress or due to their potential role in phenolic sequestration or membrane remodelling during plastid interconversion. Further studies will be needed to elucidate their function.

Lastly, we also observed changes in plastid shape and size as amoeboid plastids were seen in our study during the conversion of chloroplasts to xyloplasts. Amoeboid plastids have been previously described as common intermediates in the differentiation of various plastid types such as the differentiation from proplastid to chloroplasts in *Phaseolus vulgaris* primary leaves (Whatley, 1974; Thomson and Whatley, 1980) and during chloroplast regeneration in *Streptanthus tortuosus* tissue culture (Sjolund and Weier, 1971). It has been suggested that the changes in plastid morphology could be due to either one or a combination of (i) change in stromal sol-gel state, (ii) change in envelope character, (iii) change in volume to surface area ratio and/or iv) change in metabolic stage (Thomson and Whatley, 1980).

Cytolysosomes, formed from the endoplasmic reticulum, have also been shown to engulf portions of cytoplasm as part of an autophagic process (Villiers, 1967). Similarly, leucoplasts found in degenerating suspensor cells of *Phaseolus coccineus* showed invaginations engulfing portions of cytoplasm with acid phosphatase activity detected in the intraplastidial (IP) space (Nagl, 1977; Gärtner and Nagl, 1980). These lytic plastids were termed plastolysomes due to the degradation of soluble proteins in the engulfed cytoplasm (Nagl, 1977; Gärtner and Nagl, 1980) and could be an alternative hypothesis to explain the amoeboid plastids we observed after VND7 induction. However, lytic activity was visibly notable as the engulfed compartment was more electron-translucent than the surrounding cytosol, indicative of digestion (Nagl, 1977; Gärtner and Nagl, 1980). Similarly, plastolysomes were also reported in *Dendrobium* cv. Lucky Duan petals with detectable acid phosphatase activity and electron-translucent content in the IP space (van Doorn et al., 2011). These plastolysomes were found in freshly cut flowers and in all stages of petal development, hence no relationship was found between their formation and starvation-induced autophagy or programmed cell development, respectively (van Doorn et al., 2011). This indicated that although these plastolysomes resulted in cytoplasmic degradation, they formed part of normal cellular development (van Doorn et al., 2011).

Although at 24 HAI we observed that plastids had become swollen and started to degrade, the electron translucency of the IP space was consistent with that of the surrounding external cytoplasm which indicates lack of soluble contents, hence lack of digestion. Interestingly, structural evidence of digestion was not seen in *Brassica napus* microspores, in which 40% of the plastids transitioned into plastolysomes during the developmental switch of microspores toward embryogenesis (Parra-Vega et al., 2015). However, even with the lack of electron translucency, the presence of acid phosphatase activity, reduction in plastid number and autophagy previously associated with embryogenesis induction (Corral-Martínez et al., 2013) support the role of plastolysome-mediated autophagy in a 'cellular cleaning program' needed for the cell to adapt to the new developmental surroundings (Seguí-Simarro and Nuez, 2008; Corral-Martínez et al., 2013; Parra-Vega et al., 2015). The presence of conventional plastids in embryos derived from microspores also supports the notion that plastolysomes are a transient stage seen during developmental switches, where cytoplasm is engulfed, digested and excreted (Parra-Vega et al., 2015). In order to confirm if the amoeboid plastids we detected play a role in cellular cleaning and autophagy, it will be important to test the IP space for acid phosphatase activity.

In an ultrastructural study of pumpkin cotyledons, 2-(4-chlorophenylthio)ethyldiethylammonium chloride (CPTA) was used to induce the conversion of chromoplasts from proplastids and chloroplasts (Simpson et al., 1974). Plastids in the orange region of cotyledons exposed to CPTA and light, contained vesicles and plastid membrane invaginations that appeared to have engulfed mitochondria, whereas native chloroplasts were seen in the green regions (Simpson et al., 1974). In addition to chemical treatment, various levels of plastid regulation can be used to study plastid differentiation. This includes the hormonal induction of amyloplast differentiation from proplastids in BY-2 *Nicotiana tabacum* cells cultured in auxin-depleted medium in the presence of cytokinin (Miyazawa et al., 1999). The addition of lovastatin, which inhibits endogenous cytokinin accumulation, results in decreased starch deposition and ADP glucose pyrophosphorylase small subunit (AgpS) gene transcriptional levels needed for starch synthesis (Miyazawa et al., 2002). Artificial chloroplast-chromoplast conversion can also be elicited by synthetically inducing phytoene production in tobacco and *Arabidopsis* leaves (Llorente et al., 2020a). Phytoene is the intermediate formed from the first committed step in the carotenoid pathway (Cuttriss et al., 2011; Tian, 2016; Llorente et al., 2020a). In the first phase of interconversion, phytoene overexpression functions as a metabolic switch resulting in down

regulation of photosynthesis and weakened chloroplast identity. In the second phase, carotenoid-related genes expression and plastid morphology are concurrently reprogrammed for the conversion of phytoene into carotenoids and their subsequent storage in chromoplasts (Llorente et al., 2020a). Hence, loss of photosynthetic ability and increased carotenoid production are requirements for and not consequences of chromoplast differentiation (Llorente et al., 2020a).

Xyloplast differentiation was also accompanied by chloroplast preconditioning to loss of photosynthetic ability and the up regulation of downstream pathways *i.e.* the shikimate pathway which led to an increase in Phe synthesis, mainly provided by the arogenate pathway (Maeda et al., 2010a; Maeda et al., 2011). Two isoforms of arogenate dehydratase (ADT type-I and type-II) can catalyse and regulate the final step of Phe biosynthesis from arogenate via feedback-inhibition (Bonner and Jensen, 1987; El-Azaz et al., 2019). Although type-I enzymes are inhibited by high Phe levels, type-II enzymes evolved to overcome this inhibition (El-Azaz et al., 2019). The activity of type-II ADT enzymes allows for high levels of Phe accumulation in the plastid stroma for transport to the cytosol for monolignol synthesis, which is a major limiting step in lignin biosynthesis in vascular plants (Jung et al., 1986; Rippert et al., 2009b; Guo et al., 2018). Stable isotope labelling experiments showed that ADT1 suppression led to down regulation of carbon flux toward shikimic acid. Phe hyperaccumulation was seen in *Arabidopsis* plants overexpressing AtADT4 (Chen et al., 2016) whereas knocking out AtADT4 and AtADT5 in *A. thaliana* caused a reduction in G and S lignin monomers which highlighted their primary function in Phe biosynthesis for lignin accumulation (Corea et al., 2012). Suppression of ADT1 in *Petunia hybrida* flowers also resulted in decreased levels of Phe and the down regulation of carbon flux towards the shikimate pathway (Maeda et al., 2010b). The ADT family plays a pivotal regulatory role in carbon allocation at the branch point between the shikimate pathway and the cytosolic phenylpropanoid metabolic networks through Phe feedback inhibition (Corea et al., 2012). Future work should investigate the possible role of ADT regulation as a metabolic switch to trigger xyloplast differentiation for mass Phe synthesis.

The VND7 induction system has also previously been used to study the Golgi apparatus, central to hemicellulose biosynthesis (Meents et al., 2019). The study found that there was an increase in Golgi and mitochondrial abundance during SCW deposition, independent of xylan biosynthesis (Meents et al., 2019). Although random in distribution, the Golgi was found near SCW

deposition sites due to the free cytoplasmic space available. However, this differed from mitochondria, that were significantly found in closer proximity to SCWs (Meents et al., 2019). In our study, plastids appeared to be in close proximity to with the plasma membrane and mitochondria were often seen adjacent to plastids during cytoplasmic engulfment (**Figure 3**). However, further analysis and measurements would be required to deteremine whether plastids are randomly distributed or are significantly closer to SCWs in order to facilitate Phe supply for monolignol synthesis to these domains.

Although plastid role in secondary growth is not well studied, the electron dense regions seen in the xyloplast at 19 HAI are consistent with the up-regulated production of compounds derived from aromatic amino acids in monoterpene (Turner et al., 1999), tannin (Brillouet et al., 2013) and phytomelanin production (Coutinho et al., 2021). The leucoplasts found in peppermint secretory cells, where monoterpene synthesis is initiated (Eisenreich et al., 1997; Turner et al., 1999; Tholl et al., 2004), showed varying amoeboid-like shapes (Turner and Croteau, 2004). Brillouet *et al*. (2013) described the tannosome, a novel plastid type derived from chloroplasts involved in tannin polymerization by the 'pearling of the thylakoids'. In the Asteraceae species, phytomelanin precursors are synthesized in plastids and also follow the "pearl necklace" model of the tannosome (Brillouet et al., 2013; Brillouet, 2015; Coutinho et al., 2021). Phytomelanin production is closely related to seed sclerification, which is strongly indicative of the involvement of SCW-related phenolic compounds in phytomelanin synthesis (Britton, 1983; Solano, 2014; Glagoleva et al., 2020; Coutinho et al., 2021). Future studies should identify ways to label Phe which would allow us to determine whether the electron dense regions seen in the xyloplast represent mass Phe synthesis and accumulation.

Production of monolignols is a multi-compartmental process as it relies on Phe synthesis which takes place in the plastid stroma (Maeda et al., 2010a; Maeda et al., 2011; Yoo et al., 2013). As the inner plastidial membrane is selectively permeable (Weber et al., 2005) and Phe has a low permeability coefficient (Carruthers and Melchior, 1983; Chakrabarti and Deamer, 1992), Phe transport from plastids is unlikely to occur through simple diffusion (Widhalm et al., 2015). In the tannosome, plastid-synthesized tannins are thought to be transported to the vacuole in plastid-derived shuttles (Brillouet et al., 2013) while in *Petunia hybrida* flowers, a plastidial cationic amino-acid transporter (PhpCAT) has been identified in plastidial phenylalanine transport

(Widhalm et al., 2015). In the xyloplast, it was hypothesized that Phe transport could occur via budded off vesicles or through close membrane contacts between the plastid and ER (Pinard and Mizrachi, 2018). However, due to the absence of budded off vesicles during xyloplast differentiation, no close contact seen between plastid and ER and, the absence of PhpCAT transporter homologs in Eucalyptus and Poplar, we deduce from this work that Phe is probably made freely made available in the cytosol by bursting and degradation of plastids seen starting at 20 HAI (Figure 7). Plastid disintegration however could be the result of PCD. Using different concentrations of DEX, or selectively repressing PCD processes to prevent PCD in this system would shed more light on whether bursting of plastids holds a unique purpose in Phe availability to the cytosol.

The TEM analysis of xyloplast formation at a finer timescale has provided novel insights into how the changes in morphology between 18-24 HAI correlate with xyloplast function. Metabolite data shows that most Phe synthesis takes place between 12-24 HAI and peak Phe levels are found at 24 HAI. Plastid disintegration and PCD immediately follow the rapid appearance of Phe presumably making it available to be metabolised by the monolignol synthesis pathway. The enzymes required for the complete monolignol biosynthetic pathway are expressed at 24 HAI, which would explain the drop in Phe levels after this time point as it gets rapidly used up for monolignol synthesis. A recent study using fungal laccase containing liposomes in the presence of monolignols showed that the gradient formed by monolignol polymerisation drives the rapid diffusion of monolignols across the plasma membrane (Perkins et al., 2022). As monolignols are rapidly synthesized and polymerized in SCWs (Smith et al., 2013), rapid synthesis of Phe would be required and is supported by our findings.

More than 30% of all fixed carbon is shunted to the plastid-localised shikimate pathway (Tohge et al., 2013), a large proportion of which is channelled towards the production of AAA and derived-secondary metabolites such as lignin which is a key component of the secondary cell wall (SCW) along with cellulose and hemicellulose. In plants, about In plants, about 20–30% of carbon fixed during photosynthesis is directed towards the shikimate pathway which is involved in the production of Phe and Phe-derived compounds (Haslam, 1993) which constitute ~30–45% of plant organic matter (Razal et al., 1996). One example of such a compound is lignin, which is a key component of the SCW and is made up of monolignols derived from plastid-synthesized

Phe (Bonawitz and Chapple, 2010). However, as the SCW in woody tissues of plants hinders detailed examination our knowledge of plastids structure and function in developing xylem is very limited (Pinard and Mizrachi, 2018). The aim of this study was thus to gain a high-resolution characterization of xyloplast ultrastructure, a specialised wood-specific plastid found in developing xylem, using the VND7 induction system in *Arabidopsis* as well as to characterize the link between plastid terminal differentiation and degradation and carbon partitioning in xylogenesis. The main conclusions drawn from this study are that: (i) the VND7 induction system is a suitable model system to study plastid biology in xylem; (ii) the presence of an amoeboid plastid during the transition from chloroplasts to xyloplasts provides further evidence for the existence of a morphologically distinct plastid type found in wood; (iii) the morphological characteristics of xyloplasts present at 19/19.5 HAI in *Arabidopsis* and xyloplasts extracted from *Eucalyptus* xylem further support our findings and lastly, (iv) analysis of published VND7 expression data shows that there is a structure-function relationship between changes in xyloplast morphology and the partitioning of carbon towards phenylalanine synthesis. We conclude that the xyloplast exists for a short period of time where it rapidly synthesizes Phe, which is made available for monolignol biosynthesis as the xyloplasts degrade due to programmed cell death. This study highlights the central role of organellar metabolism during SCW formation and provides novel insight into the ultrastructural dynamics accompanying the shunt of carbon from sugar to phenolics during secondary growth.

2.6. Acknowledgments

The research conducted during the course of this dissertation was done by myself in the African Plant Systems biology for the Bioeconomy (APSB) Programme at the Forestry and Agricultural Biotechnology Institute (FABI), Department of Biochemistry, Genetics and Microbiology, University of Pretoria, under the guidance of my supervisors, Prof. Eshchar Mizrachi, Dr Desrre Pinard, Prof. Vida Van Staden and Dr Victoria Maloney, with financial support from South Africa's National Research Foundation (Grant UID 116239) and the Technology Innovation Agency of South Africa through the Forest Molecular Genetics Cluster Program. The authors would also like to acknowledge Erna van Wilpe and Charity Maepa for their technical assistance in setting up the light microscopy and transmission electron microscopy experiments.

2.7. References

Abdelkader, A.F., Aronsson, H., Solymosi, K., Böddi, B., and Sundqvist, C. (2007). High salt stress induces swollen prothylakoids in dark-grown wheat and alters both prolamellar body transformation and reformation after irradiation. JExB **58,** 2553-2564.

Archibald, J.M. (2009). The puzzle of plastid evolution. Curr. Biol. **19,** R81-R88.

Austin, J.R., Frost, E., Vidi, P.-A., Kessler, F., and Staehelin, L.A. (2006). Plastoglobules are lipoprotein subcompartments of the chloroplast that are permanently coupled to thylakoid membranes and contain biosynthetic enzymes. The Plant Cell **18,** 1693-1703.

Bailey, J.L., and Whyborn, A. (1963). The osmiophilic globules of chloroplasts II. Globules of the spinach-beet chloroplast. AcBB **78,** 163-174.

Beltrán, J., Wamboldt, Y., Sanchez, R., LaBrant, E.W., Kundariya, H., Virdi, K.S., Elowsky, C., and Mackenzie, S.A. (2018). Specialized plastids trigger tissue-specific signaling for systemic stress response in plants. Plant Physiol. **178,** 672-683.

Bonawitz, N.D., and Chapple, C. (2010). The genetics of lignin biosynthesis: connecting genotype to phenotype. Annu. Rev. Genet. **44,** 337-363.

Bonner, C., and Jensen, R. (1987). [57] Prephenate aminotransferase. Methods Enzymol. **142,** 479-487.

Bréhélin, C., and Kessler, F. (2008). The plastoglobule: a bag full of lipid biochemistry tricks. PcPb **84,** 1388-1394.

Brillouet, J.-M. (2015). On the role of chloroplasts in the polymerization of tannins in Tracheophyta: A monograph. Am. J. Plant Sci. **6,** 1401.

Brillouet, J.-M., Verdeil, J.-L., Odoux, E., Lartaud, M., Grisoni, M., and Conéjéro, G. (2014). Phenol homeostasis is ensured in vanilla fruit by storage under solid form in a new chloroplast-derived organelle, the phenyloplast. JExB **65,** 2427-2435.

Brillouet, J.-M., Romieu, C., Schoefs, B., Solymosi, K., Cheynier, V., Fulcrand, H., Verdeil, J.-L., and Conéjéro, G. (2013). The tannosome is an organelle forming condensed tannins in the chlorophyllous organs of Tracheophyta. Ann. Bot. **112,** 1003-1014.

Britton, G. (1983). The biochemistry of natural pigments. (Cambridge University Press).

Brodersen, C.R., Roddy, A.B., Wason, J.W., and McElrone, A.J. (2019). Functional Status of Xylem Through Time. Annu. Rev. Plant Biol. **70,** 407-433.

Burgess, J. (1985). Introduction to plant cell development. (CUP Archive).

Buschmann, C., Meier, D., Kleudgen, H., and Lichtenthaler, H. (1978). Regulation of chloroplast development by red and blue light. In Annual European Symposium on Photomorphogenesis (Elsevier), pp. 195-198.

Carruthers, A., and Melchior, D. (1983). Study of the relationship between bilayer water permeability and bilayer physical state. Biochemistry **22,** 5797-5807.

Chakrabarti, A.C., and Deamer, D.W. (1992). Permeability of lipid bilayers to amino acids and phosphate. Biochim. Biophys. Acta - Biomembr. **1111,** 171-177.

Chen, Q., Man, C., Li, D., Tan, H., Xie, Y., and Huang, J. (2016). Arogenate dehydratase isoforms differentially regulate anthocyanin biosynthesis in Arabidopsis thaliana. Molecular Plant **9,** 1609-1619.

Cheung, A.Y., McNellis, T., and Piekos, B. (1993). Maintenance of chloroplast components during chromoplast differentiation in the tomato mutant green flesh. Plant Physiol. **101,** 1223-1229.

Choi, H., Yi, T., and Ha, S.-H. (2021). Diversity of plastid types and their interconversions. Front. Plant Sci. **12**.

Chuartzman, S.G., Nevo, R., Shimoni, E., Charuvi, D., Kiss, V., Ohad, I., Brumfeld, V., and Reich, Z. (2008). Thylakoid membrane remodeling during state transitions in Arabidopsis. The Plant Cell **20,** 1029-1039.

Corea, O.R.A., Ki, C., Cardenas, C.L., Kim, S.-J., Brewer, S.E., Patten, A.M., Davin, L.B., and Lewis, N.G. (2012). Arogenate dehydratase isoenzymes profoundly and differentially modulate carbon flux into lignins. J. Biol. Chem. **287,** 11446-11459.

Corral-Martínez, P., Parra-Vega, V., and Seguí-Simarro, J.M. (2013). Novel features of *Brassica napus* embryogenic microspores revealed by high pressure freezing and freeze substitution: evidence for massive autophagy and excretion-based cytoplasmic cleaning. JExB **64,** 3061-3075.

Coutinho, J.W., Rodrigues, A.C., Appezzato-da-Gloria, B., Oliveira, E.M., Oliveira, F.M., and Lusa, M.G. (2021). Plastid role in phytomelanin synthesis in *Piptocarpha axillaris* (Less.) Baker stems (Asteraceae, Vernonieae). Protoplasma**,** 1-15.

Cuttriss, A.J., Cazzonelli, C.I., Wurtzel, E.T., and Pogson, B.J. (2011). Carotenoids. In Advances in Botanical Research, F. Rébeillé and R. Douce, eds (Academic Press), pp. 1-36.

de Vries, J., Stanton, A., Archibald, J.M., and Gould, S.B. (2016). Streptophyte terrestrialization in light of plastid evolution. Trends Plant Sci. **21,** 467-476.

Derbyshire, P., Ménard, D., Green, P., Saalbach, G., Buschmann, H., Lloyd, C.W., and Pesquet, E. (2015). Proteomic analysis of microtubule interacting proteins over the course of xylem tracheary element formation in *Arabidopsis*. The Plant Cell **27,** 2709-2726.

Dilley, R., and Rothstein, A. (1967). Chloroplast membrane characteristics. Biochim. Biophys. Acta - Biomembr. **135,** 427-443.

Egea, I., Barsan, C., Bian, W., Purgatto, E., Latché, A., Chervin, C., Bouzayen, M., and Pech, J.-C. (2010). Chromoplast differentiation: current status and perspectives. PCPhy **51,** 1601-1611.

Eisenreich, W., Sagner, S., Zenk, M.H., and Bacher, A. (1997). Monoterpenoid essential oils are not of mevalonoid origin. Tetrahedron Lett. **38,** 3889-3892.

El-Azaz, J., Cánovas, F.M., Barcelona, B., Ávila, C., and de la Torre, F. (2019). Allosteric deregulation of phenylalanine biosynthesis evolved with the emergence of vascular plants. bioRxiv**,** 834747.

Eugeni Piller, L., Abraham, M., Dörmann, P., Kessler, F., and Besagni, C. (2012). Plastid lipid droplets at the crossroads of prenylquinone metabolism. JExB **63,** 1609-1618.

Farquharson, K.L. (2018). Microtubules direct lignin and xylan deposition in a cellulose-independent manner (American Society of Plant Biologists).

Gärtner, P.-J., and Nagl, W. (1980). Acid phosphatase activity in plastids (plastolysomes) of senescing embryo-suspensor cells. Planta **149,** 341-349.

Gaude, N., Bréhélin, C., Tischendorf, G., Kessler, F., and Dörmann, P. (2007). Nitrogen deficiency in *Arabidopsis* affects galactolipid composition and gene expression and results in accumulation of fatty acid phytyl esters. PlJ **49,** 729-739.

Glagoleva, A.Y., Shoeva, O.Y., and Khlestkina, E.K. (2020). Melanin pigment in plants: Current Knowledge and Future Perspectives. Front. Plant Sci. **11**.

Gracen, V., Hilliard, J.H., Brown, R., and West, S. (1972). Peripheral reticulum in chloroplasts of plants differing in CO 2 fixation pathways and photorespiration. Planta **107,** 189-204.

Greenwood, A., Leech, R.M., and Williams, J. (1963). The osmiophilic globules of chloroplasts: I. Osmiophilic globules as a normal component of chloroplasts and their isolation and composition in Vicia faba L. AcBB **78,** 148-162.

Guo, L., Wang, P., Jaini, R., Dudareva, N., Chapple, C., and Morgan, J.A. (2018). Dynamic modeling of subcellular phenylpropanoid metabolism in Arabidopsis lignifying cells. Metab. Eng. **49,** 36-46.

Hanson, M.R., and Sattarzadeh, A. (2014). Fluorescent labeling and confocal microscopic imaging of chloroplasts and non-green plastids. In Chloroplast Biotechnology (Springer), pp. 125-143.

Harris, W.M., and Spurr, A.R. (1969). Chromoplasts of tomato fruits. II. The red tomato. Am. J. Bot. **56,** 380-389.

Haslam, E. (1993). Shikimic acid: metabolism and metabolites. (Wiley).

Huang, C.X., and van Steveninck, R.F. (1990). Salinity induced structural changes in meristematic cells of barley roots. New Phytol. **115,** 17-22.

Jain, R., Katavic, V., Agrawal, G.K., Guzov, V.M., and Thelen, J.J. (2008). Purification and proteomic characterization of plastids from *Brassica napus* developing embryos. Proteomics **8,** 3397-3405.

Jarvis, P., and López-Juez, E. (2013). Biogenesis and homeostasis of chloroplasts and other plastids. Nat. Rev. Mol. Cell Biol. **14,** 787-802.

Jung, E., Zamir, L.O., and Jensen, R.A. (1986). Chloroplasts of higher plants synthesize L-phenylalanine via L-arogenate. PNAS **83,** 7231-7235.

Keeling, P.J. (2010). The endosymbiotic origin, diversification and fate of plastids. Philosophical Transactions of the Royal Society B: Biological Sciences **365,** 729-748.

Kessler, F., and Vidi, P.-A. (2007). Plastoglobule lipid bodies: their functions in chloroplasts and their potential for applications. Green Gene Technology**,** 153-172.

Kohn, S., and Klein, S. (1976). Light-induced structural changes during incubation of isolated maize etioplasts. Planta **132,** 169-175.

Larkin, R.M. (2014). Influence of plastids on light signalling and development. Philosophical Transactions of the Royal Society B: Biological Sciences **369,** 20130232.

Larkin, R.M., and Ruckle, M.E. (2008). Integration of light and plastid signals. Curr. Opin. Plant Biol. **11,** 593-599.

Laubscher, M., Brown, K., Tonfack, L.B., Myburg, A.A., Mizrachi, E., and Hussey, S.G. (2018). Temporal analysis of *Arabidopsis* genes activated by *Eucalyptus grandis* NAC transcription factors associated with xylem fibre and vessel development. Sci. Rep. **8,** 10983.

Li, Z., Omranian, N., Neumetzler, L., Wang, T., Herter, T., Usadel, B., Demura, T., Giavalisco, P., Nikoloski, Z., and Persson, S. (2016). A transcriptional and metabolic framework for secondary wall formation in *Arabidopsis*. Plant Physiol. **172,** 1334-1351.

Lichtenthaler, H. (1968). Plastoglobuli and fine structure of plastids. Endvr **27,** 144-+.

Liebers, M., Grübler, B., Chevalier, F., Lerbs-Mache, S., Merendino, L., Blanvillain, R., and Pfannschmidt, T. (2017). Regulatory shifts in plastid transcription play a key role in morphological conversions of plastids during plant development. Front. Plant Sci. **8**.

Liere, K., and Börner, T. (2013). Development-dependent changes in the amount and structural organization of plastid DNA. In Plastid development in leaves during growth and senescence (Springer), pp. 215-237.

Lindquist, E., Solymosi, K., and Aronsson, H. (2016). Vesicles are persistent features of different plastids. Traffic **17,** 1125-1138.

Liu, X., Li, Y., and Zhong, S. (2017). Interplay between light and plant hormones in the control of *Arabidopsis* seedling chlorophyll biosynthesis. Front. Plant Sci. **8,** 1433.

Llorente, B., Torres-Montilla, S., Morelli, L., Florez-Sarasa, I., Matus, J.T., Ezquerro, M., D'andrea, L., Houhou, F., Majer, E., and Picó, B. (2020). Synthetic conversion of leaf chloroplasts into

carotenoid-rich plastids reveals mechanistic basis of natural chromoplast development. PNAS **117,** 21796-21803.

López-Juez, E. (2007). Plastid biogenesis, between light and shadows. JExB **58,** 11-26.

Maeda, H., Yoo, H., and Dudareva, N. (2011). Prephenate aminotransferase directs plant phenylalanine biosynthesis via arogenate. Nat. Chem. Biol. **7,** 19-21.

Maeda, H., Shasany, A.K., Schnepp, J., Orlova, I., Taguchi, G., Cooper, B.R., Rhodes, D., Pichersky, E., and Dudareva, N. (2010a). RNAi suppression of arogenate dehydratase1 reveals that phenylalanine is synthesized predominantly via the arogenate pathway in petunia petals The Plant Cell **22,** 832-849.

Maeda, H., Shasany, A.K., Schnepp, J., Orlova, I., Taguchi, G., Cooper, B.R., Rhodes, D., Pichersky, E., and Dudareva, N. (2010b). RNAi suppression of Arogenate Dehydratase1 reveals that phenylalanine is synthesized predominantly via the arogenate pathway in petunia petals. The Plant Cell **22,** 832-849.

Marin, B., M. Nowack, E.C., and Melkonian, M. (2005). A plastid in the making: evidence for a second primary endosymbiosis. Protist **156,** 425-432.

Martin, W., Rujan, T., Richly, E., Hansen, A., Cornelsen, S., Lins, T., Leister, D., Stoebe, B., Hasegawa, M., and Penny, D. (2002). Evolutionary analysis of *Arabidopsis*, cyanobacterial, and chloroplast genomes reveals plastid phylogeny and thousands of cyanobacterial genes in the nucleus. PNAS **99,** 12246-12251.

McFadden, G.I. (2001). Primary and secondary endosymbiosis and the origin of plastids. J. Phycol. **37,** 951-959.

Meents, M.J., Watanabe, Y., and Samuels, A.L. (2018). The cell biology of secondary cell wall biosynthesis. Ann. Bot. **121,** 1107-1125.

Meents, M.J., Motani, S., Mansfield, S.D., and Samuels, A.L. (2019). Organization of xylan production in the golgi during secondary cell wall biosynthesis [OPEN]. Plant Physiol. **181,** 527-546.

Miyazawa, Y., Kato, H., Muranaka, T., and Yoshida, S. (2002). Amyloplast formation in cultured tobacco BY-2 cells requires a high cytokinin content. PCPhy **43,** 1534-1541.

Miyazawa, Y., Sakai, A., Miyagishima, S.-y., Takano, H., Kawano, S., and Kuroiwa, T. (1999). Auxin and cytokinin have opposite effects on amyloplast development and the expression of starch synthesis genes in cultured bright yellow-2 tobacco cells. Plant Physiol. **121,** 461-470.

Mustárdy, L., Buttle, K., Steinbach, G., and Garab, G.z. (2008). The three-dimensional network of the thylakoid membranes in plants: quasihelical model of the granum-stroma assembly. The Plant Cell **20,** 2552-2557.

Nagl, W. (1977). «Plastolysomes»—Plastids involved in the autolysis of the embryo-suspensor in Phaseolus. Zeitschrift für Pflanzenphysiologie **85,** 45-51.

Noguchi, M., Fujiwara, M., Sano, R., Nakano, Y., Fukao, Y., Ohtani, M., and Demura, T. (2018). Proteomic analysis of xylem vessel cell differentiation in VND7-inducible tobacco BY-2 cells by two-dimensional gel electrophoresis. Plant Biotechnol. **35,** 31-37.

Nordby, H., and Yelenosky, G. (1985). Change in citrus leaf lipids during freeze-thaw stress. Phytochemistry **24,** 1675-1679.

Ohtani, M., and Demura, T. (2019). The quest for transcriptional hubs of lignin biosynthesis: beyond the NAC-MYB-gene regulatory network model. Curr. Opin. Biotechnol. **56,** 82-87.

Ohtani, M., Morisaki, K., Sawada, Y., Sano, R., Uy, A.L.T., Yamamoto, A., Kurata, T., Nakano, Y., Suzuki, S., and Matsuda, M. (2016). Primary metabolism during biosynthesis of secondary wall polymers of protoxylem vessel elements. Plant Physiol. **172,** 1612-1624.

Orsenigo, M., Rascio, N., and Bonatti, P.M. (1976). Fine structure of the etioplast in two mutants of maize. J. Ultrastruct. Res. **55,** 42-49.

Parra-Vega, V., Corral-Martínez, P., Rivas-Sendra, A., and Seguí-Simarro, J.M. (2015). Formation and excretion of autophagic plastids (plastolysomes) in *Brassica napus* embryogenic microspores. Front. Plant Sci. **6,** 94.

Perkins, M.L., Schuetz, M., Unda, F., Chen, K.T., Bally, M.B., Kulkarni, J.A., Yan, Y., Pico, J., Castellarin, S.D., and Mansfield, S.D. (2022). Monolignol export by diffusion down a polymerization-induced concentration gradient. The Plant Cell.

Pinard, D., and Mizrachi, E. (2018). Unsung and understudied: plastids involved in secondary growth. Curr. Opin. Plant Biol. **42,** 30-36.

Pinard, D., Fierro, A.C., Marchal, K., Myburg, A.A., and Mizrachi, E. (2019). Organellar carbon metabolism is coordinated with distinct developmental phases of secondary xylem. New Phytol. **222,** 1832-1845.

Platt-Aloia, K., Thomson, W., and Terry, N. (1983). Changes in plastid ultrastructure during iron nutrition-mediated chloroplast development. Protoplasma **114,** 85-92.

Razal, R.A., Ellis, S., Singh, S., Lewis, N.G., and Towers, G.N. (1996). Nitrogen recycling in phenylpropanoid metabolism. Phytochemistry **41,** 31-35.

Rippert, P., Puyaubert, J., Grisollet, D., Derrier, L., and Matringe, M. (2009). Tyrosine and phenylalanine are synthesized within the plastids in *Arabidopsis*. Plant Physiol. **149,** 1251-1260.

Rudowska, Ł., Gieczewska, K., Mazur, R., Garstka, M., and Mostowska, A. (2012). Chloroplast biogenesis — Correlation between structure and function. Biochim. Biophys. Acta **1817,** 1380-1387.

Sarafis, V. (1998). Chloroplasts: a structural approach. J. Plant Physiol. **152,** 248-264.

Seguí-Simarro, J.M., and Nuez, F. (2008). How microspores transform into haploid embryos: changes associated with embryogenesis induction and microspore-derived embryogenesis. Physiol. Plant. **134,** 1-12.

Simkin, A.J., Gaffé, J., Alcaraz, J.-P., Carde, J.-P., Bramley, P.M., Fraser, P.D., and Kuntz, M. (2007). Fibrillin influence on plastid ultrastructure and pigment content in tomato fruit. Phytochemistry **68,** 1545-1556.

Simpson, D., Chichester, C., and Lee, T. (1974). Chemical regulation of plastid development. I. inhibition of chlorophyll biosynthesis in detached pumpkin cotyledons by CPTA. A Pigment and Ultrastructual Study. Funct. Plant Biol. **1,** 119-133.

Sjolund, R., and Weier, T. (1971). An ultrastructural study of chloroplast structure and dedifferentiation in tissue cultures of *Streptanthus tortuosus* (Cruciferae). Am. J. Bot. **58,** 172-181.

Smith, R.A., Schuetz, M., Roach, M., Mansfield, S.D., Ellis, B., and Samuels, L. (2013). Neighboring parenchyma cells contribute to *Arabidopsis* xylem lignification, while lignification of interfascicular fibers is cell autonomous. The Plant cell **25,** 3988-3999.

Solano, F. (2014). Melanins: skin pigments and much more—types, structural models, biological functions, and formation routes. New J. Sci. **2014**.

Solymosi, K., and Bertrand, M. (2010). Heavy metals and plastid metabolism. Handbook of plant and crop stress**,** 675-711.

Solymosi, K., Lethin, J., and Aronsson, H. (2018). Diversity and plasticity of plastids in land plants. Plastids**,** 55-72.

Spurr, A.R., and Harris, W.M. (1968). Ultrastructure of chloroplasts and chromoplasts in *Capsicum annuum* I. Thylakoid membrane changes during fruit ripening. Am. J. Bot. **55,** 1210-1224.

Sundell, D., Street, N.R., Kumar, M., Mellerowicz, E.J., Kucukoglu, M., Johnsson, C., Kumar, V., Mannapperuma, C., Delhomme, N., and Nilsson, O. (2017). AspWood: high-spatial-resolution transcriptome profiles reveal uncharacterized modularity of wood formation in *Populus tremula*. The Plant Cell **29,** 1585-1604.

Suzuki, S. (1974). Ultrastructural development of plastids in cherry peppers during fruit ripening. The botanical magazine = Shokubutsu-gaku-zasshi **87,** 165-178.

Szczepanik, J., and Sowiński, P. (2014). The occurrence of chloroplast peripheral reticulum in grasses: a matter of phylogeny or a matter of function? Acta Physiol. Plant **36,** 1133-1142.

Tan, T.T., Demura, T., and Ohtani, M. (2019). Creating vessel elements in vitro: Towards a comprehensive understanding of the molecular basis of xylem vessel element differentiation. Plant Biotechnol. J **36,** 1-6.

Tan, T.T., Endo, H., Sano, R., Kurata, T., Yamaguchi, M., Ohtani, M., and Demura, T. (2018). Transcription factors VND1-VND3 contribute to cotyledon xylem vessel formation. Plant Physiol. **176,** 773-789.

Tholl, D., Kish, C.M., Orlova, I., Sherman, D., Gershenzon, J., Pichersky, E., and Dudareva, N. (2004). Formation of monoterpenes in *Antirrhinum majus* and *Clarkia breweri* flowers involves heterodimeric geranyl diphosphate synthases. The Plant Cell **16,** 977-992.

Thomson, W., and Whatley, J.M. (1980). Development of nongreen plastids. Annu. Rev. Plant Physiol. **31,** 375-394.

Tian, L. (2016). Chapter 32 - Carotenoids, genetically modified foods, and vitamin A nutrition. In Genetically Modified Organisms in Food, R.R. Watson and V.R. Preedy, eds (San Diego: Academic Press), pp. 353-360.

Timmis, J.N., Ayliffe, M.A., Huang, C.Y., and Martin, W. (2004). Endosymbiotic gene transfer: organelle genomes forge eukaryotic chromosomes. Nat Rev Genet **5,** 123-135.

Tong, H., Chen, H., and Williams, C.M. (2021). Gene regulatory network of secondary cell wall biosynthesis during VND7 induced *de novo* xylem formation. Gene **11**.

Turner, G., Gershenzon, J., Nielson, E.E., Froehlich, J.E., and Croteau, R. (1999). Limonene synthase, the enzyme responsible for monoterpene biosynthesis in peppermint, is localized to leucoplasts of oil gland secretory cells. Plant Physiol. **120,** 879-886.

Turner, G.W., and Croteau, R. (2004). Organization of monoterpene biosynthesis in Mentha. Immunocytochemical localizations of geranyl diphosphate synthase, limonene-6-hydroxylase, isopiperitenol dehydrogenase, and pulegone reductase. Plant Physiol. **136,** 4215-4227.

van Doorn, W.G., Kirasak, K., Sonong, A., Srihiran, Y., van Lent, J., and Ketsa, S. (2011). Do plastids in *Dendrobium* cv. Lucky Duan petals function similar to autophagosomes and autolysosomes? Autophagy **7,** 584-597.

Vidi, P.-A., Kanwischer, M., Baginsky, S., Austin, J.R., Csucs, G., Dörmann, P., Kessler, F., and Bréhélin, C. (2006). Tocopherol cyclase (VTE1) localization and vitamin E accumulation in chloroplast plastoglobule lipoprotein particles. J. Biol. Chem. **281,** 11225-11234.

Villiers, T.A. (1967). Cytolysomes in long-dormant plant embryo cells. Nature **214,** 1356-1357.

Watanabe, Y. (2018). The cell biology of cellulose deposition in secondary cell walls of protoxylem tracheary elements in Arabidopsis thaliana (University of British Columbia).

Watanabe, Y., Schneider, R., Barkwill, S., Gonzales-Vigil, E., Hill, J.L., Samuels, A.L., Persson, S., and Mansfield, S.D. (2018). Cellulose synthase complexes display distinct dynamic behaviors during xylem transdifferentiation. PNAS **115,** E6366-E6374.

Waters, M.T., Fray, R.G., and Pyke, K.A. (2004). Stromule formation is dependent upon plastid size, plastid differentiation status and the density of plastids within the cell. PlJ **39,** 655-667.

Weber, A.P., Schwacke, R., and Flügge, U.-I. (2005). Solute transporters of the plastid envelope membrane. Annu. Rev. Plant Bio. **56,** 133-164.

Whatley, J. (1974). Chloroplast development in primary leaves of *Phaseolus vulgaris*. New Phytol. **73,** 1097-1110.

Widhalm, J.R., Gutensohn, M., Yoo, H., Adebesin, F., Qian, Y., Guo, L., Jaini, R., Lynch, J.H., McCoy, R.M., and Shreve, J.T. (2015). Identification of a plastidial phenylalanine exporter that

influences flux distribution through the phenylalanine biosynthetic network. Nat. Commun. **6,** 1-11.

Wise, R.R. (2007). The diversity of plastid form and function. In The structure and function of plastids (Springer), pp. 3-26.

Yamaguchi, M., Kubo, M., Fukuda, H., and Demura, T. (2008). VASCULAR-RELATED NAC-DOMAIN7 is involved in the differentiation of all types of xylem vessels in *Arabidopsis* roots and shoots. PlJ **55,** 652-664.

Yamaguchi, M., Mitsuda, N., Ohtani, M., Ohme-Takagi, M., Kato, K., and Demura, T. (2011). VASCULAR-RELATED NAC-DOMAIN 7 directly regulates the expression of a broad range of genes for xylem vessel formation. PlJ **66,** 579-590.

Yamaguchi, M., Goué, N., Igarashi, H., Ohtani, M., Nakano, Y., Mortimer, J.C., Nishikubo, N., Kubo, M., Katayama, Y., and Kakegawa, K. (2010). VASCULAR-RELATED NAC-DOMAIN6 and VASCULAR-RELATED NAC-DOMAIN7 effectively induce transdifferentiation into xylem vessel elements under control of an induction system. Plant Physiol. **153,** 906-914.

Yoo, H., Widhalm, J.R., Qian, Y., Maeda, H., Cooper, B.R., Jannasch, A.S., Gonda, I., Lewinsohn, E., Rhodes, D., and Dudareva, N. (2013). An alternative pathway contributes to phenylalanine biosynthesis in plants via a cytosolic tyrosine: phenylpyruvate aminotransferase. Nat. Commun. **4,** 1-11.

Ytterberg, A.J., Peltier, J.-B., and Van Wijk, K.J. (2006). Protein profiling of plastoglobules in chloroplasts and chromoplasts. A surprising site for differential accumulation of metabolic enzymes. Plant Physiol. **140,** 984-997.

Zhong, R., Lee, C., and Ye, Z.-H. (2010). Global analysis of direct targets of secondary wall NAC master switches in *Arabidopsis*. Mol Plant **3,** 1087-1103.

Zhong, R., Cui, D., and Ye, Z.H. (2019). Secondary cell wall biosynthesis. New Phytol. **221,** 1703-1723.

Zimmermann, M.H. (2013). Xylem structure and the ascent of sap. (Springer Science & Business Media).

2.8. Supporting Information

Supplemental Figure S1

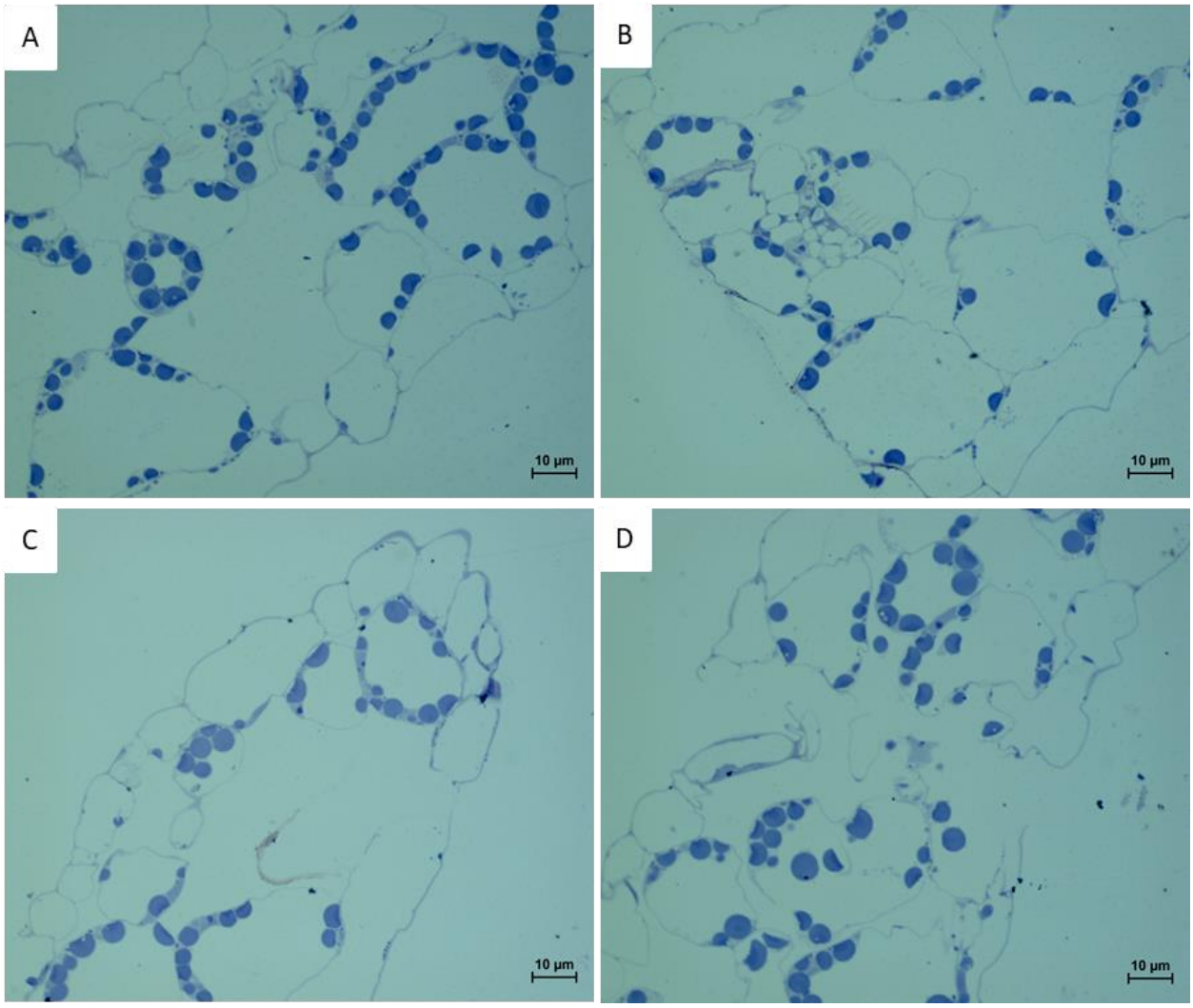

Figure S1 Globular chloroplasts can be seen in wild type *Arabidopsis thaliana* leaves. Light micrographs of transverse sections of leaves from 1-week-old WT *Arabidopsis* plants stained with toluidine blue. Scale bars – 10um

Supplemental Figure S2

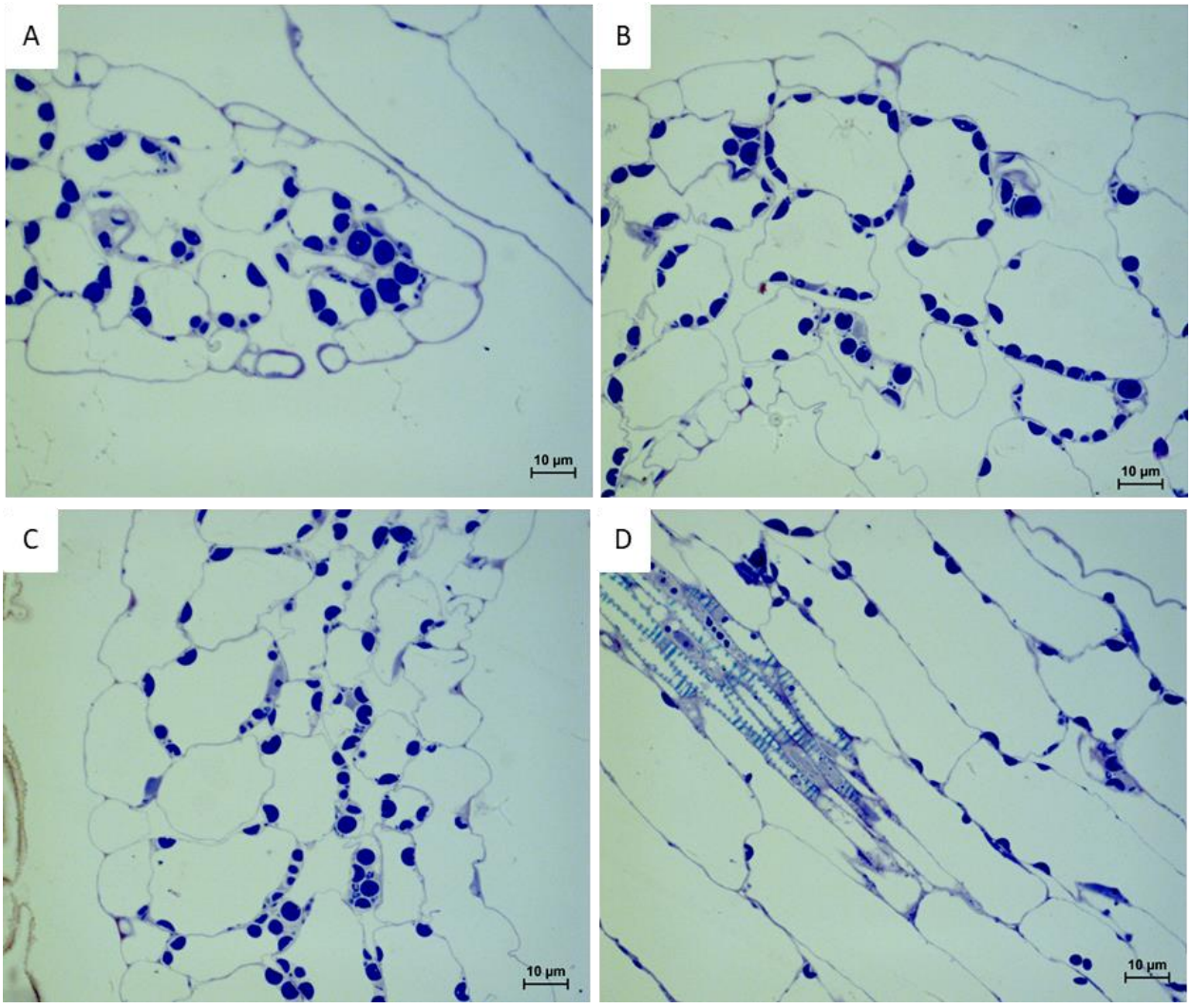

Figure S2 Chloroplasts comparable to wild type seen in un-induced VND7 *Arabidopsis thaliana* leaves. Light micrographs of transverse sections of leaves from 1-week-old VND7 *Arabidopsis* plants without induction, stained with toluidine blue. Scale bars – 10um

Supplemental Figure S3

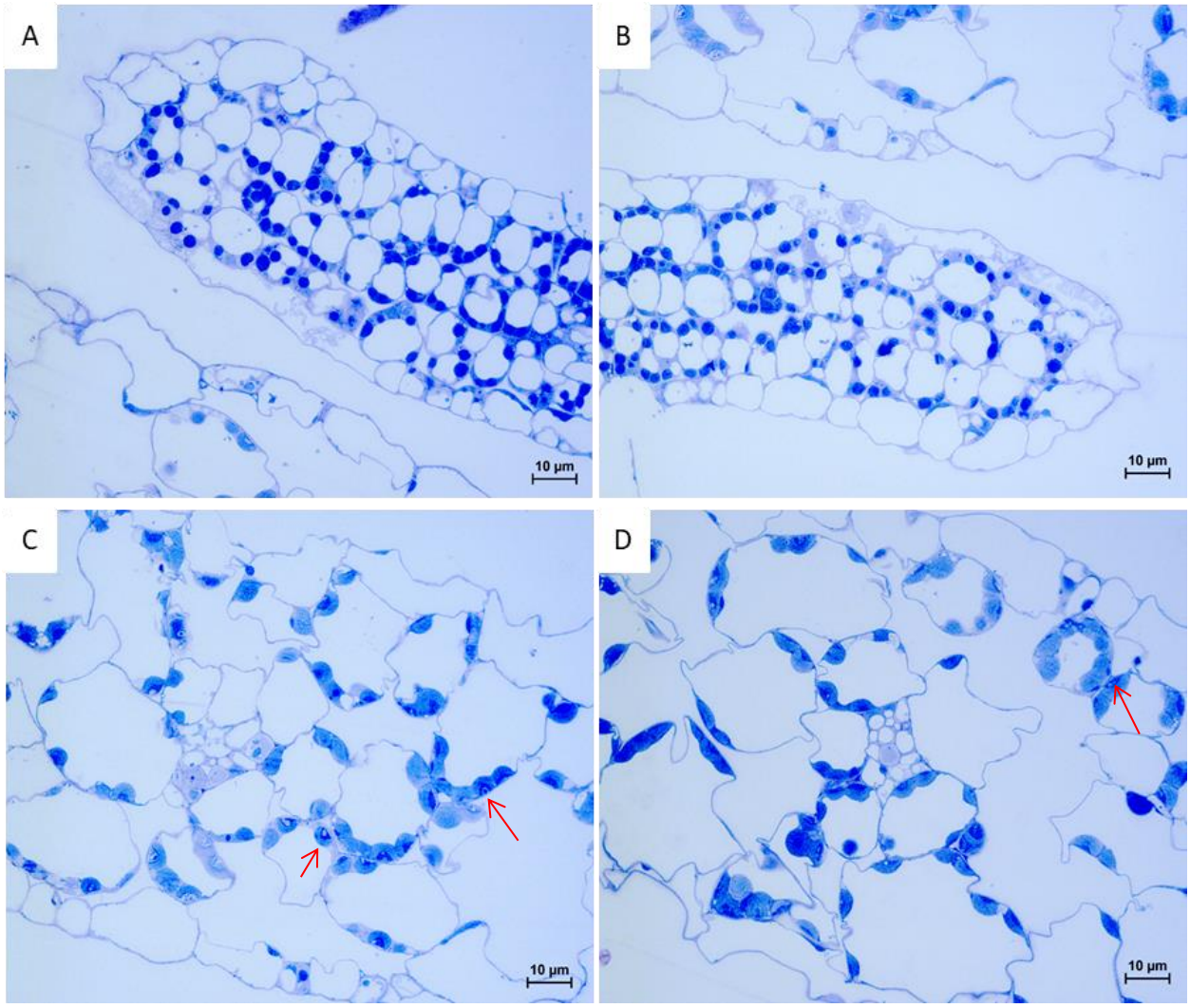

Figure S3 Transition of disc-shaped chloroplasts into unique amoeboid shapes. Light micrographs of transverse sections of leaves from 1-week-old VND7 *Arabidopsis* plants 8 HAI, stained with toluidine blue. Some chloroplasts appeared to be engulfing cytoplasmic material (red arrows in C and D) while others remained a globular shape. Scale bars – 10um

Supplemental Figure S4

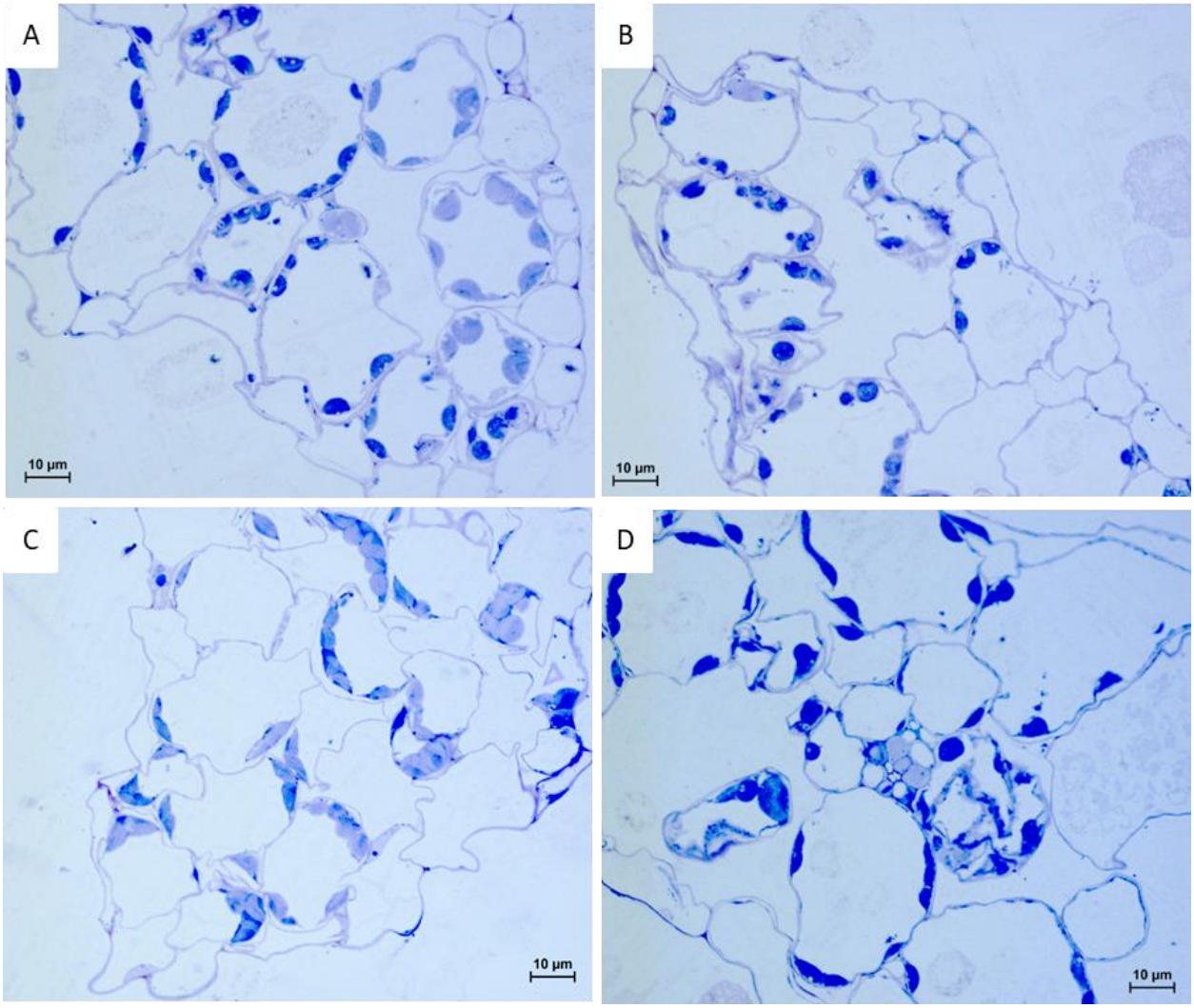

Figure S4 Cytoplasmic engulfment seen at 12 HAI. Light micrographs of transverse sections of leaves from 1-week-old VND7 *Arabidopsis* plants 12 HAI, stained with toluidine blue. Chloroplasts appeared to be engulfing cytoplasmic material. Scale bars – 10um

Supplemental Figure S5

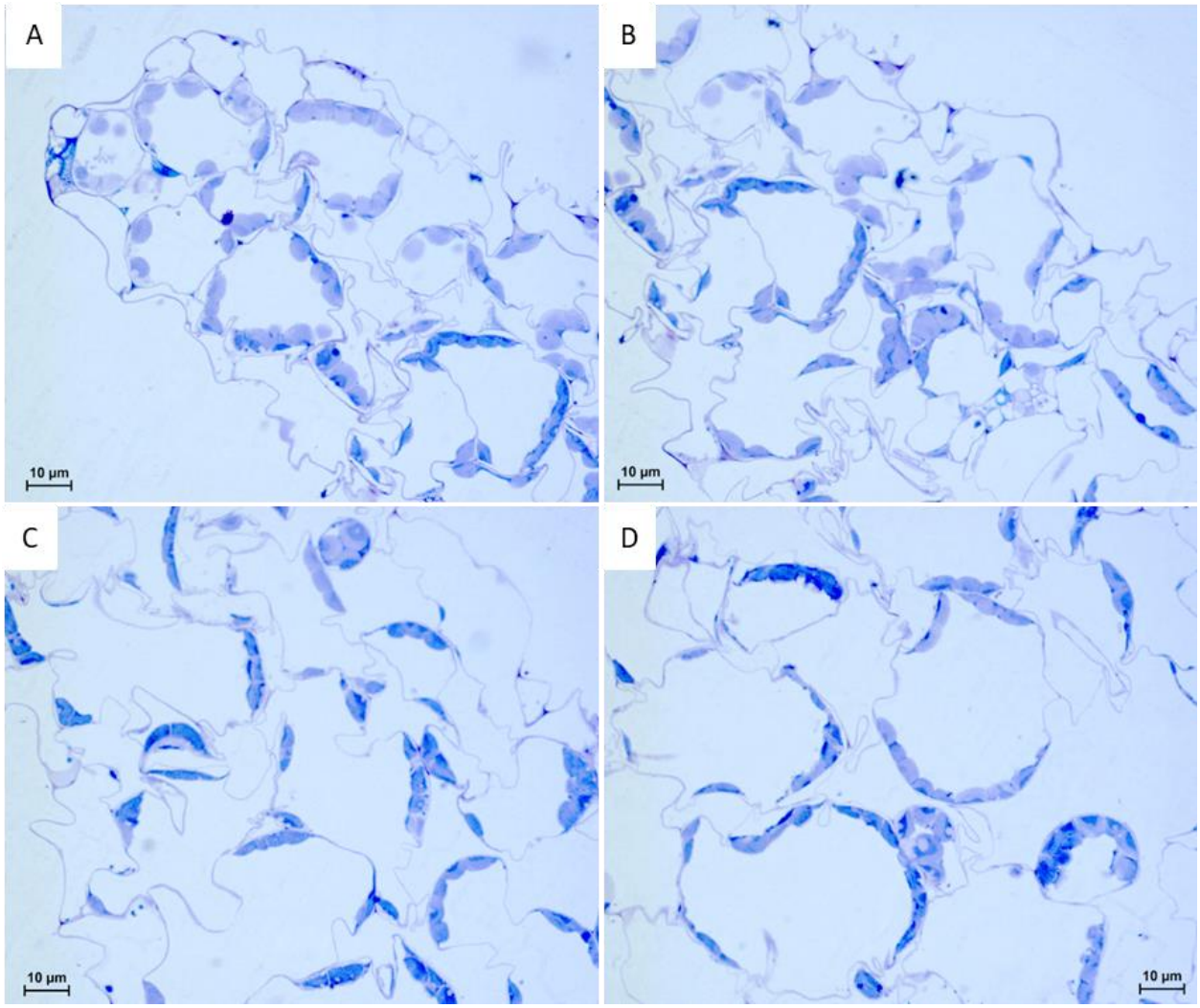

Figure S5 Globular chloroplasts can no longer be seen at 18 HAI. Light micrographs of transverse sections of leaves from 1-week-old VND7 *Arabidopsis* plants 18 HAI, stained with toluidine blue. Scale bars – 10um

Supplemental Figure S6

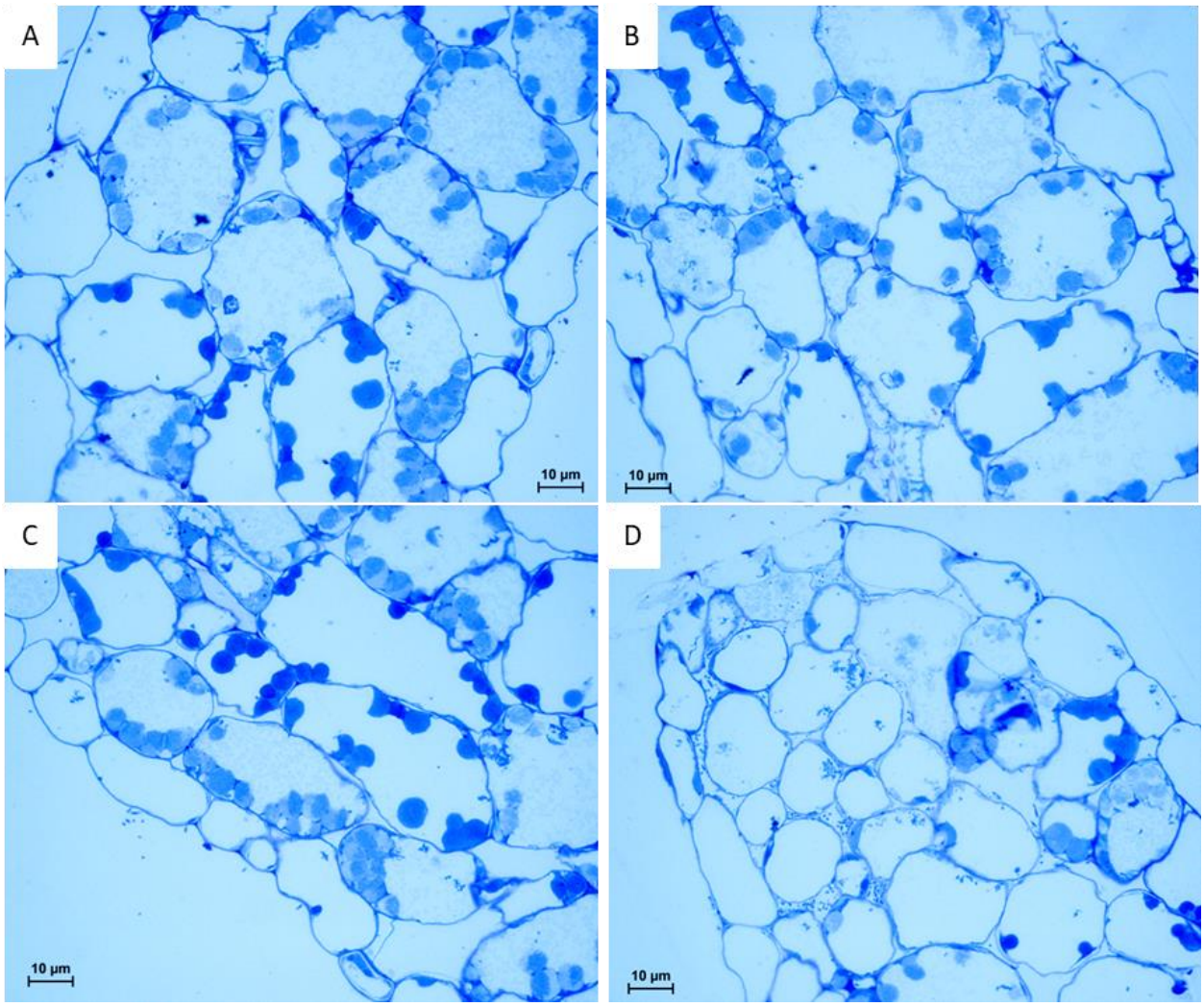

Figure S6 The plastids appear rounder at 24 HAI however SCW thickening is not clearly visible. Light micrographs of transverse sections of leaves from 1-week-old VND7 *Arabidopsis* plants 24 HAI, stained with toluidine blue. SCW deposition cannot be seen at this magnification. Scale bars – 10um

Supplemental Figure S7

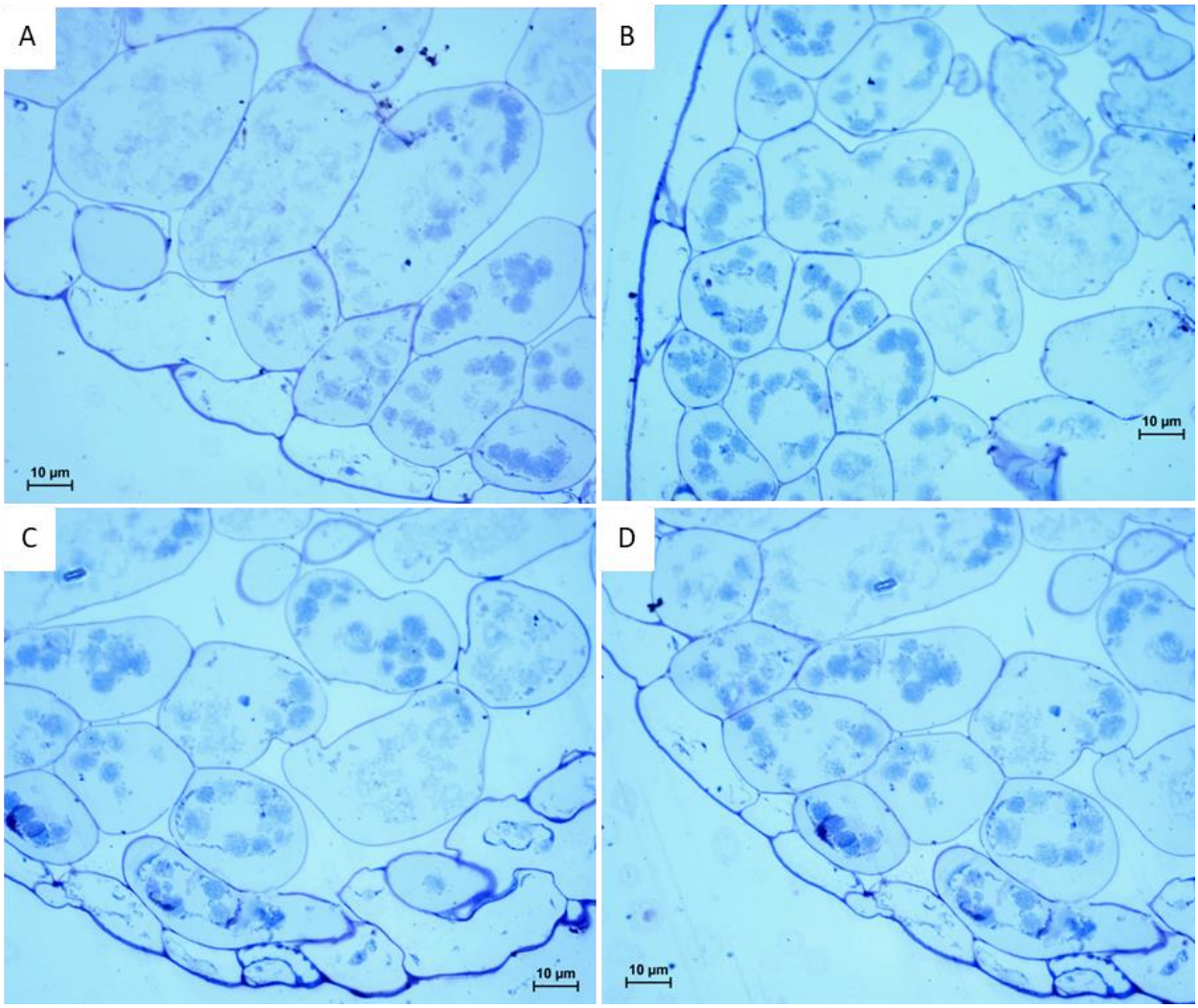

Figure S7 Plastids appear enlarged and degraded. Light micrographs of transverse sections of leaves from 1-week-old VND7 *Arabidopsis* plants 36 HAI, stained with toluidine blue. The plastids appear to have lost their membrane integrity and degraded. Scale bars – 10um

Supplemental Figure S8

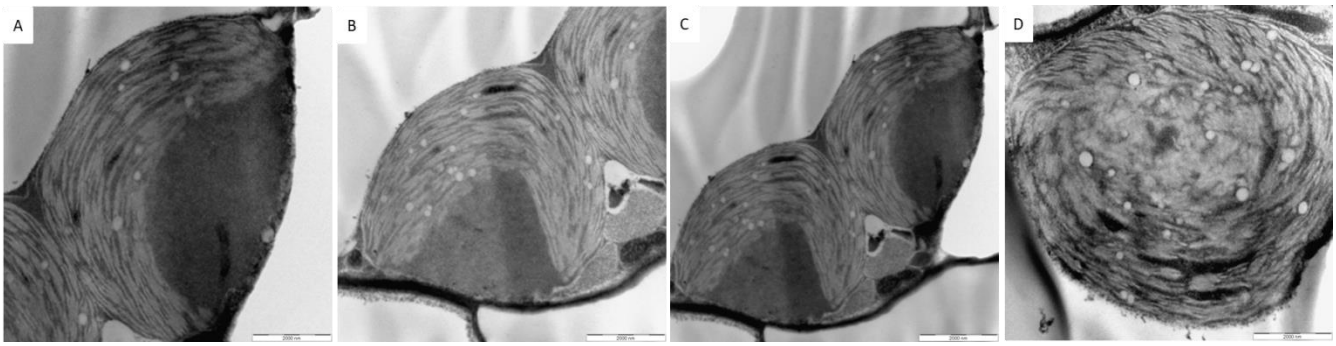

Figure S8 Transition of disc-shaped chloroplasts into unique amoeboid shapes. Transmission electron microscope images (trial 1) of VND7*Arabidopsis thaliana* leaf cross sections showing changes in plastid ultrastructure at 8 HAI. The chloroplasts transitioned into a horse-shoe shape known as an amoeboid plastid. Scale bars – 1000nm

Supplemental Figure S9

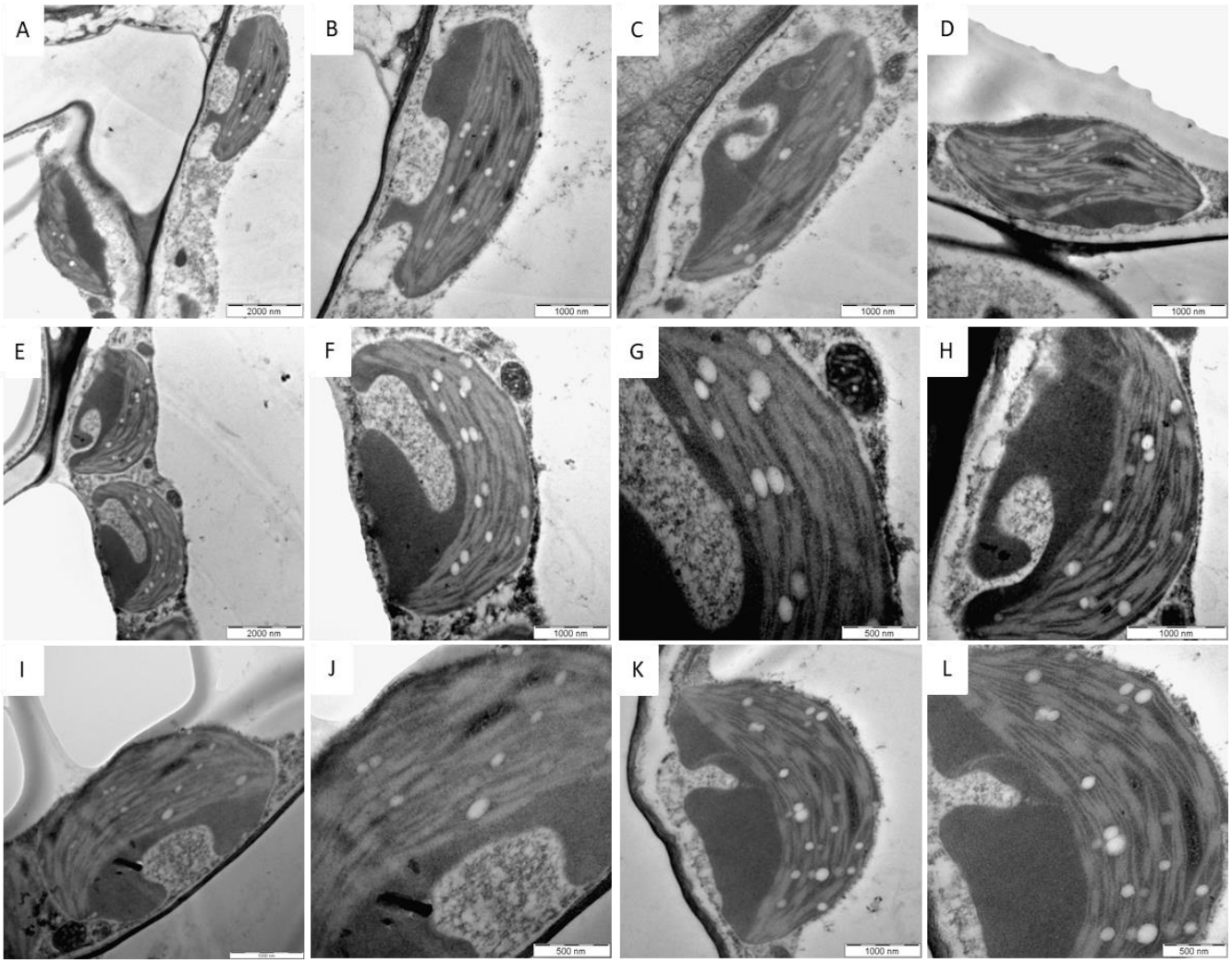

Figure S9 Transition of disc-shaped chloroplasts into unique amoeboid shapes. Transmission electron microscope images (trial 1) of VND7*Arabidopsis thaliana* leaf cross sections showing changes in plastid ultrastructure at 12 HAI. The plastids appeared to be engulfing the surrounding cytoplasmic material. Scale bars: A; E – 2000nm, B; C; D; F; H; I; K – 1000nm, G; J; L – 500nm

Supplemental Figure S10

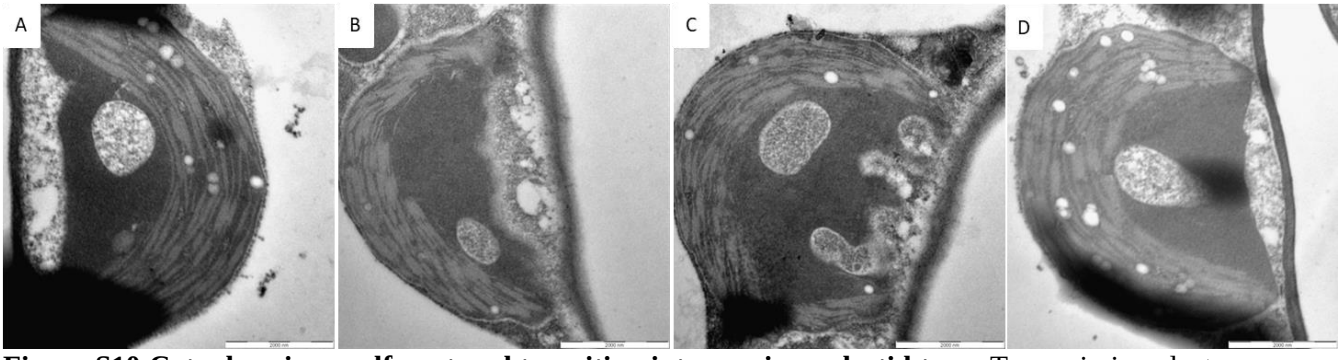

Figure S10 Cytoplasmic engulfment and transition into a unique plastid type. Transmission electron microscope images (trial 1) VND7 *Arabidopsis thaliana* leaf cross sections showing changes in plastid

ultrastructure at 18 HAI. The engulfed cytoplasmic material appeared to be surrounded by the plastidial membrane. Scale bars – 2000nm

Supplemental Figure S11

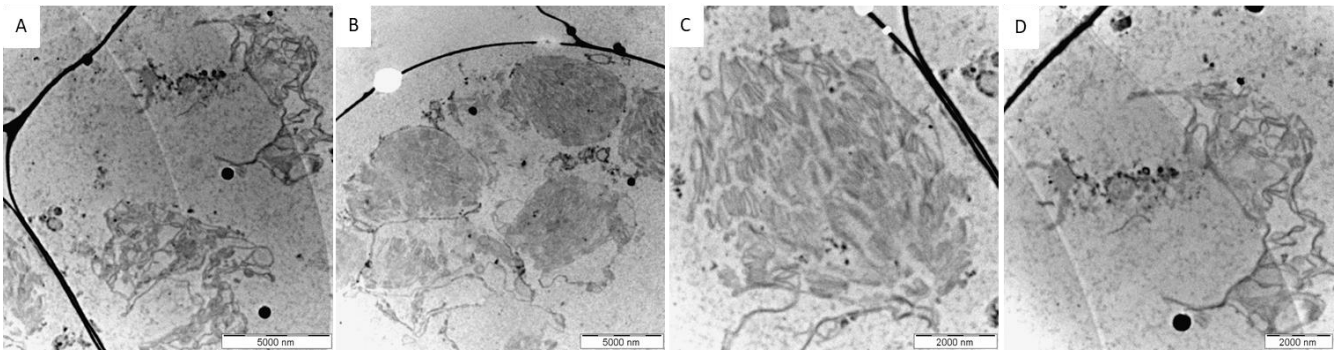

Figure S11 Plastids swell and subsequently degrade at 24 HAI. Transmission electron microscope images (trial 1) of VND7 *Arabidopsis thaliana* leaf cross sections showing changes in plastid ultrastructure at 24 HAI. The plastids had lost their inner membrane structure and appeared degraded. Scale bars – A; B – 5000nm, C; D – 2000nm

Supplemental Figure S12

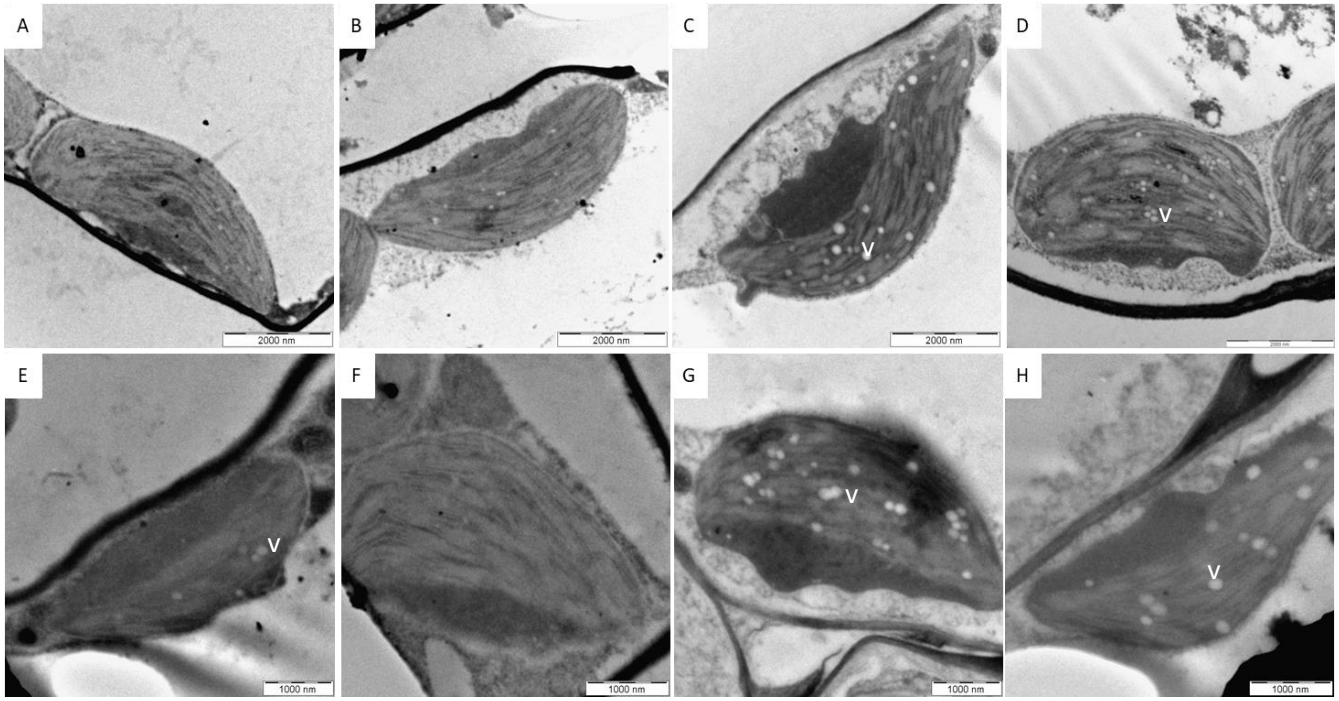

Figure S12 Transition of disc-shaped chloroplasts into unique amoeboid shapes. Transmission electron microscope images (trial 2) of VND7*Arabidopsis thaliana* leaf cross sections showing changes in plastid ultrastructure at 8 HAI. The amoeboid plastid can be seen forming with an increase in vesicle (v) number. Scale bars – A-D - 2000nm; E-H – 1000nm.

Supplemental Figure S13

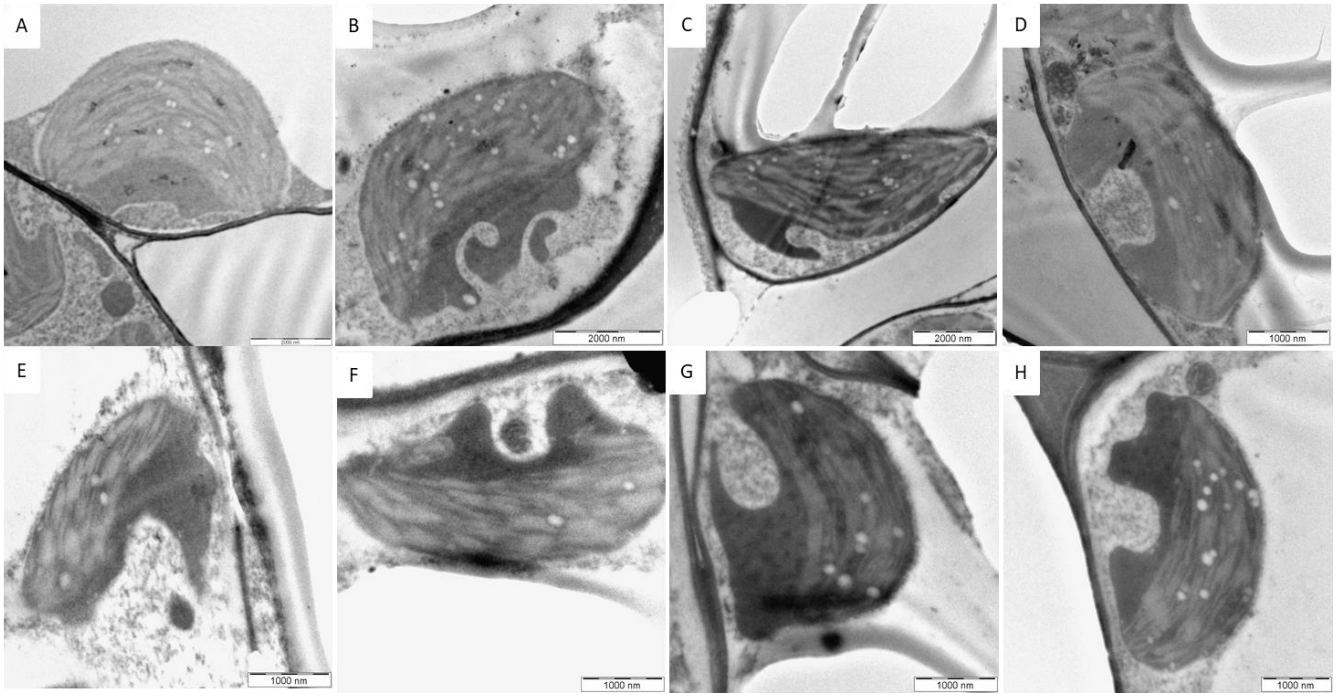

Figure S13 Transition of disc-shaped chloroplasts into unique amoeboid shapes. Transmission electron microscope images (trial 2) of VND7*Arabidopsis thaliana* leaf cross sections showing changes in plastid ultrastructure at 12 HAI. The plastids appeared to be engulfing the surrounding cytoplasmic material. Scale bars – A-C - 2000nm; D-H – 1000nm

Supplemental Figure S14

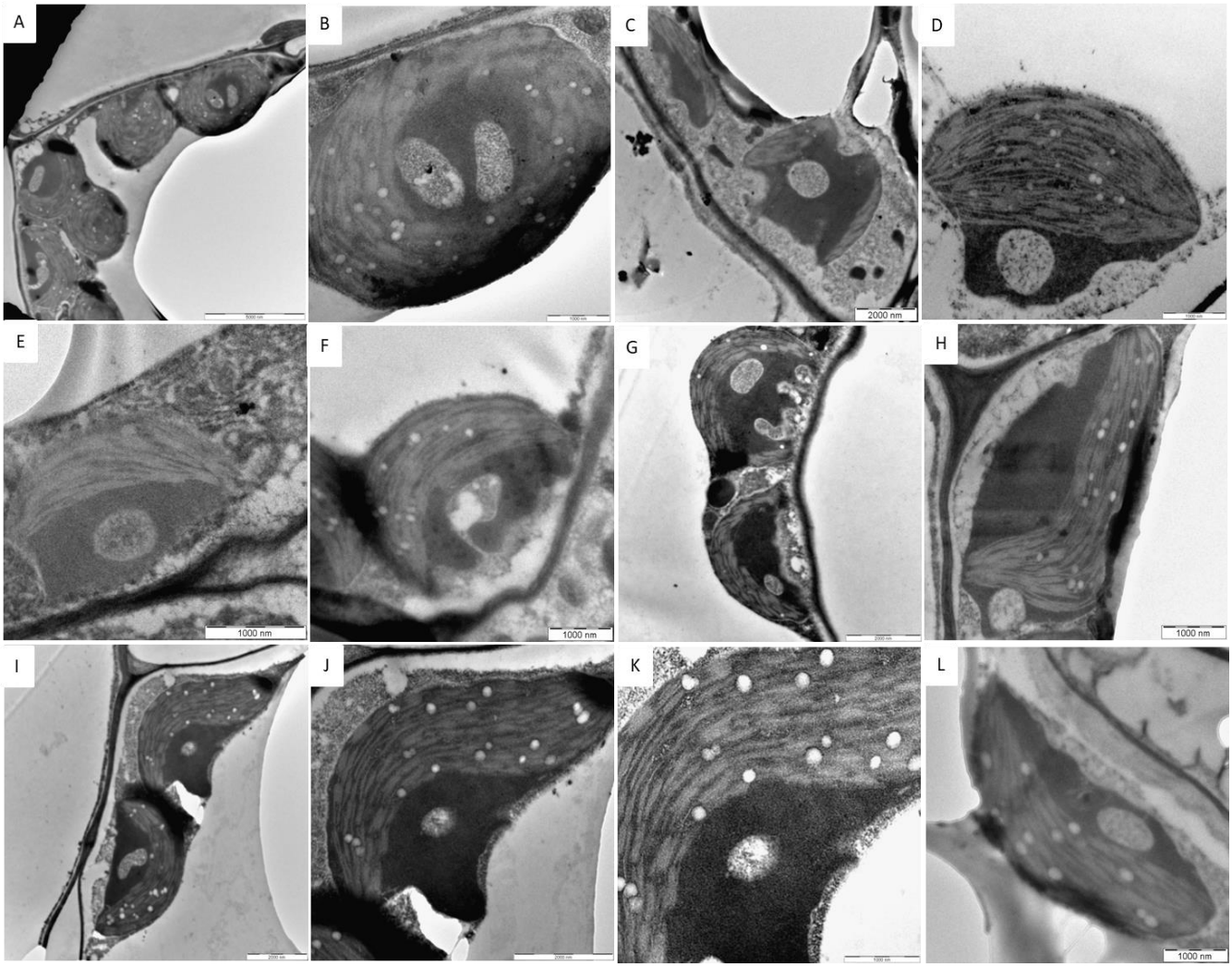

Figure S14 Cytoplasmic engulfment and transition into a unique plastid type. Transmission electron microscope images (trial 2) of VND7*Arabidopsis thaliana* leaf cross sections showing changes in plastid ultrastructure at 18 HAI. The engulfed cytoplasm appears to be surrounded by the plastid membrane. Some plastids appeared to engulf a second portion of cytoplasm (A, B, G). B is a higher magnification of A, J and K are magnifications of I. Scale bars – A- 5000nm, B; D; E; F; H; K; L – 1000nm, C;G; I; J - 2000nm

Supplemental Figure S15

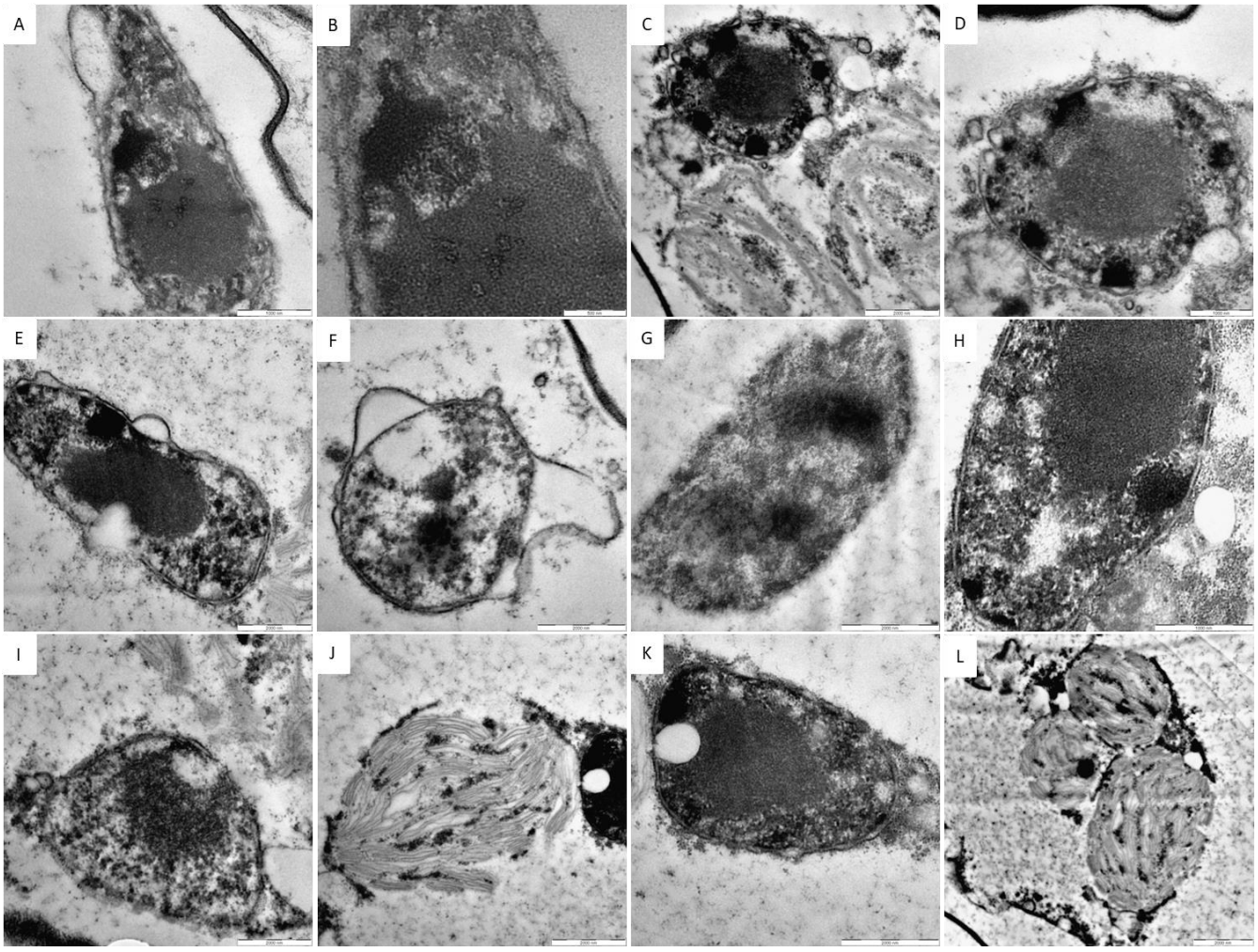

Figure S15 Formation of a unique plastid type, the xyloplast. Transmission electron microscope images (trial 2) of VND7*Arabidopsis thaliana* leaf cross sections showing changes in plastid ultrastructure at 19HAI. The newly formed xyloplast contains electron dense material in the centre and a diffuse outer membrane. Some plastids appear to have already started to degrade at this time point (J&L). B is a magnification of A, D is a magnification of C. Scale bars – A; D; H – 1000nm, B – 500 nm, C; E; F; G; I-L – 2000nm

Supplemental Figure S16

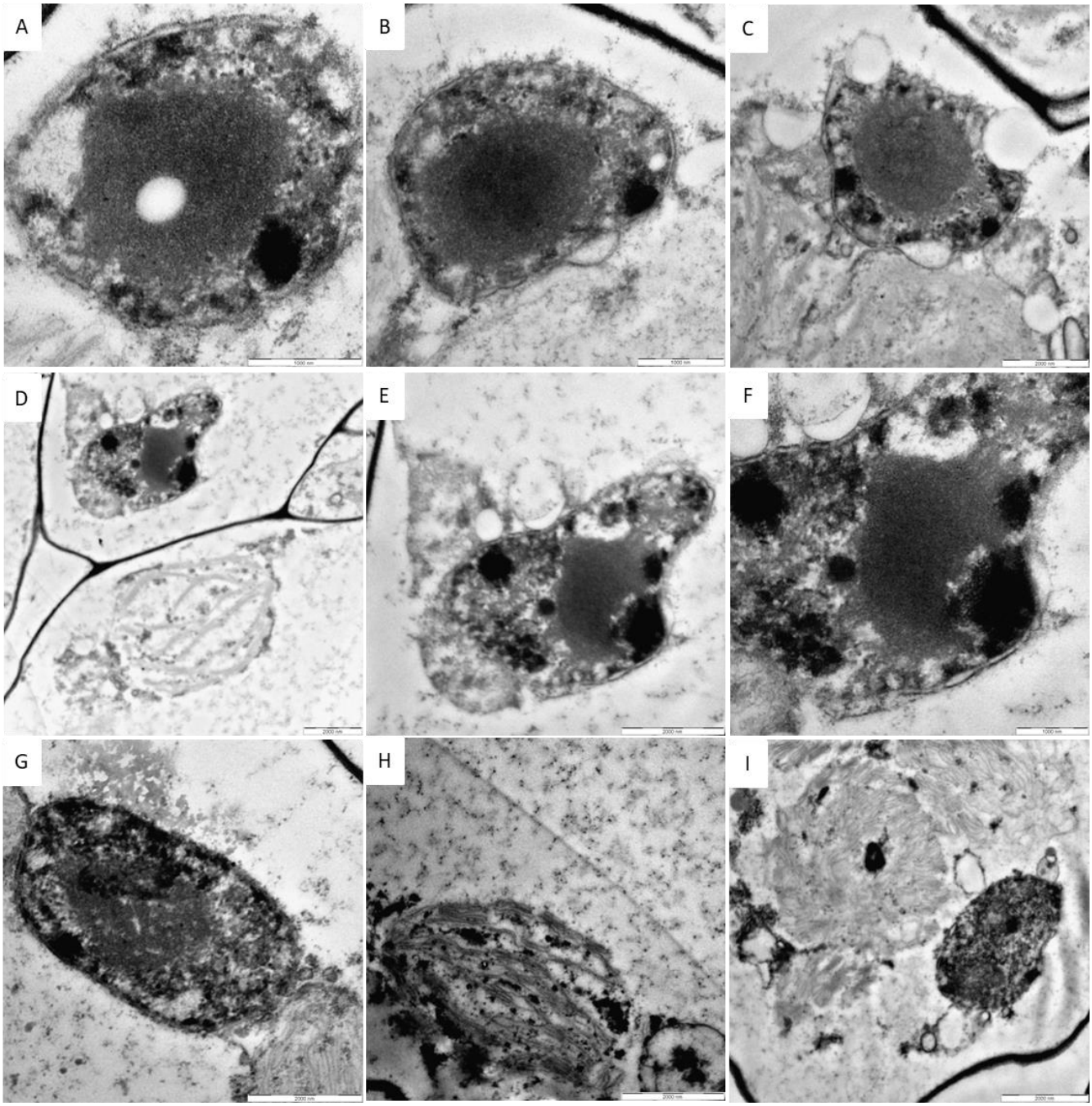

Figure S16 Formation of a unique plastid type, the xyloplast. Transmission electron microscope images (trial 2) of VND7 *Arabidopsis thaliana* leaf cross sections showing changes in plastid ultrastructure at 19.5 HAI. The xyloplast can still be seen however the electron dense material appears to have moved to the outer membrane of the plastid for possible secretion into the cytoplasm. Degraded xyloplasts can be seen in D, H and I. E and F are a magnification of D. Scale bars – A; B; G – 1000nm, C-E; G-I -2000nm

Supplemental Figure S17

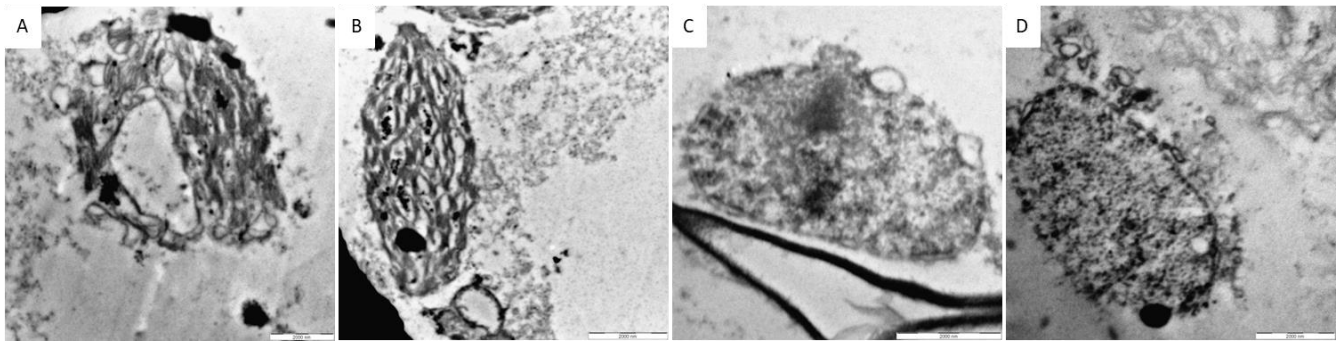

Figure S17 Xyloplasts swell and begin to release intraplastidial contents after 20 HAI. Transmission electron microscope images (trial 2) of VND7 *Arabidopsis thaliana* leaf cross sections showing changes in plastid ultrastructure at 20 HAI. A and B show degrading xyloplasts lacking inner contents while C and D show relatively intact xyloplasts. Scale bars – 2000nm

Supplemental Figure S18

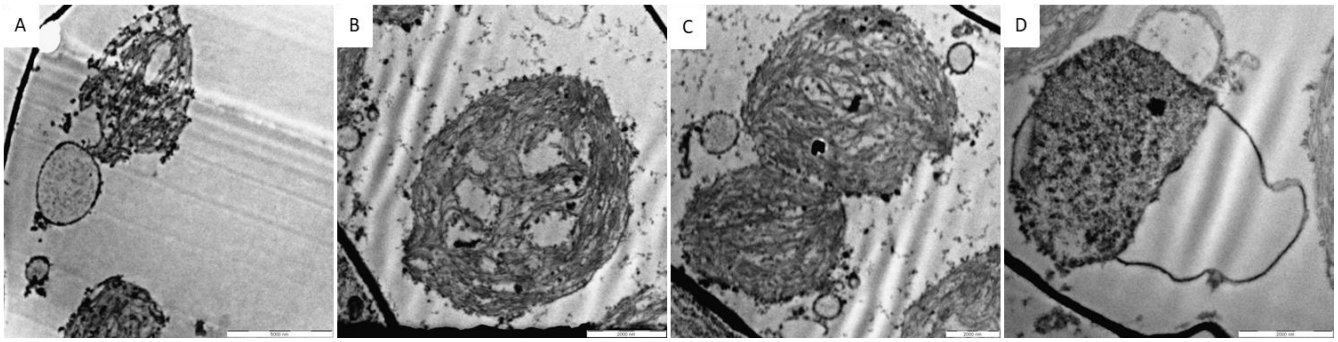

Figure S18 Xyloplasts swell and release intraplastidial contents. Transmission electron microscope images (trial 2) of VND7 *Arabidopsis thaliana* leaf cross sections showing changes in plastid ultrastructure at 20.5 HAI. The surrounding dark spots could be indicative of released plastid contents. Scale bars – A – 5000nm, B-D – 2000nm

Supplemental Figure S19

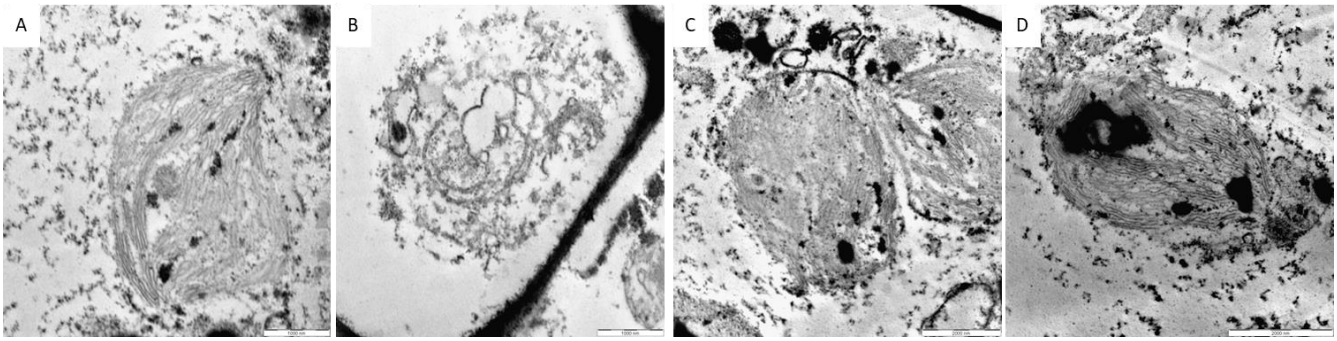

Figure S19 Xyloplasts swell and release intraplastidial contents. Transmission electron microscope images (trial 2) of VND7 *Arabidopsis thaliana* leaf cross sections showing changes in plastid

ultrastructure at 21 HAI. The surrounding dark spots could be indicative of released plastid contents. Scale bars – A; B – 1000nm, C; D – 2000nm

Supplemental Figure S20

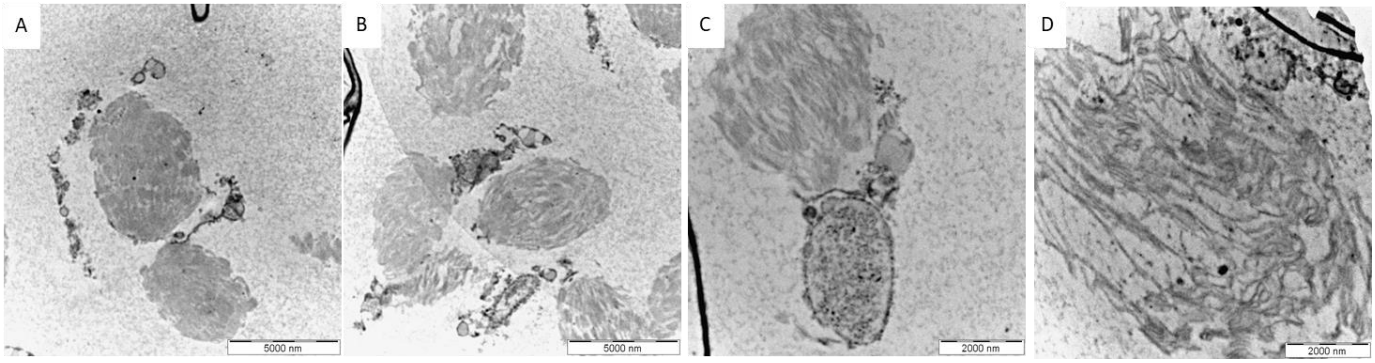

Figure S20 Xyloplasts swell and release intraplastidial contents after which they degrade. Transmission electron microscope images (trial 2) of VND7 *Arabidopsis thaliana* leaf cross sections showing changes in plastid ultrastructure at 22 HAI. C shows a relatively intact xyloplast next to a degraded xyloplast. Scale bars – A; B – 5000nm, C; D – 2000nm

Supplemental Figure S21

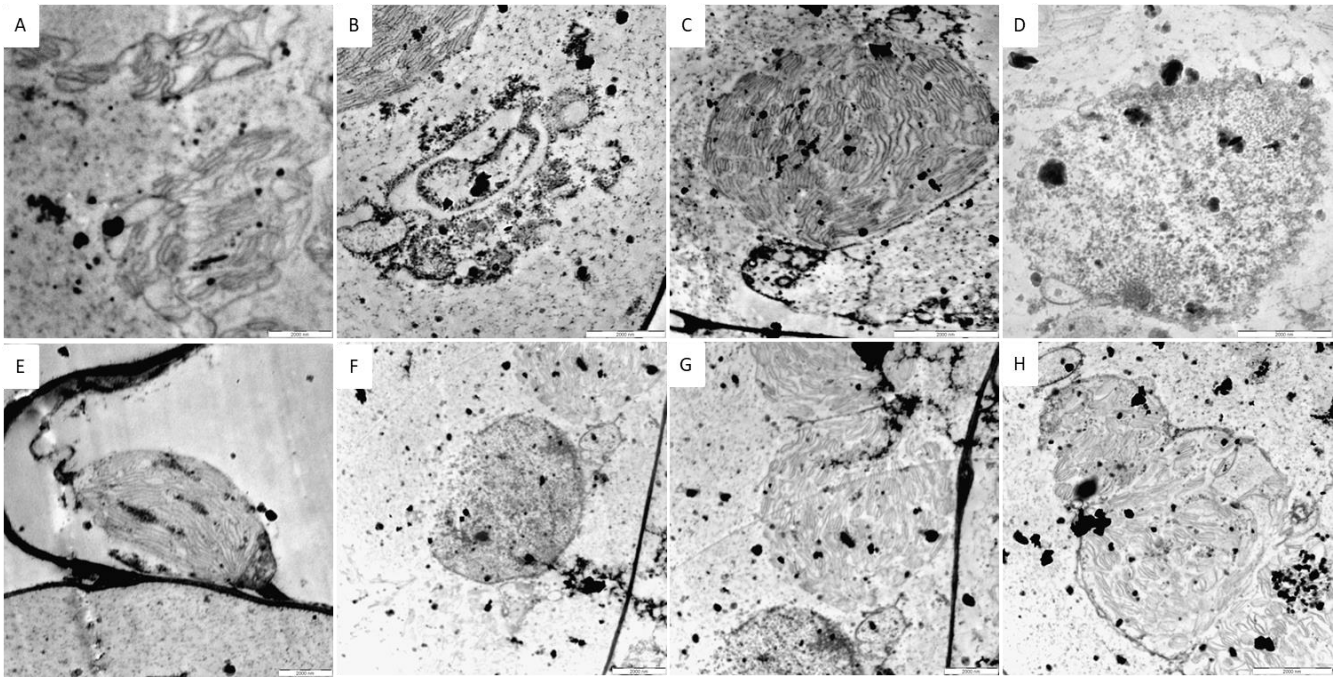

Figure S21 Xyloplasts swell and get degraded. Transmission electron microscope images (trial 2) of VND7*Arabidopsis thaliana* leaf cross sections showing changes in plastid ultrastructure at 22.5 HAI. All the plastids appeared to have released plastidial contents and degraded by 22.5 HAI. Degraded thylakoid membranes can be seen in most plastids. Scale bars – 2000nm

Supplemental Figure S22

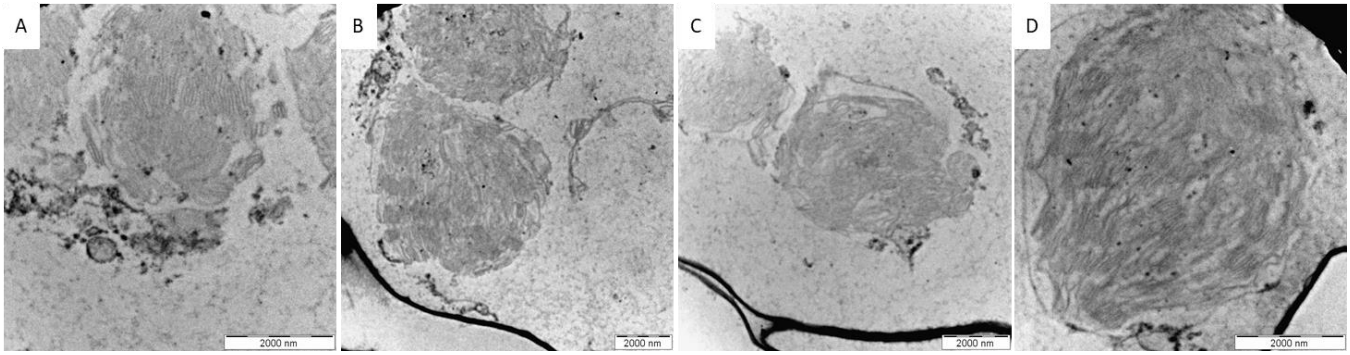

Figure S22 Degraded xyloplasts present in the cell at 23 HAI. Transmission electron microscope images (trial 2) of VND7*Arabidopsis thaliana* leaf cross sections showing changes in plastid ultrastructure at 23 HAI. Scale bars – 2000nm

Supplemental Figure S23

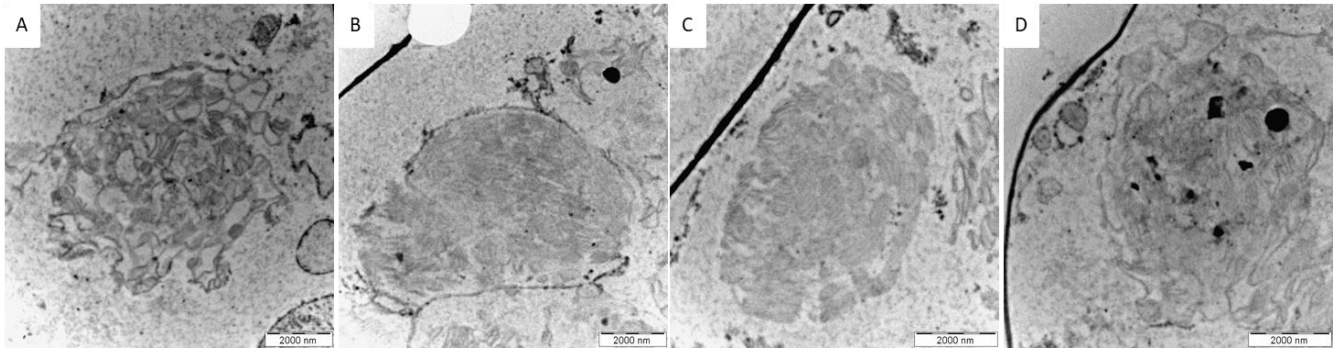

Figure S23 Degraded xyloplasts present in the cell at 24 HAI. Transmission electron microscope images (trial 2) of VND7*Arabidopsis thaliana* leaf cross sections showing changes in plastid ultrastructure at 24 HAI. SCW deposition at 24 HAI (not shown here) is accompanied by plastid and cell death. Scale bars – 2000nm

Supplemental Figure S24

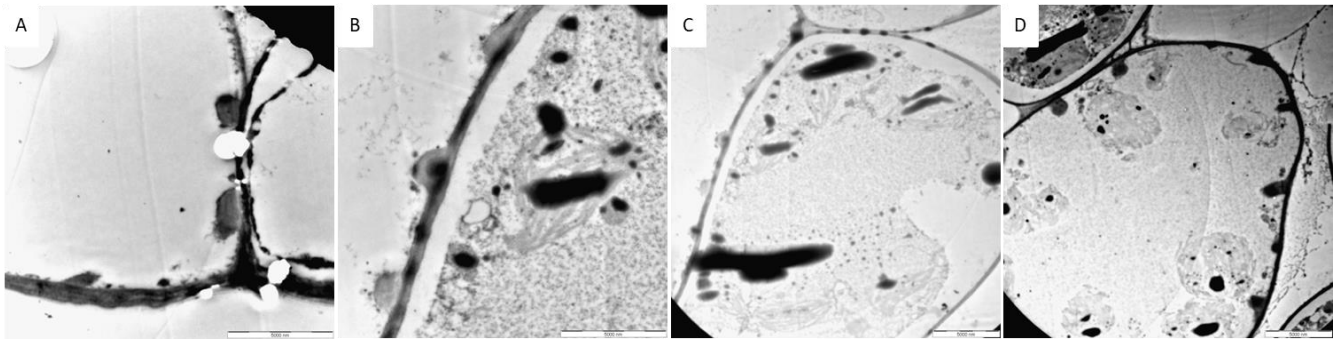

Figure S24 Degraded xyloplasts present in the cell at 36 HAI accompanied by SCW deposition. Transmission electron microscope images (trial 2) of VND7*Arabidopsis thaliana* leaf cross sections showing changes in plastid ultrastructure and SCW deposition at 36 HAI. Plastids are degraded and SCW deposition can be seen. Scale bars – 5000nm

Supplemental Figure S25

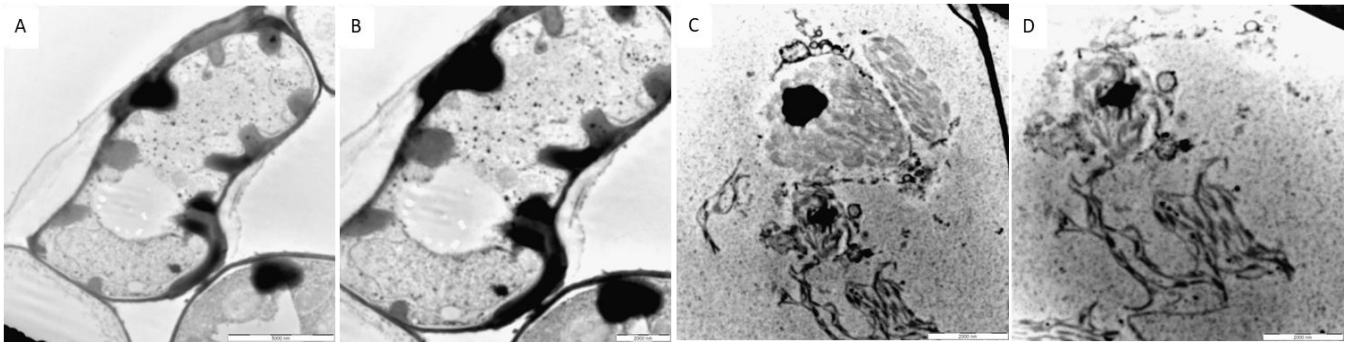

Figure S25 SCW deposition at 48 HAI and degraded xyloplasts in the cell. Transmission electron microscope images (trial 2) of VND7*Arabidopsis thaliana* leaf cross sections showing changes SCW deposition (A and B) deposition at 48 HAI as well as plastid degradation(C and D). Scale bars – A - 5000nm, C; D; B – 2000nm

Supplemental Figure S26

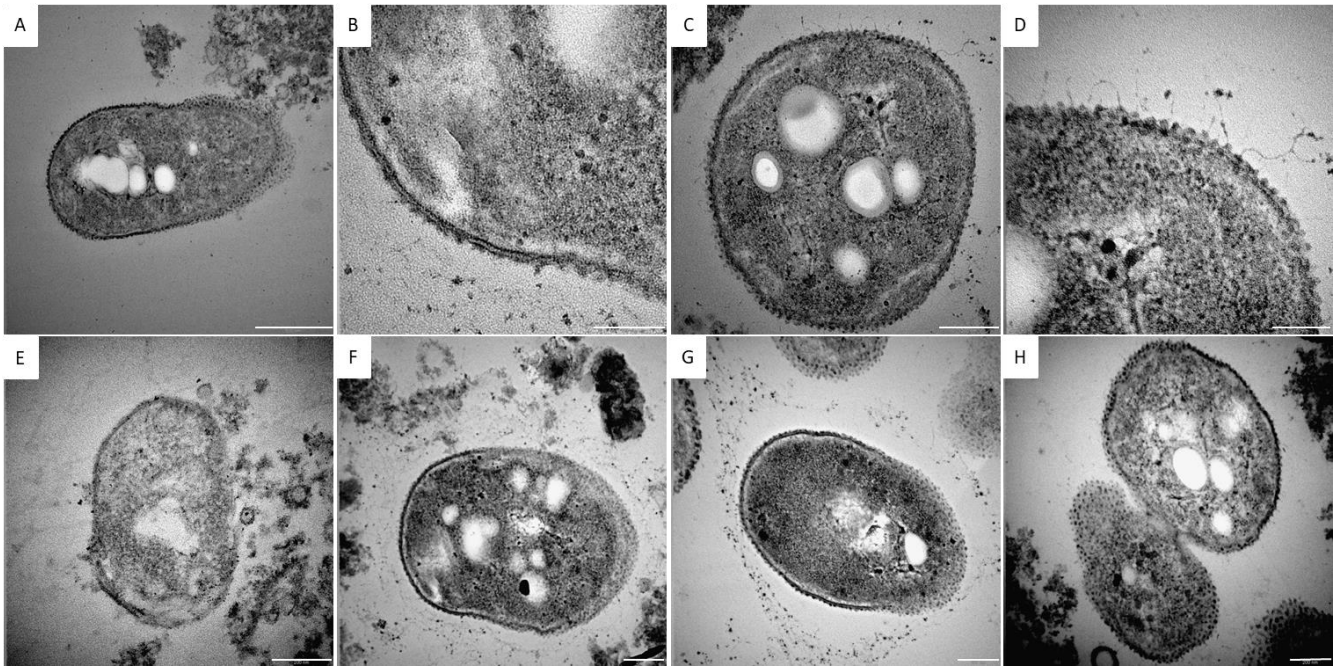

Figure S26 Xyloplasts extracted from 7 year old *E grandis* immature xylem scrapings. Xyloplasts extracted from xylem are comparable to the plastids seen at 19&19.5 HAI in the VND7 system (**Fig. S15 & S16**). The xyloplasts show a diffuse outer membrane (B &D) however, starch granules can be seen. B is a magnification of A; D is a magnification of C. Scale bars – A – 500nm, B; D – 100nm, C; E - H – 200nm.

Chapter 3

3.1. Concluding remarks

Terrestrial plants account for ~82% of carbon in living biomass and an estimated 70% of this exists in the woody tissues of vascular plants (Bar-On et al., 2018). Plastids found in vascular plants play a key role in sequestering atmospheric carbon through photosynthesis and more than 30% of all fixed carbon is shunted to the plastid-localised shikimate pathway (Tohge et al., 2013) which provides phenylalanine (Phe), the phenolic precursor for lignin, which is a key component of the secondary cell wall (SCW) along with cellulose and hemicellulose. In this study, we performed ultrastructural studies to gain a deeper insight into the role of plastids in woody tissues. We describe a morphologically distinct plastid, the xyloplast, found in xylem using the VND7 induction system in *Arabidopsis.* Analysis of published transcriptomic and metabolic data revealed that rapid Phe synthesis is accompanied by the formation of the xyloplast and that xyloplast degradation as a result of programmed cell death (PCD) is central to making Phe available for monolignol synthesis in the cytoplasm.

Although this study provided new insights into organellar metabolism during SCW formation, some missing gaps in knowledge remain. In our study, the conversion of chloroplasts into amoeboid plastids served as an indicator of the xyloplast being a distinct plastid type, as amoeboid plastids are commonly seen during plastid interconversion (Whatley, 1974). Between 8 HAI and 18 HAI, there is evidence of structural and morphological changes in the plastid that are indicative of increased interaction with cytoplasmic contents due to increased surface area contact. It would be interesting to see whether the cytoplasmic uptake is a result of the morphological reprogramming of chloroplasts or cytoplasmic enzymes/ pathways are being taken up by the plastid. One way of doing this would be to use immunogold labelling targeted to PPP and shikimate biosynthetic pathway enzymes. In peppermint, immunogold labeling using polyclonal antibodies was previously used to determine the localization of limonene synthase, involved in the first step of monoterpene biosynthesis (Turner et al., 1999). It was found that limonene synthase was exclusively localized in the leucoplasts while the remaining steps of the pathway were not localized in the plastid (Turner et al., 1999).

Previously, amoeboid plastids have been identified as plastolysosomes containing acid phosphatase activity involved in autophagy (Nagl, 1977; Gärtner and Nagl, 1980). These autophagic plastids have been implicated to play a role in a cellular cleaning program where

cytoplasm is engulfed, digested and excreted in response to new developmental surroundings (Seguí-Simarro and Nuez, 2008; Corral-Martínez et al., 2013; Parra-Vega et al., 2015). An indication of autophagy is the translucency of the intraplastidial (IP) space after digestion compared to the surrounding cytoplasm. Although in our images, the IP space maintained the same electron density as the surrounding cytoplasm, future work should test the IP space for acid phosphatase activity to rule out whether any cytoplasmic digestion is taking place.

It is also not known how Phe synthesized in the plastid is made available to the cytosolic monolignol biosynthetic pathway, as the first step (PAL) committing Phe into monolignol synthesis is cytoplasmic and endoplasmic reticulum-localized (Boerjan et al., 2003). It has been hypothesized that Phe could either be transported across the plastid double membrane through diffusion, active transporters or by vesicle-mediated transport (Pinard and Mizrachi, 2018). Our findings suggest that vesicle-mediated transport is unlikely and that Phe is most likely made freely available to the cell as a result of the plastid bursting. This is due to the up regulation of programmed cell death (PCD) genes resulting in homeostasis no longer being maintained as the cell is fated to die. This is supported by our observation of electron dense material being present in the plastid before they burst and the up-regulation of the full lignin pathway post plastid degradation. However, it is important to confirm whether plastid degradation plays a central role in making Phe available and is not just a result of PCD. One way to bypass PCD would be to create CRISPR constructs which target the PCD genes in VND7-inducible *Arabidopsis* plants. This would prevent the successful expression of PCD genes upon induction. Another way would be to trigger xyloplast formation at the metabolic level and bypass VND7 and PCD gene induction.

Previously, the synthetic conversion of chloroplasts to chromoplasts has been metabolically triggered by the up regulation of phytoene, the metabolite formed from the first committed step of the carotenoid pathway (Llorente et al., 2020a). In plants, two isoforms of arogenate dehydratase (ADT type-I and type-II) can catalyse and regulate the final step of Phe biosynthesis from arogenate via feedback-inhibition (Bonner and Jensen 1987; El-Azaz et al. 2019). While ADT1 suppression reduces Phe levels by 75% to 82% in mutant *Petunia hybrida* flowers (Maeda et al., 2010a), the up regulation of AtADT4 in *Arabidopsis* leads to Phe hyperaccumulation (Chen et al., 2016). In transgenic ADT1-RNAi *Petunia* petals, there was a reduction in shikimate

levels and stable isotope labelling showed that the flux toward shikimate was reduced relative to controls, which resulted in the arogenate pool remaining unaltered (Maeda et al., 2010). This shows that ADT1 expression regulates carbon flux towards the shikimate pathway. Further research is needed to determine the role of ADT expression as a metabolic switch in xyloplast differentiation.

CRISPR/Cas9 has emerged as an efficient gene editing tool and is a step towards revolutinizing molecular research and breeding in crops and in forestry (Belhaj et al., 2015; Tsai and Xue, 2015; Ma and Liu, 2016; Weeks et al., 2016; Zhang et al., 2016) and may used in novel applications such as imaging chromatin (Chen et al., 2013), cleaving RNA (O'Connell et al., 2014) and in epigenomic regulation (Hilton et al., 2015; Kearns et al., 2015). Although not reported in the dissertation, I have created four CRISPR/Cas9 knock out lines in the VND7-inducible system which could not be analysed due to time contraints (See Supplementary Note). The four targeted genes these included the starch metabolism genes phosphoglucomutase (PGM) and beta-amylase, a lignin biosynthesis gene cinnamoyl CoA-reductase (CCR) as well as transaldolase (TAL) which is central to the pentose phosphate pathway (PPP). For future studies, these mutants could be used to dissect the role starch plays as a carbon source for the xyloplast and will serve as proof of concept that combination knock outs with the VND7 system can add even more insight into xyloplast biology in the future.

It is clear that organellar biology is central to wood formation as plastids are the exclusive sites of phenylalanine synthesis for monolignol precursors (Henkes et al., 2001; Pinard et al., 2019). Organellar genome variation has been shown to have a large effect on metabolite variation as well as plant fitness and growth in various plant species (Budar and Roux, 2011; Joseph et al., 2013; Roux et al., 2016). It has been shown in *Arabidopsis* that optimally combining organellar and nuclear genomes results in a 23% increase in biomass (Flood et al., 2020). As organellar genomes have an effect on xylem metabolism, dissecting organellar biology during wood formation is crucial in understanding wood formation as a whole (Pinard and Mizrachi, 2018). One limitation to this study is the slight variation seen in the timing of SCW differentiation in the VND7-inducible system. Although the inferences made between plastid morphology and transcriptomic data in this study are consistent with what is expected during xylem differentiation, microscopy and expression analysis can be performed using seedlings induced in

the same experiment/ biological replicates. In the broader context, the work in this thesis has both fundamental plant biology and ecology as well as biotechnology implications. Understanding xyloplast biology will provide us with novel targets for organellar bioengineering of biosynthetic pathways that lead to Phe synthesis and subsequently many other phenolic compounds in a variety of plants. Engineering plastids to synthesize various terpenes and metabolites could be the key step to not only engineering wood in trees, but engineering biomass overall.

3.2. References

Bar-On, Y.M., Phillips, R., and Milo, R. (2018). The biomass distribution on Earth. PNAS **115,** 6506-6511.

Belhaj, K., Chaparro-Garcia, A., Kamoun, S., Patron, N.J., and Nekrasov, V. (2015). Editing plant genomes with CRISPR/Cas9. Curr. Opin. Biotechnol. **32,** 76-84.

Boerjan, W., Ralph, J., and Baucher, M. (2003). Lignin biosynthesis. Annu. Rev. Plant Biol. **54,** 519-546.

Budar, F., and Roux, F. (2011). The role of organelle genomes in plant adaptation: time to get to work! Plant Signal. Behav. **6,** 635-639.

Chen, B., Gilbert, L.A., Cimini, B.A., Schnitzbauer, J., Zhang, W., Li, G.-W., Park, J., Blackburn, E.H., Weissman, J.S., and Qi, L.S. (2013). Dynamic imaging of genomic loci in living human cells by an optimized CRISPR/Cas system. Cell **155,** 1479-1491.

Chen, Q., Man, C., Li, D., Tan, H., Xie, Y., and Huang, J. (2016). Arogenate dehydratase isoforms differentially regulate anthocyanin biosynthesis in Arabidopsis thaliana. Mol Plant **9,** 1609-1619.

Corral-Martínez, P., Parra-Vega, V., and Seguí-Simarro, J.M. (2013). Novel features of Brassica napus embryogenic microspores revealed by high pressure freezing and freeze substitution: evidence for massive autophagy and excretion-based cytoplasmic cleaning. JExB **64,** 3061-3075.

Flood, P.J., Theeuwen, T.P., Schneeberger, K., Keizer, P., Kruijer, W., Severing, E., Kouklas, E., Hageman, J.A., Wijfjes, R., and Calvo-Baltanas, V. (2020). Reciprocal cybrids reveal how organellar genomes affect plant phenotypes. Nat. Plants **6,** 13-21.

Gärtner, P.-J., and Nagl, W. (1980). Acid phosphatase activity in plastids (plastolysomes) of senescing embryo-suspensor cells. Planta **149,** 341-349.

Henkes, S., Sonnewald, U., Badur, R., Flachmann, R., and Stitt, M. (2001). A small decrease of plastid transketolase activity in antisense tobacco transformants has dramatic effects on photosynthesis and phenylpropanoid metabolism. The Plant Cell **13,** 535-551.

Hilton, I.B., D'ippolito, A.M., Vockley, C.M., Thakore, P.I., Crawford, G.E., Reddy, T.E., and Gersbach, C.A. (2015). Epigenome editing by a CRISPR-Cas9-based acetyltransferase activates genes from promoters and enhancers. Nat. Biotechnol. **33,** 510-517.

Joseph, B., Corwin, J.A., Li, B., Atwell, S., and Kliebenstein, D.J. (2013). Cytoplasmic genetic variation and extensive cytonuclear interactions influence natural variation in the metabolome. Elife **2,** e00776.

Kearns, N.A., Pham, H., Tabak, B., Genga, R.M., Silverstein, N.J., Garber, M., and Maehr, R. (2015). Functional annotation of native enhancers with a Cas9–histone demethylase fusion. Nat. Methods **12,** 401-403.

Llorente, B., Torres-Montilla, S., Morelli, L., Florez-Sarasa, I., Matus, J.T., Ezquerro, M., D'andrea, L., Houhou, F., Majer, E., and Picó, B. (2020). Synthetic conversion of leaf chloroplasts into carotenoid-rich plastids reveals mechanistic basis of natural chromoplast development. PNAS **117,** 21796-21803.

Ma, X., and Liu, Y. (2016). CRISPR/Cas9-based genome editing systems and the analysis of targeted genome mutations in plants. Yi chuan= Hereditas **38,** 118-125.

Maeda, H., Shasany, A.K., Schnepp, J., Orlova, I., Taguchi, G., Cooper, B.R., Rhodes, D., Pichersky, E., and Dudareva, N. (2010). RNAi suppression of Arogenate Dehydratase1 reveals that phenylalanine is synthesized predominantly via the arogenate pathway in petunia petals. The Plant Cell **22,** 832-849.

Nagl, W. (1977). «Plastolysomes»—Plastids involved in the autolysis of the embryo-suspensor in Phaseolus. Zeitschrift für Pflanzenphysiologie **85,** 45-51.

O'Connell, M.R., Oakes, B.L., Sternberg, S.H., East-Seletsky, A., Kaplan, M., and Doudna, J.A. (2014). Programmable RNA recognition and cleavage by CRISPR/Cas9. Nature **516,** 263-266.

Parra-Vega, V., Corral-Martínez, P., Rivas-Sendra, A., and Seguí-Simarro, J.M. (2015). Formation and excretion of autophagic plastids (plastolysomes) in Brassica napus embryogenic microspores. Front. Plant Sci. **6,** 94.

Pinard, D., and Mizrachi, E. (2018). Unsung and understudied: plastids involved in secondary growth. Curr. Opin. Plant Biol. **42,** 30-36.

Pinard, D., Fierro, A.C., Marchal, K., Myburg, A.A., and Mizrachi, E. (2019). Organellar carbon metabolism is coordinated with distinct developmental phases of secondary xylem. New Phytol. **222,** 1832-1845.

Roux, F., Mary-Huard, T., Barillot, E., Wenes, E., Botran, L., Durand, S., Villoutreix, R., Martin-Magniette, M.-L., Camilleri, C., and Budar, F. (2016). Cytonuclear interactions affect adaptive traits of the annual plant *Arabidopsis thaliana* in the field. PNAS **113,** 3687-3692.

Seguí-Simarro, J.M., and Nuez, F. (2008). How microspores transform into haploid embryos: changes associated with embryogenesis induction and microspore-derived embryogenesis. Physiol. Plant. **134,** 1-12.

Tohge, T., Watanabe, M., Hoefgen, R., and Fernie, A. (2013). Shikimate and Phenylalanine Biosynthesis in the Green Lineage. Front. Plant Sci. **4**.

Tsai, C.-J., and Xue, L.-J. (2015). CRISPRing into the woods. GM crops & food **6,** 206-215.

Turner, G., Gershenzon, J., Nielson, E.E., Froehlich, J.E., and Croteau, R. (1999). Limonene synthase, the enzyme responsible for monoterpene biosynthesis in peppermint, is localized to leucoplasts of oil gland secretory cells. Plant Physiol. **120,** 879-886.

Weeks, D.P., Spalding, M.H., and Yang, B. (2016). Use of designer nucleases for targeted gene and genome editing in plants. Plant Biotechnol. J. **14,** 483-495.

Whatley, J. (1974). Chloroplast development in primary leaves of Phaseolus vulgaris. New Phytol. **73,** 1097-1110.

Zhang, Z., Mao, Y., Ha, S., Liu, W., Botella, J.R., and Zhu, J.-K. (2016). A multiplex CRISPR/Cas9 platform for fast and efficient editing of multiple genes in *Arabidopsis*. Plant Cell Rep. **35,** 1519-1533.

3.3. Supplementary note

3.3.1. Background

The analysis of plastid-encoded genes in the total mRNA-seq data from *E. grandis* (Pinard et al., in preparation) as well as the ultrastructural studies and gene expression analysis performed in this study support the notion of a developing secondary xylem-specific plastid, the xyloplast and makes it important to understand their role in carbon partitioning (Pinard and Mizrachi, 2018). An important step in dissecting xyloplast biology would be to determine what the supply of carbon is for normal xyloplast functioning during SCW formation. For future studies, we used CRISPR/Cas9 technology and the VND7 post-translational induction system to determine whether plastids import free sugars like glucose-6-phophate from the cytoplasm or break down the starch present in the plastid to produce Phe. CRISPR/Cas9 was used to target genes including phosphoglucomutase (PGM), which involved in starch biosynthesis, plastidial beta-amylase (BAM3) responsible for plastidial starch breakdown, transaldolase (TAL) which is crucial to the PPP and cinnamoyl-CoA reductase (CCR) which is needed for normal lignin synthesis to serve as a positive control. In future studies, these mutant plants can be induced to form SCW using DEX and analysed using light microscopy and TEM imaging to determine the effects on SCW formation and xyloplast integrity.

3.3.2. CRISPR/Cas9 target site selection and sgRNAs design

The coding regions of the target genes were obtained as FASTA files from NCBI. The mutation target site for each gene was selected using the sgRNA design online tool "E-CRISP" (www.e-crisp.org) through the *Arabidopsis thaliana* TAIR10 database. The top three sgRNA sequences for all genes were selected and RGenome (http://www.rgenome.net/cas-offinder) was used to detect any off-target effects. From the 3 sgRNAs sequences, one was selected to be cloned into the vector of choice for each gene **(table 1)**. The first base of the target sites selected had a 'G' to function as the start site for RNA polymerase III transcription.

Supplemental table S1 gRNA sequences for each of the six target genes.

Gene	gRNA sequence (5'to 3')
TAL **(AT1G12230)**	GCGTCTTCGTCTCTCGAAGC
CCR (**AT1G15950**)	GCCGAGACCGCACTTCACCG
BAM3 (**AT4G17090)**	GATTCTGTGCCTGTCCTAAG
PGM (**AT5G51820)**	GCACGTTCTATGCCGACAAG

3.3.3. Cloning and plant transformation

The PKI1.1R vector (Addgene) was cultured on selective LB plates containing spectinomycin. A single colony was selected and inoculated into liquid LB containing spectinomycin and grown in a shaking incubator at 37°C overnight. Plasmid DNA was extracted using the GeneJET plasmid miniprep kit (ThermoScientific) as per the manufacturer's instructions. Sticky end ligation of sgRNA into the PKI1.1R vector was performed as per the authors' protocol (Tsutsui and Higashiyama, 2017) and transformed into competent DH5alpha *E.coli* cells using heat shock. The transformed cells were plated onto LB plates containing 100ug/mL Spectinomycin and incubated at 37°C for 24 h. Colonies were selected, grown and plasmid DNA was extracted as previously described. Plasmid containing insert was then transformed into chemically competent *Agrobacterium tumefaciens* cells (Lifeasible). Plasmid (1 ng) was added to 100 µl competent cells and incubated on ice for 5 minutes, flash frozen in liquid nitrogen for 5 minutes, heat shocked in a 37°C water bath for 5 minutes followed by incubation on ice for another 5 minutes. Liquid YEP medium (700 ul) was added to the reactions at room temperature and incubated with shaking at 28°C for 3 hours. The cell culture was centrifuged for 1 minute at 6000 rpm and 700 ul of supernatant was disposed of. Cell pellet was resuspended in 100 ul of YEP medium and plated on selective YEP plates (100 ug/ml spectinomycin, 50 ug/ml rifampicin, 30 µg/ml streptomycin) and incubated at 28°C for 3 days. A single colony was used to inoculate 5 ml YEP medium (containing antibiotics) and incubated at 28°C for 1-2 days with shaking. 500 mL of YEP medium was inoculated with the 5 ml starter culture and incubated overnight with shaking

at 28°C till and OD600 of 0.8 (monitored on a spectrophotometer (ThermoScientific Multiskan GO)). *Agrobacterium* was centrifuged at 5500 x g at 20°C for 20 min. Cells were resuspended in 5% sucrose solution to OD600 approximately 0.8. Silwet L-77 was added to solution to a concentration of 0.05% (500 ul/l). *A. tumefaciens*-mediated transformation of *A. thaliana* was done by a floral dipping (Clough and Bent, 1998). Plants were grown in short day conditions (16h dark, 8h light) for 4 weeks followed by long day conditions (8h dark, 16h light) for 2 weeks. First bolts that appeared were dipped for 2 – 3 seconds with gentle agitation in *Agrobacterium*. Dipped plants were placed on their sides and sealed to create a humid environment for no longer than 24 hours. The plants were dipped again with the four-day interval to increase transformation percentage (Davis et al., 2009). After transformation, dry seeds were collected. Successfully transformed seeds fluoresced red due to the expressed Cas9-red fluorescent protein and were selected using fluorescent microscopy (Leica EZ4 microscope and fluorescent light) (Tsutsui and Higashiyama, 2017).

3.3.4. Conclusion

In conclusion, determining whether plastids import free sugars from the cytoplasm or break down the starch they make/have to produce Phe for normal lignin and cell wall formation will provide novel insights into the xyloplast and would be a major step forward in our fundamental understanding of plant vasculature and secondary growth.